CO_2/epoxide Coupling Reactions and Thiirane Desulphurization with Ru-Mn Bimetallic Complex, Manganese Carbonylates, and PPN Salts

By

Wing Nga SIT

A Thesis Presented to
The Hong Kong Polytechnic University
Department of Applied Biology and Chemical Technology
in Partial Fulfillment
of the Requirements
for the Degree of Master of Philosophy
in chemistry

Hong Kong, October 2005

Declaration

I hereby declare that this thesis summarized my own work carried out since my registration for the Degree of Master of Philosophy in September, 2003; and that has not been previously included in a thesis, dissertation or report submitted to this or any other institution for a degree, diploma or other qualification.

Wing Nga, SIT

Oct, 2005

Acknowledgements

I would like to express my deepest gratitude to my supervisor Prof. C. P. Lau for his valuable advice and patience throughout the course of my study. His guidance, encouragement and devoted attitude in research have made my study a truly rewarding experience.

Thanks are also expressed to Prof. Z. Y. Lin and his research group in the Department of Chemistry, The Hong Kong University of Science and Technology, for their support on the study of mechanism via theoretical calculations.

I would like to thank my postgraduate colleagues and the undergraduate students in Prof. Lau's research group, Dr. W. K. Fung, Mr. T. C. Chan, Mr. D. X. Wang, Mr. C. W. Leung, Dr. Z. C. Li, Mr. P. H. Leung, Mr. P. K. So, Mr. H. W. Cheung and Miss P. C. Shum, all of whom have made my study more pleasant. Special thanks are expressed to Dr. M. L. Man, Mr. S. M. Ng, Dr. K. C. Cheung, Dr. F. Y. Kwong and Dr. S. K. Wo, for their valuable discussion, assistance and encouragement.

I am obliged to the staff and the technical service crew of the Chemical

Technology section of the Department of Applied Biology and Chemical Technology, The Hong Kong Polytechnic University for their assistance throughout my postgraduate study, especially thanks to Miss P. S. Chan, Mr. Y. K. Au, and Mr. W. K. Kwan for their assistance in running the MS and NMR spectra respectively.

I am greatly indebted to my parents, friends and the whole family for their love, support, and forbearance, especially thanks to Mr. Roberto Leung for his understanding, support, and concern while I was engaged in this research project.

Finally, I would like to acknowledge the Research Degree Committee of The Hong Kong Polytechnic University for the award of a studentship, and for a grant supporting my conference presentation in the International Conference on Organometallic Chemistry Directed Towards Organic Synthesis (OMCOS 13) held in Geneva in July, 2005.

Abstract of thesis entitled "CO_2/epoxide coupling reactions and thiirane desulphurization with Ru-Mn bimetallic complex, manganese carbonylates, and PPN salts."

Submitted by Wing-Nga SIT

For the Degree of Master of Philosophy

at The Hong Kong Polytechnic University

in October, 2005.

Abstract

The coupling reactions of carbon dioxide with epoxides to produce five-membered cyclic carbonates were efficiently catalyzed by heterobimetallic complex $[(\eta^5\text{-}C_5H_5)Ru(CO)(\mu\text{-dppm})Mn(CO)_4]$ (**1**) and complex $Li^+[Mn(CO)_4(PPh_3)]^-$ **(2)**. We have studied and compared the reactivity of the two complexes in the coupling reactions. The reactions were carried out under 40 bar of CO_2 at 100 °C and in the absence of solvents and additives. The higher activity of **1** compared to **2** is attributed to the proximity of the metal centers in the former. Two possible reaction pathways for **1-**catalyzed CO_2/epoxide coupling reaction have been proposed. Both routes begin with heterolytic cleavage of the Ru-Mn bond and coordination of an epoxide molecule to the Lewis acidic Ru center. In **route I**, the Lewis basic Mn center activates the CO_2 by forming the metallocarboxylate anion, which then ring-opens the epoxide; ring-closure gives the cyclic carbonate. In **route II**, the nucleophilic Mn center ring-opens the Ru-attached epoxide to afford an alkoxide intermediate; CO_2 insertion into the Ru-O bond, followed by ring-closure yields the product. Density functional calculations at the B3LYP levels were carried out to understand the structural and energetic aspects of the two possible reaction pathways. The results of the calculations indicate that **route II** is favored over **route I**.

We also found that the bimetallic complex $[(\eta^5\text{-}C_5H_5)Ru(CO)(\mu\text{-dppm})Mn(CO)_4]$ (**1**) is active in catalyzing the desulphurization reaction of thiiranes to produce the corresponding olefins. The reactions were conducted at 100°C and dioxane was used as solvent without other additives. The thiiranes were converted to the corresponding olefins with good yields.

Comparing the catalytic reactivities of complex **1** with other complexes $Li^+[Mn(CO)_4(PPh_3)]^-$ **(2)** and $[(\eta^5\text{-}C_5H_5)Ru(CO)(PPh_3)(CH_3CN)]^+[BF_4]^-$ **(3)** in the desulphurization reactions found that **1** showed the highest catalytic activity. We believe that some sort of bimetallic co-operativity in **1** facilities the desulphurization reaction.

The off-the-shelf reagent $[PPN]^+[Cl]^-$ (**4**) and the PPN-manganese carbonylate complexes $[PPN]^+[Mn(CO)_5]^-$ (**5**) and $[PPN]^+[Mn(CO)_4(PPh_3)]^-$ (**6**) were found to be good catalysts for the coupling reactions of CO_2 with neat epoxides, under 5 bar CO_2, at 100°C or lower temperature (80°C) without the use of organic solvents, to afford the corresponding cyclic carbonates in good yields.

The three catalysts were found to show very similar catalytic activity. However, PPN salts with weak nucleophilic anions such as BF_4^- and OTf^- are inactive for the coupling reactions. Two possible mechanisms for the **4-**, **5-** and **6-**catalyzed CO_2/epoxide coupling reactions have been proposed.

Table of Contents

Chapter One

Chapter Two

Chapter Three

Chapter Four

Chapter Five

List of Figures

List of Tables

List of Schemes

Abbreviation

δ	Chemical shift (NMR)
η	Descriptor for hapticity
μ	Decriptor for bridging
L	Generalized ligand, in particular a 2e^- ligand
[M]	Generalized metal fragment with n ligands
ESI-MS	Electro-spray ionization mass spectrometry
FAB-MS	Fast atom bombardment mass spectrometry
IR	Infra-red
NMR	Nuclear magnetic resonance spectroscopy
THF	Tetrahydrofuran
TMS	Tetramethylsilane
MeOH	Methanol
EtOH	Ethanol
CH_3CN	Acetonitrile
Cp	Cyclopentadienyl
PPN	Bis(triphenylphosphine)immium
Ph	Phenyl
PPh_3	Triphenylphosphine
dppm	Bis(diphenylphosphino)methane
dppe	Bis(diphenylphosphino)ethane
OTf	Trifluoromethane sulfonate

BF_4	Tetrafluoroborate
R	Generalized alkyl group
Me	Methyl
Et	Ethyl
^{i}Pr	Isopropyl
Pz	Pyrazolate
Bu	Butyl
nod	nobornadiene
sh	Sharp
br	Broad
vs	Very strong
w	Weak
s	Singlet
d	Doublet
t	Triplet
q	Quartet
m	Multiplet
TS	Transition state

(1)

η^5-$C_5H_5Ru(CO)(\mu$-dppm$)Mn(CO)_4$

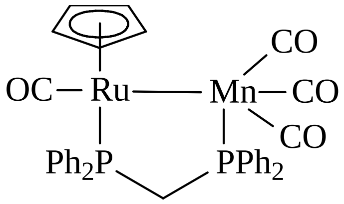

(2) $Li^+[Mn(CO)_4(PPh_3)]^-$

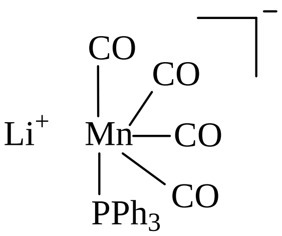

(3)

$[\eta^5$-$C_5H_5Ru(CO)(PPh_3)(CH_3CN)]^+[BF_4]^-$

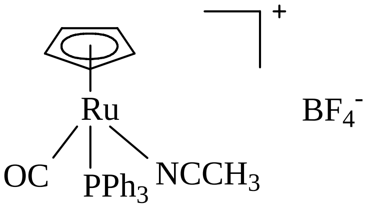

(4) $[PPN]^+[Cl]^-$

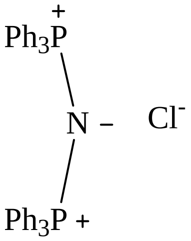

(5) $[PPN]^+[Mn(CO)_5]^-$

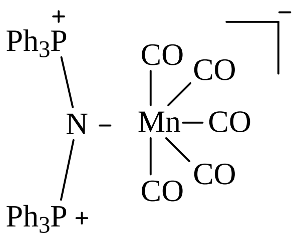

(6) $[PPN]^+[Mn(CO)_4(PPh_3)]^-$

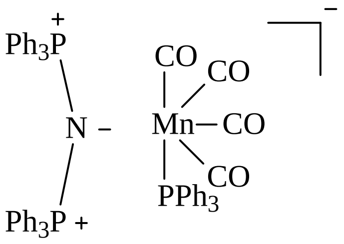

(7) $[PPN]^+[BF_4]^-$

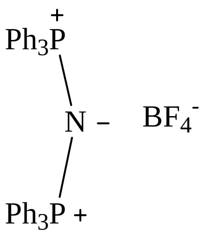

(8) $[PPN]^+[OTf]^-$

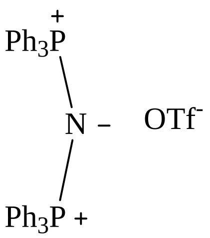

Chapter 1 Introduction

1.1 Bimetallic complexes and synergism

Bimetallic complexes have attracted much attention because it is believed that by having two metal centers in proximity, the reactivity of the individual metal atoms might complement each other, giving rise to the so-called cooperative reactivity. Moreover, these systems have the potential of giving distinct chemistry and are promising candidates for new chemical reactions and catalysis. Heterobimetallic complexes are of particular interest since it is relatively easy in these systems to introduce metal-metal bond polarity, which can provide bifunctional activity and direct selectivity of the substrate-system interaction. Furthermore, heterolytic cleavage of the polar metal-metal bond in the course of reaction might generate a pair of metal nucleophile and electrophile, the former could act as a Lewis base to activate a substrate and the latter as a Lewis acid to activate a second one. The pair might also activate a polar substrate in a cooperative manner.

For bimetallic systems, much research on early-late heterobimetallic complexes, in which direct participation of both metal centers in activating or reacting with organic compounds have been reported. [1-8] Recently, Oro and co-workers have reported that a pyrazolate-bridged diiridium complex containing a bridging hydride catalyzes the hydrogenation of alkynes to alkenes in a new dinuclear mechanistic route. [3] The novelty of this mechanism lies on the fact that two labile positions of the dinuclear species are used for reactant coordination and product release in a cooperative way. The necessary communication between the metal centers is established by hydride migration (**Scheme 1.1**).

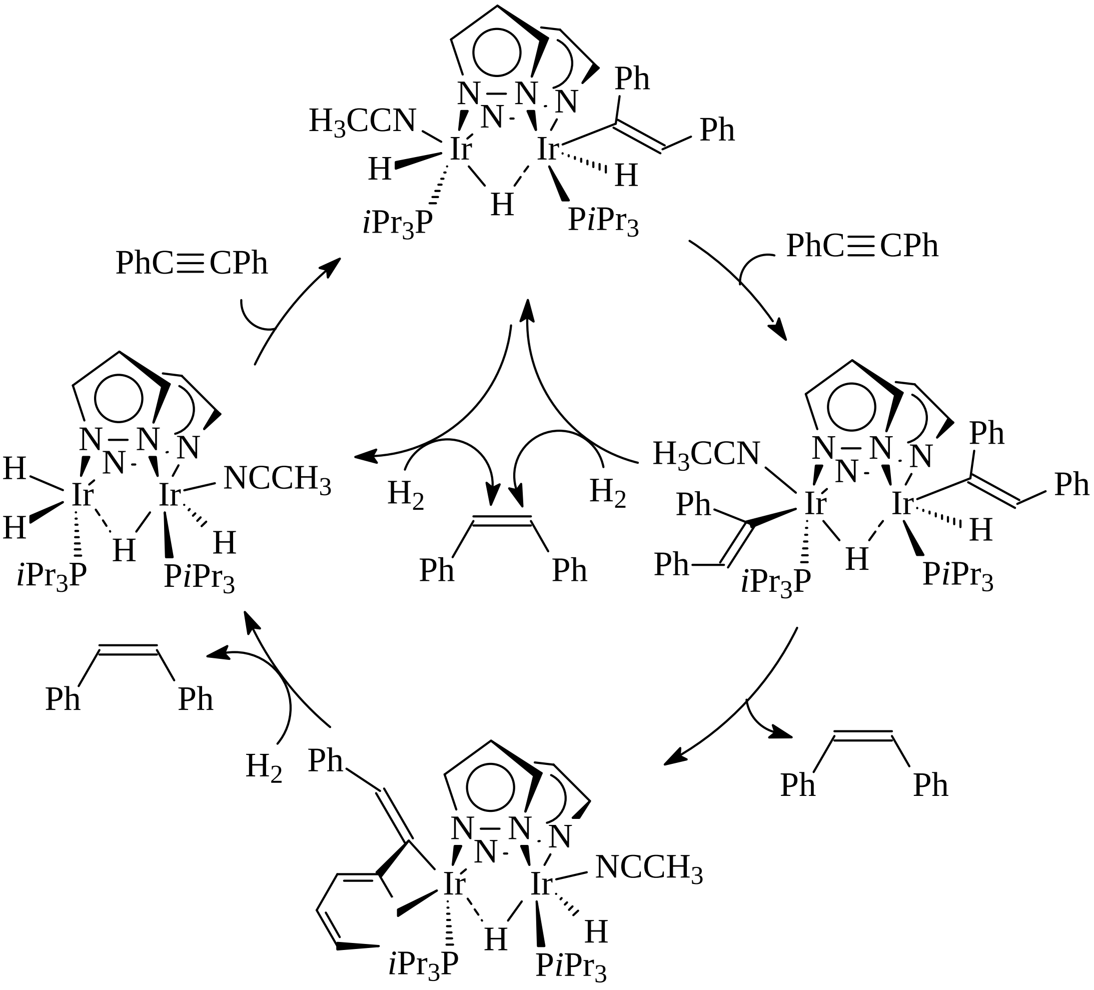

Scheme 1.1: Proposed mechanism for the hydrogenation of diphenylacetylene catalyzed by [Ir_2(μ-H)-(μ-pz)$_2$($NCCH_3$)(P^iPr_3)$_2$]

Stanley *et al*. reported that an electron-rich binucleating tetraphosphine ligand (et,ph-P4 = ($Et_2PCH_2CH_2$)(Ph)PCH_2P(Ph)(CCH_2PEt_2) was used to prepare the homobimetallic rhodium norbornadiene complex [Rh_2(nod)$_2$(et,ph-P4)](BF_4)$_2$. [1] The *racemic* bimetallic Rh complex is a highly active and regioselective catalyst for the hydroformylation of 1-alkenes to give linear aldehydes. A mechanism involving bimetallic cooperativity between the two rhodium centers in the form of an intramolecular hydride transfer is proposed (**Scheme 1.2**).

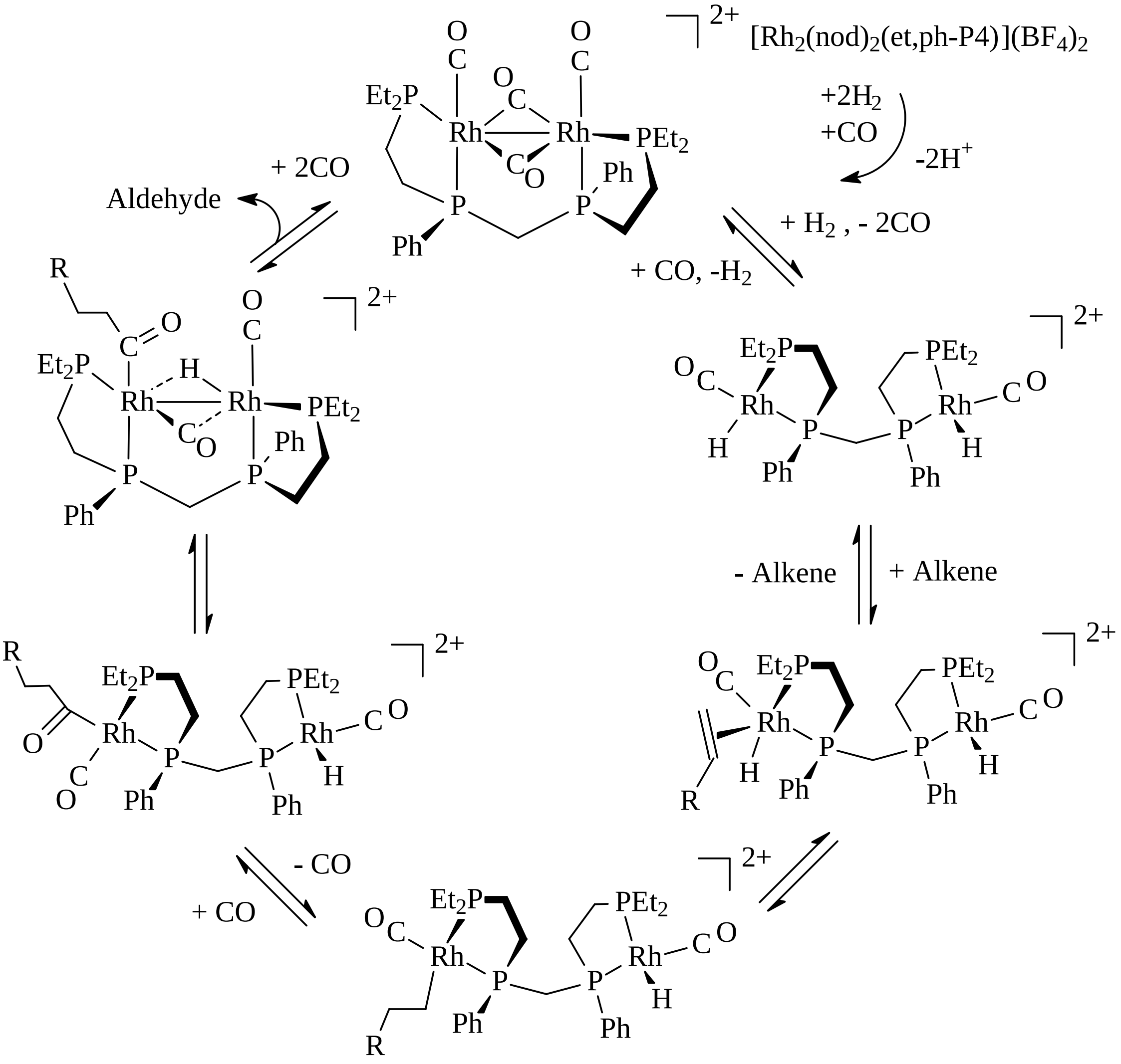

Scheme 1.2: Proposed mechanism for the bimetallic complex $[Rh_2(nod)_2(et,ph\text{-}P_4)](BF_4)_2$-catalyzed hydroformylation

Coates and co-workers recently reported that the [Lewis Acid]$^+$[Co(CO)$_4$]$^-$ bimetallic systems including [Cp$_2$Ti(THF)$_2$][Co(CO)$_4$] and [(salph)Al(THF)$_2$][Co(CO)$_4$] are efficient catalysts for the carbonylation of epoxides and aziridines. [8] They proposed that the carbonylations of both epoxides and aziridines proceed through an unified mechanism involving a backside nucleophilic attack by the [Co(CO)$_4$]$^-$ ion at the least-substituted carbon center (**Scheme 1.3**). The role of the cationic Lewis acid counterpart is to bind and activate the substrate. Insertion of CO followed by ring-closure results in the formation of lactone and lactam as products.

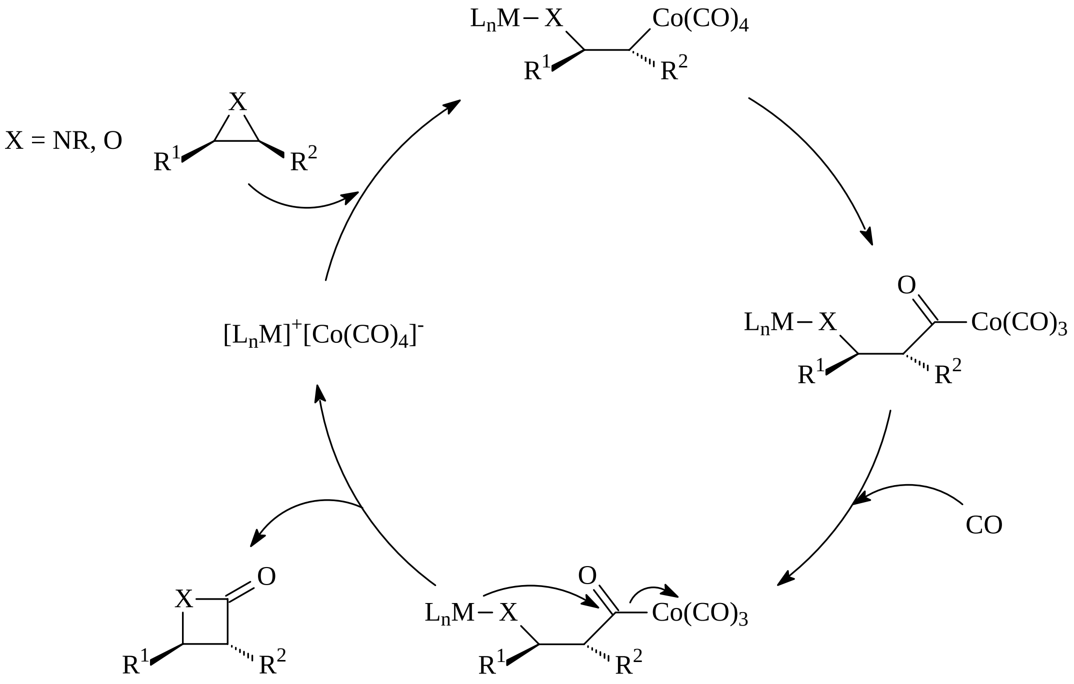

In $[L_nM]^+[Co(CO)_4]^-$ = $[(Cp)_2Ti(THF)_2][Co(CO)_4]$ X = NR, O

In $[L_nM]^+[Co(CO)_4]^-$ = [(salph)Al(THF)2][Co(CO)4] X = O

Scheme 1.3: Proposed mechanism for epoxide and aziridine carbonylation with $[\text{Lewis Acid}]^+[Co(CO)_4]^-$

Jacobsen *et al.* [9] reported that the chiral (salen)Cr^{III} complexes effectively catalyzed the asymmetric ring-opening of epoxides by trimethylsily (TMS) azide. In this reaction, several critical findings were disclosed, including the characterization of the active catalyst, and the identification of the initially-formed intermediate in the ring-opening reaction. They also provided kinetic data to strongly support a mechanism involving activation of both the nucleophile and electrophile in a bimetallic rate-determining step (**Scheme 1.4**)

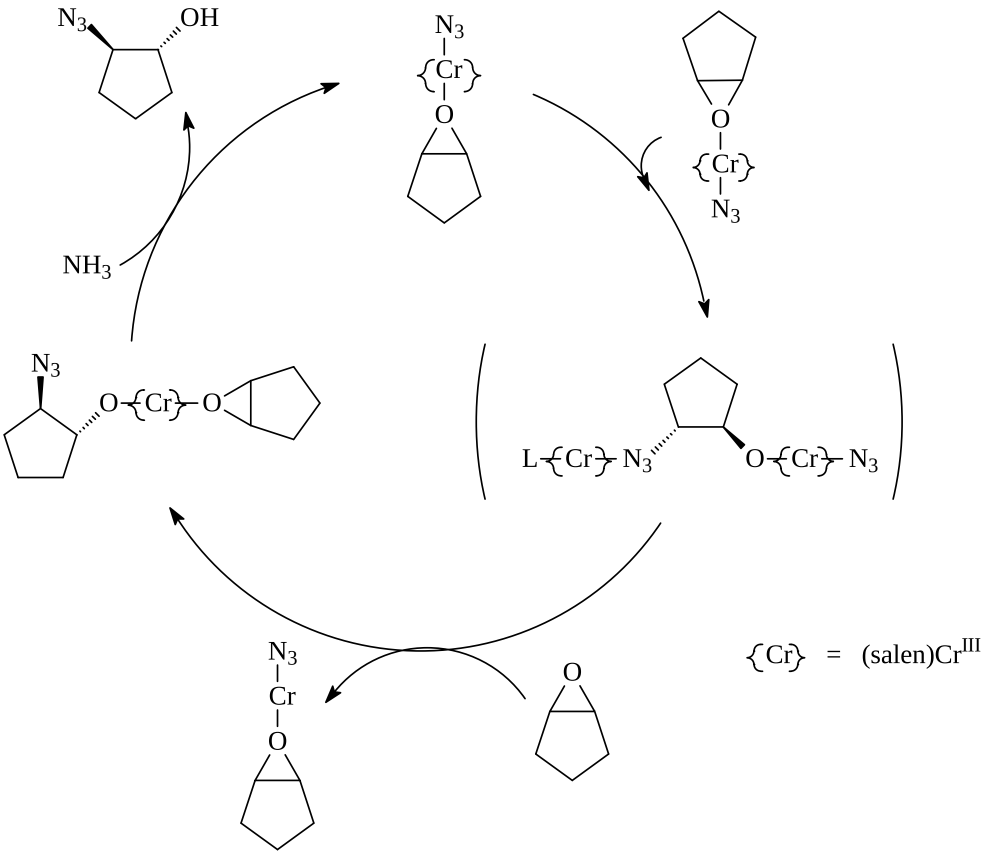

Scheme 1.4: Mechanism for the (salen)Cr^{III} complex-catalyzed ring-opening reaction of epoxide by trimethylsily (TMS) azide

In our research, we utilize our bimetallic systems, which contain polar metal-metal bonds, for the catalysis of CO_2/epoxide coupling reactions. Other catalyst systems such as PPN^+Cl^- and PPN manganese carbonylates have also been studied for their activities in catalyzing the coupling reactions.

1.2 Production of cyclic carbonates by coupling reaction of CO_2 and epoxides

Carbon dioxide is released into the atmosphere when carbon-containing fossil fuels such as oil, natural gas, and coal are burned. It is the largest individual contributor to the ever-growing greenhouse effect, and the amount of CO_2 in the atmosphere has greatly increased over the past century. An efficient way to reduce greenhouse effect is to fix CO_2 to produce harmless chemicals and other useful products. Therefore, the utilization of carbon dioxide as a feedstock for the production of chemical products has attracted much attention owing to its economic and environmental benefits. [10, 11] Currently, there are only a few important large-scale industrial processes that make use of CO_2 in organic synthesis (**Scheme 1.5**), [11-13] including the producting of urea, salicyclic acid, cyclic carbonate, and polycarbonates. [14]

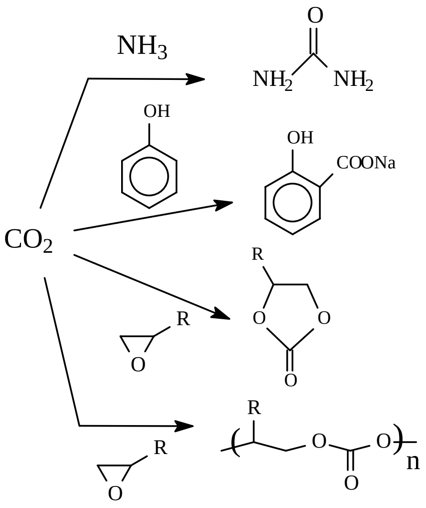

Scheme 1.5: Examples of large-scale production of organic compounds using CO_2 as raw material

In our studies, we have focused on the synthesis of cyclic carbonates from the CO_2/epoxide coupling reaction, which is one of the promising approaches in chemical CO_2 fixation. Cyclic carbonates are valuable as aprotic polar solvents, fine chemical intermediates, and sources for polymer and engineering plastic syntheses. [12] Traditional methods of synthesising cyclic carbonate involved the use of highly toxic materials like phosgene and pyridine. [15] The benefit of the CO_2/epoxide coupling reaction is the elimination of the use of highly toxic materials. Inoue and co-workers first discovered the production of polycarbonates from epoxide and carbon dioxide co-polymerization catalyzed by Et_2Zn/H_2O in 1969. [16] After this discovery, many catalysts were found to enable the coupling reactions of epoxides and carbon dioxide forming only cyclic carbonates (**eq 1.1**), whereas many other catalysts lead to the formation of both polymers and cyclic carbonates. Some previous reports on the synthesis of cyclic carbonates from CO_2 and epoxides suggest that parallel Lewis-base-activation of CO_2 and Lewis-acid-activation of epoxides are important for the success of the reaction. [17-22]

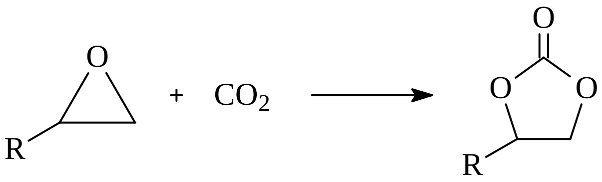

(1.1)

Of the catalysts used for producing cyclic carbonates, some of them are simple alkali metal salts. For example, Endo and co-worker demonstrated the catalytic activity of various alkali metal salts, including lithium halide salts and sodium halide salts in the epoxide/CO_2 coupling reaction using 2,3-epoxypropyl phenyl ether as model substrate. [19] They proposed a mechanism for the reaction in which CO_2 can be easily introduced into the organic molecules under one atmosphere of CO_2 (**Scheme 1.6**). In path I of Scheme 1.6, the alkali metal cations behave as Lewis acids to activate the epoxide; the halide ion acts as Lewis base to ring-open the epoxide because of its appropriate nucleophilicity. In path II, the halide ion activates the CO_2 as the first step, then ring-open the epoxide to afford the cyclic carbonate.

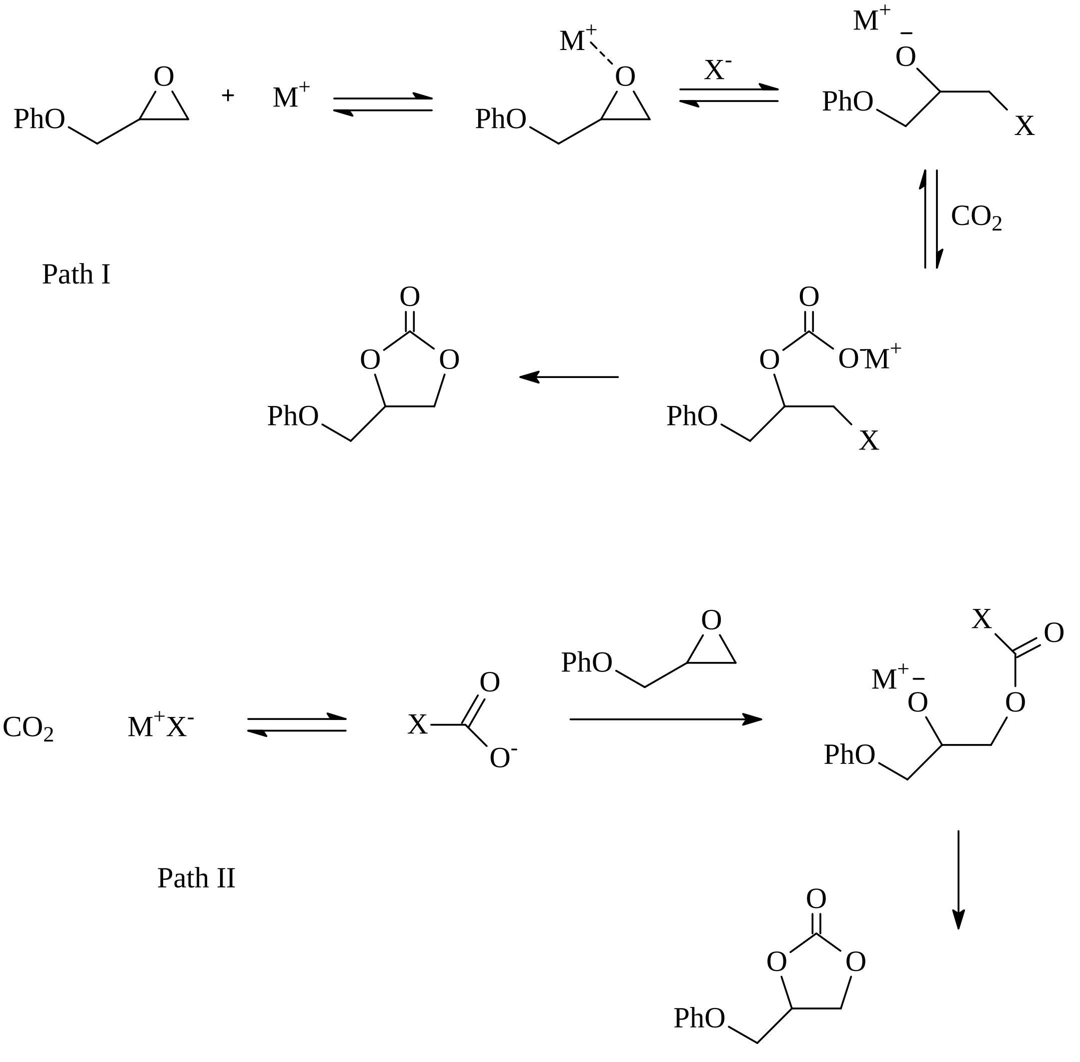

Scheme 1.6: Mechanism of epoxide/CO_2 coupling reaction catalyzed by alkali metal salts

Apart from the above simple alkali salts, metal oxide-catalyzed epoxide/CO_2 coupling reactions have also been reported. In 1997, Yoshihara and co-workers reported the use of magnesium oxide to catalyze the cycloaddition of carbon dioxide to epoxides under mild conditions with retention of stereochemistry. [20] They proposed a mechanism showing that magnesium oxide could control the stereochemistry of the reaction (**Scheme 1.7**). Carbon dioxide is attached to the oxygen and the epoxide is activated by the Mg cation of MgO and then the carboxylate anion attacks the β-carbon atom of the epoxide to generate the oxy anion, which subsequently attacks the carbonate group to afford the cyclic carbonate.

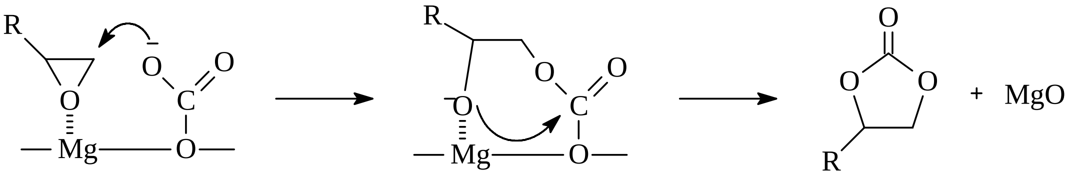

Scheme 1.7: Mechanism of magnesium oxide catalyzes cycloaddition of carbon dioxide to epoxides

Kaneda and co-workers reported that the Mg-Al mixed oxides are effective catalysts for the fixation of CO_2 to various epoxides to form the corresponding five-membered cyclic carbonates. [21] They proposed a mechanism for the addition reaction as shown in **Scheme 1.8**. It is initiated by the attachment of the CO_2 molecule to the Lewis basic site to form a carbonate species, and independently, an epoxide is coordinated to the neighboring acid site on the metal surface. The coordinated epoxide is ring-opened by nucleophilic attack of the carbonate species, leading to an oxy anionic species; finally ring-closure yields the corresponding cyclic carbonate as product.

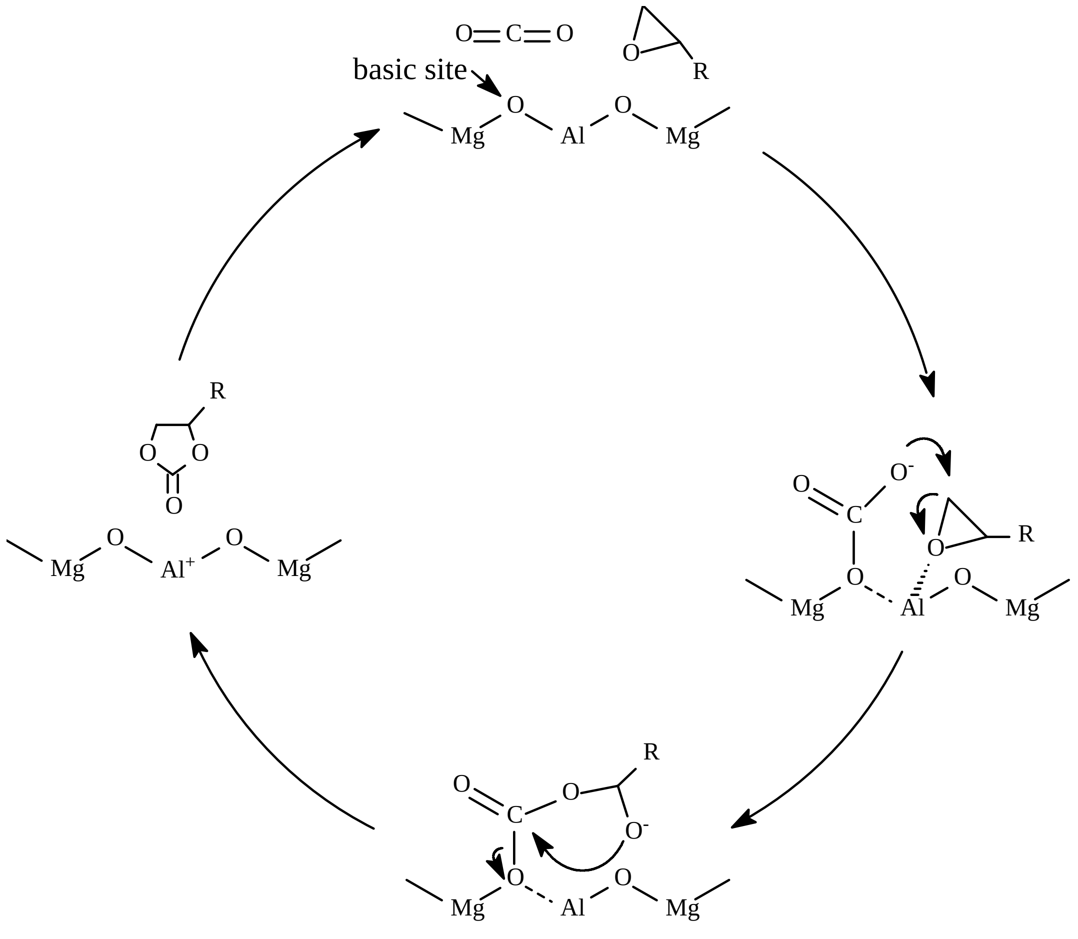

Scheme 1.8: Mechanism of coupling of epoxides and CO_2 catalyzed by Mg-Al mixed oxides

Apart from the above catalytic systems, metal complexes of Cu [23], Ni [24], Pd [25], Zn, [26], Cr [27, 28], and even Al [29, 30] had been proved to be capable of catalyzing the CO_2/epoxide coupling reactions. For example, Dellar and co-workers found that chromium (III) tetra-*p*-tolylporphyrinate (CrTTPCl) or chromium (IV) tetra-*p*-tolylporphyrinate (CrTTPO) in concert with an amine cocatalyst, promotes the formation of the dioxalanones or cyclic carbonates from carbon dioxide and epoxides. [27] Recently, Nguyen et al. [28] reported a similar chromium salen catalyst for the coupling reaction. In this case, the authors proposed a mechanism as shown in **Scheme 1.9**. The DMAP co-catalyst is necessary for coordination to the (salen)-Cr(III) complex. It donates electron to the Cr center forming the (salen)-Cr(III)·DMAP, in which the Cr(III) center is rendered more electron-rich to activate CO_2 by forming the metallo-carboxylate; on the other hand, the epoxide is activated by the (salen)CrCl complex towards ring-opening by the carboxylate.

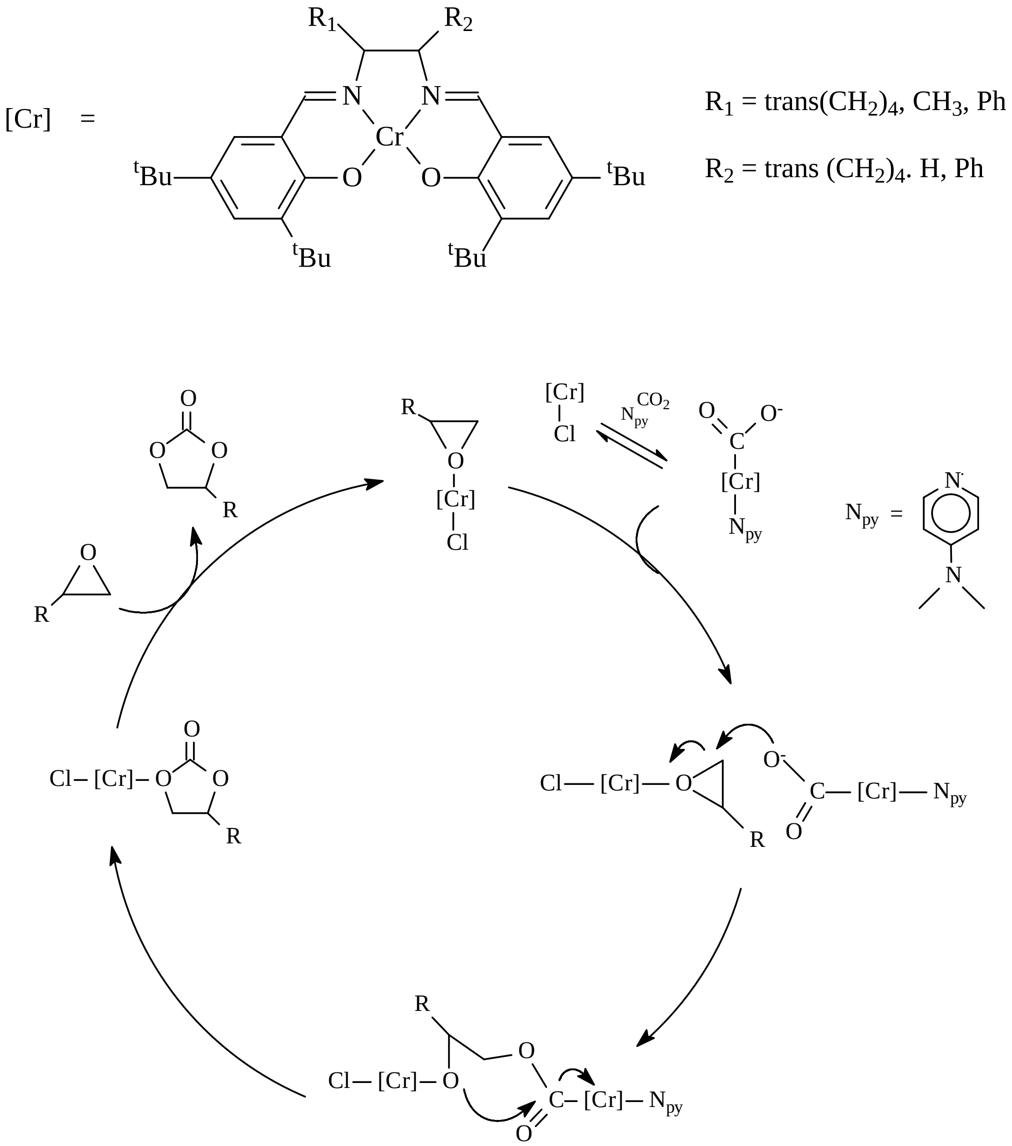

R_1 = trans$(CH_2)_4$, CH_3, Ph

R_2 = trans $(CH_2)_4$. H, Ph

Scheme 1.9: Proposed mechanism of the coupling reaction of epoxide and CO_2 catalyzed by (salen)CrCl

Fanizzi *et al.* [31] discovered a straightforward method for chemical fixation of CO_2 onto epoxides by simply dissolving epoxide in molten tetrabutylammonium salts bearing halides as counterions and stirring the solution under atmospheric pressure of carbon dioxide. A plausible mechanism for this reaction proposed by the authors consists of ring-opening of the epoxide through a nucleophilic attack by the bromide ion, subsequent CO_2 inserting and ring-closure to produce the cyclic carbonate (**Scheme 1.10**).

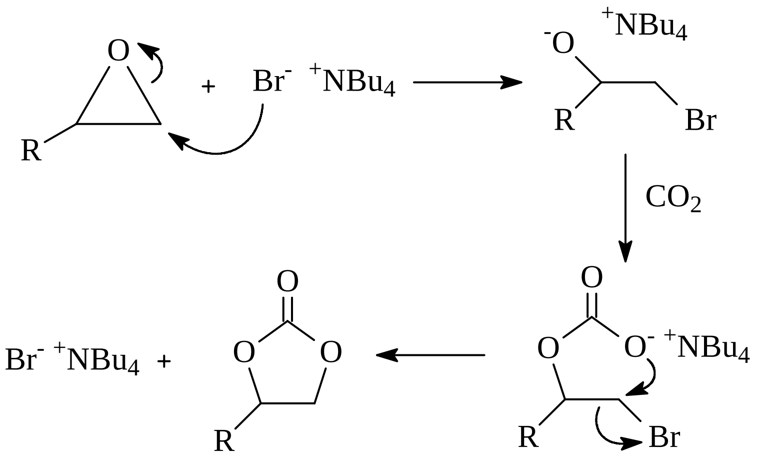

Scheme 1.10: Proposed mechanism for the coupling reaction of epoxide and CO_2 catalyzed by TBAB

Other catalytic systems have also been reported, including those that involve the application of electrochemical methods [32, 33], assistance of microwave [24], the use of supercritical CO_2 [34, 35], and the use of ionic liquids. [31, 36, 37]

Ikushima and co-workers [35] discovered that the synthesis of propylene carbonate from propylene oxide and carbon dioxide is achievable under supercritical conditions in the presence of an ionic liquid (**Figure 1.1**). For example, using 1-octyl-3-methylimidazolium tetrafluoroborate (IL) as solvent, the epoxide/CO_2 coupling reaction could achieve nearly 100% yield and 100% selectivity within 5 minutes. The high catalysis rate might be due to an increase of the solubilities of CO_2 and epoxide in the ionic liquid phase with long alkyl chain.

Ionic Liquid =
[Cn-mim][X]

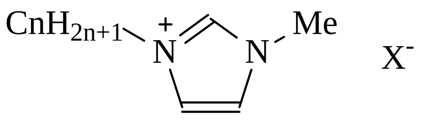

n = 1 to 8
X = BF_4, OTf, PF_6, NO_3

Figure 1.1: Structure of the ionic liquids for the $scCO_2$-ionic liquid reaction systems

1.3 Desulphurization reaction of thiiranes

In addition to the CO_2/epoxide coupling reactions, we also studied the coupling reaction of CO_2 with thiirane, which is the sulphur analogue of epoxide (**Figure 1.2**). The coupling reactions of thiiranes and CO_2, however, were not successful. Interestingly, we discovered that our catalyst systems are able to catalyze the desulphurization of thiiranes.

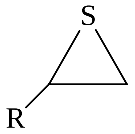

Fig 1.2: Thiiranes (the sulfur analogues of epoxides)

Thiiranes is a three-membered system with a sulphur heteroatom in the ring. Thiiranes can undergo a variety of reactions including polymerization, dimerization, desulphurization to olefins and reaction with halogens, (**Scheme 1.11**); [38] however, reactivity studies of thiirane are scarce. Thiirane chemistry is a neglected area of research, its ring-opening reactions are, in particular scarcely studied, probably due to the fact that thiirane derivatives are generally unstable, making them difficult to synthesize and handle.

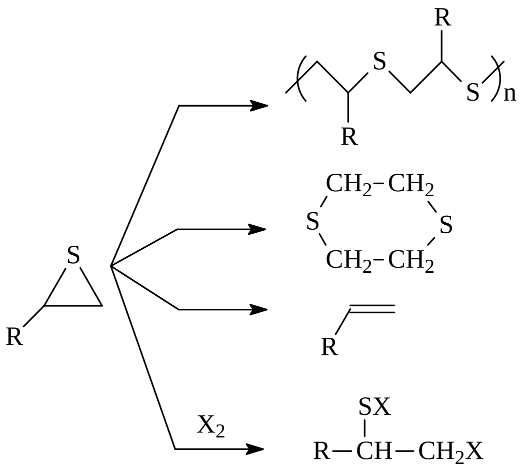

Scheme 1.11: Some reactions of thiiranes

The traditional method to prepare thiiranes is from the cooresponding epoxides, by attack of the latter with an appropriate sulfur nucleophile and subsequent cyclization. In contrast, the conversion of an alkene to the reluctant thiiranes by desulphurization of simple thiirane as sulphur source is yet a scarce transformation and remains a synthetic challenge of timely interest. This metathesis process is sometime efficient enough to convert usually reluctant alkenes (cyclopentene, cycloheptene, norbornene and bicyclopropylidene) to their corresponding episulfides. For example: Kendall and Simpkins reported the rhodium-catalyzed sulfur transfer to norbornene and norbornadiene, using the commercial available propylene sulfide as the sulfur donor (**Scheme 1.12**). [39]

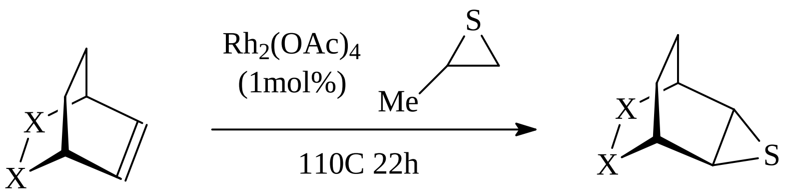

$X-X = H_2C-CH_2,\ HC=CH$

Scheme 1.12: Rhodium-catalyzed sulfur transfer to norbornene and norbornadiene

Desulphurization of thiiranes can occur thermally, [40] photochemically, [41] and chemically. Reagents widely used in this process include trivalent phosphorus compounds, [42] organometallic reagents, tungsten carbonyl complexes, [43-45] iron carbonyl complexes, and cobalt carbonyl complexes. [46]

Jacob *et al*. [42] reported that methyltrioxorhenium (MTO) catalyzes the efficient and stereospecific desulphurization of thiiranes in the presence of triphenylphosphine at room temperature (**eq 1.2**). They proposed that the active catalyst is the Re(V) species, which is formed from $MeReO_3$ and Ph_3P. The Re(V) species adsorbed the sulfur atom of thiirane to produce a Re(VII) sulfide complex, which can easily transfer a sulfur atom to a phosphine to give phosphine sulfide and regenerate the Re(V) species (**Scheme 1.13**).

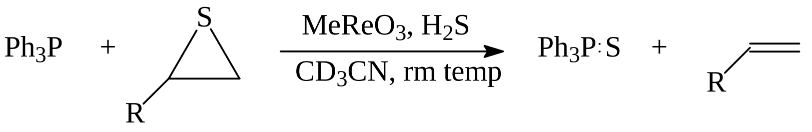

(1.2)

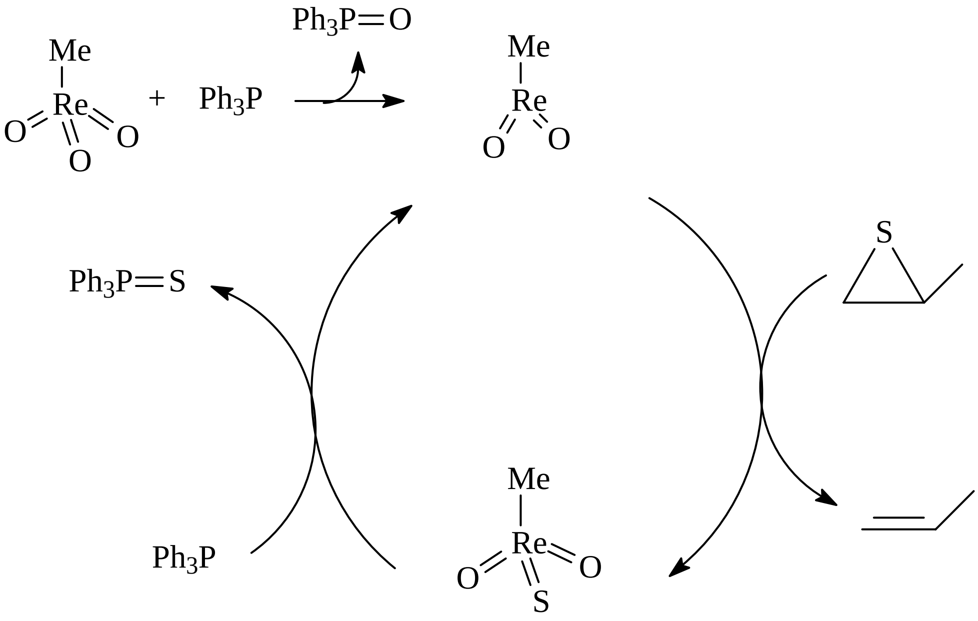

Scheme 1.13: MTO-catalyzed defulphurization of thiiranes

Adams and co-workers [43-45] have discovered that $W(CO)_5(NCCH_3)$ catalyzes the transformation of thiiranes to cyclic polydisulfides and olefins. The reaction of an excess of thiiranes with $W(CO)_5(NCCH_3)$ leads to the formation of the cyclic polydisulfides $(CH_2CH_2SS)_n$, (n= 2-5), (**1-4**) and ethylene catalytically (**Scheme 1.14**). From the reaction, they have been able to isolate the thiirane complex

$W(CO)_5(\overline{SCHRCHR})$. Using X-ray crystallography, they have proven that the thiirane coordinates to the tungsten metal center with pyramidal coordination at the sulphur atom.

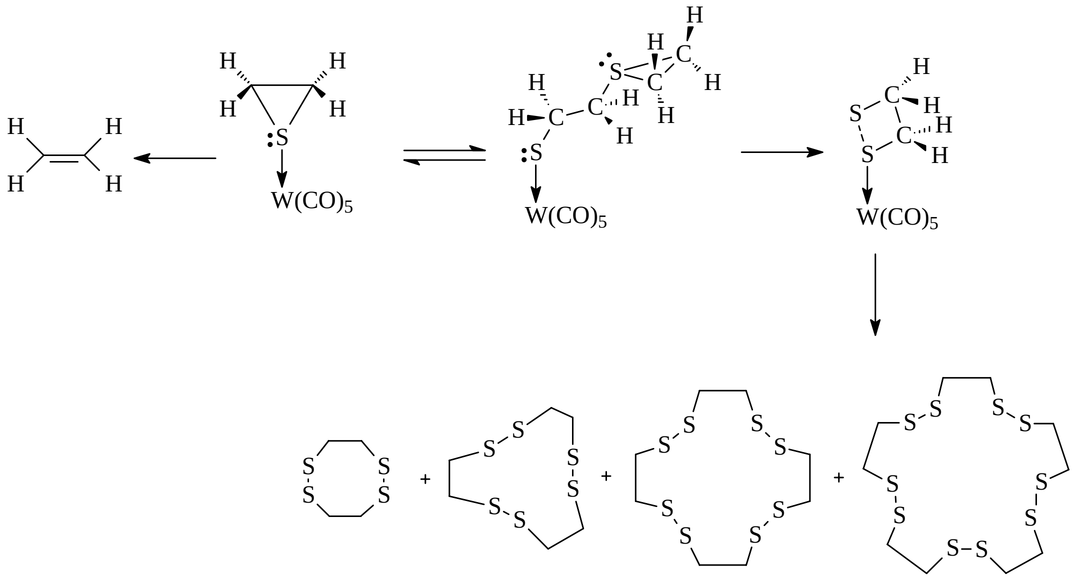

1 2 3 4

Scheme 1.14: Transformation of thiiranes to the cyclic polydisulfides and olefins catalyzed by $W(CO)_5(NCCH_3)$

Recently, Fasi *et al.* [47] studied the transformations of ethylene sulfide at three reaction temperatures 423, 473, and 523K on different acidic molecular sieves (HZSM-5, HY and AIMCM-41) and alumina. The main reaction pathways were found to be desulphurization and cyclo-oligomerisation, the latter being more important. In this reaction, the products are mainly the dimer (1,4-dithiane,), trimer

(1,4,7-trithiacyclononane) and ethylene. The dimer and trimer always predominates (**Scheme 1.15**).

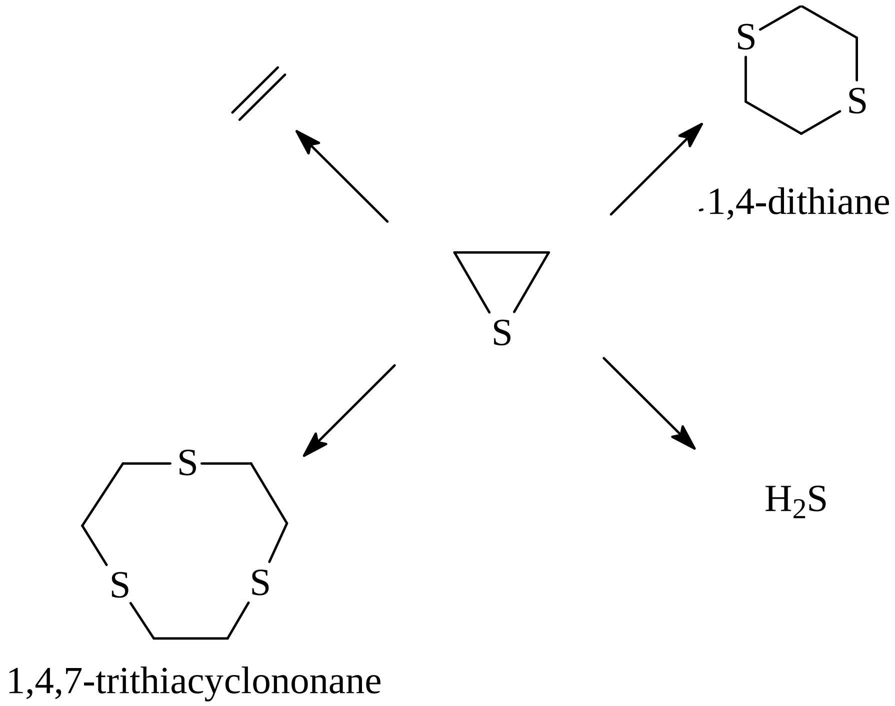

Scheme 1.15: Transformation pathways for the ring opening of thiiranes on solid acids

Komiya and co-worker [48] have found a highly regio- and stereocontrolled ring-opening reaction of thiiranes with organoplatium-manganese (or rhenium) complexes (dppe)RPtM$(CO)_5$ (M = Mn or Re), (R = Me or Et) giving new heterodinuclear complexes (dppe)RPt$SC_1R_2RCH_2M(CO)_5$ or *anti*- and *syn*-(dppe)RPt$\overline{\text{SCMeHCMeHCOMn}}(CO)_4$, from which steroselective desulfurization occurs to afford olefin and the sulfide-bridged Pt-S-M complexes (**Scheme 1.16**).

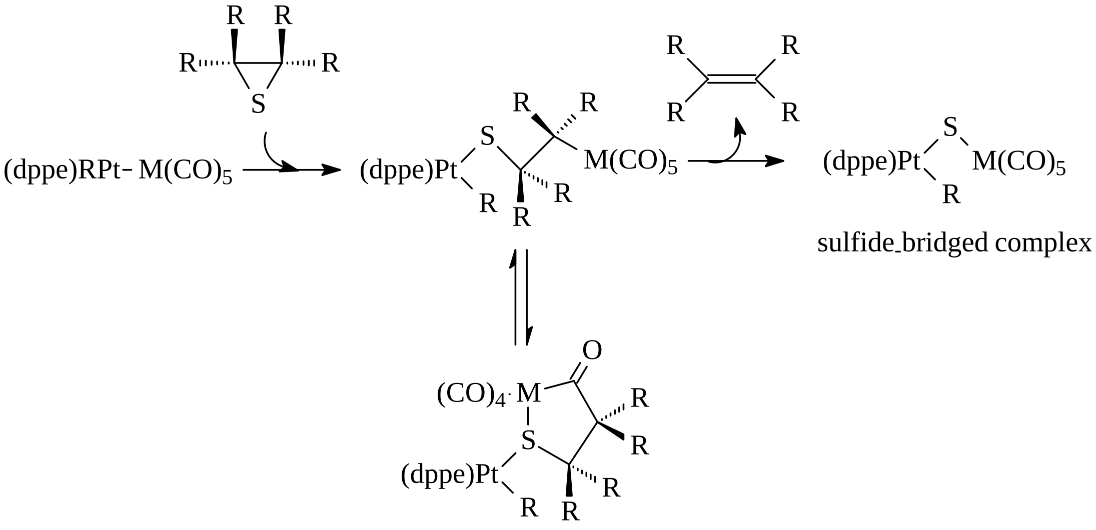

Scheme 1.16: Desulfurization of thiirane by the platinum-manganese(rhenium) complexes to afford olefin and the Pt-S-M complexes

Chapter 2 Heterobimetallic complex $[(\eta^5\text{-}C_5H_5)Ru(CO)(\mu\text{-dppm})Mn(CO)_4]$, and $Li^+[Mn(CO)_4(PPh_3)]^-$ catalyzed coupling reactions of CO_2 with neat epoxides

2.1 Introduction

Our research group has previously synthesized the heterobimetallic complex $(\eta^5\text{-}C_5H_5)Ru(CO)(\mu\text{-dppm})Mn(CO)_4$ (**1**), in which the two metal centers exhibit different electronic properties. Proximity of the metal centers in the heterobimetallic complex **1** offers the possibility of cooperative reactivity.

It has been proposed that the Lewis base activation of CO_2 and Lewis acid activation of epoxides are important for the coupling reaction of the two substrates to form cyclic carbonate. [17, 20, 21, 28] For example, it has been proposed that in the Cr^{III}salen complex/(4-dimethylamino)pyridine (DMAP)-catalyzed CO_2/epoxide coupling reaction, Cr^{III}salen complex acts as a Lewis acid to activate the epoxide; the Cr^{III}salen·DMAP complex, in which the Cr^{III} center is rendered more electron-rich by the coordination of the DMAP molecule, activates the CO_2 by forming a metallocarboxylate intermediate. [28] It is also likely that the catalytic activity of the

Mg-Al mixed oxides in the coupling of carbon dioxide with epoxides originates from the cooperative action of both the neighboring basic and acidic sites on the surface. [21]

Jacobsen and co-workers reported that the chiral (salen)Cr^{III} complexes catalyze the ring-opening of epoxides by trimethylsilyl (TMS) azide. In this reaction, they disclosed several findings, including the characterization of the active catalyst, the identification of the initially formed intermediate in the ring-opening reaction, and kinetic and structural evidence that this transformation proceeds by catalyst activation of both the nucleophile and electrophile centers of a substrate in a bimetallic enantioselectivity-determining step. They proposed a mechanism showing activation of both the oxygen atom and the β-carbon of the epoxide in the bimetallic rate-determining step (**Scheme 2.1**). Their results have been elucidated and reveal an important design principle for bimetallic system capable of activation of both the electron rich and deficiency centers in a substrate. [9]

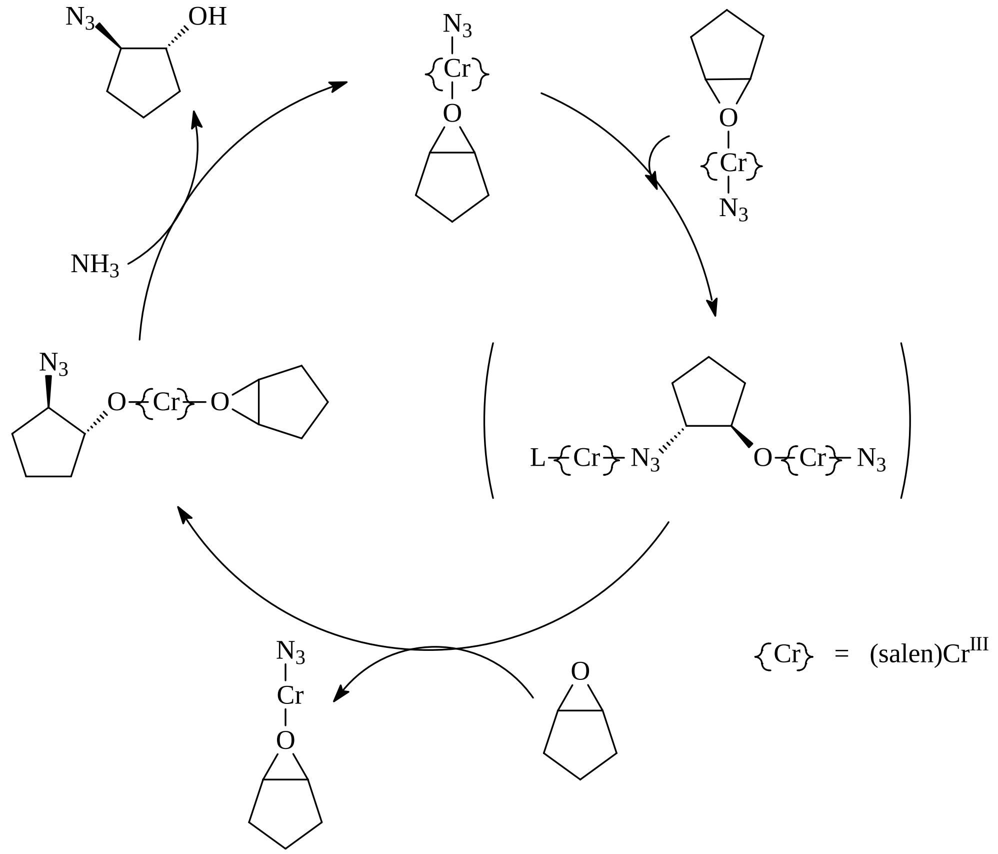

Scheme 2.1: Mechanism of the (salen)Cr^{III} complexes catalyzed ring-opening of epoxides

In this chapter, we report our work on the study and the comparison of the activities of the bimetallic complex **1** and $Li^+[Mn(CO)_4(PPh_3)]^-$ (**2**) in the catalytic coupling reactions of epoxides with CO_2 to yield the cyclic carbonates.

2.2 Experimental

2.2.1 Reagents

The preparative reactions were carried out under a dry N_2 atmosphere using Schlenk. All solvents were distilled and degassed prior to use. Dichloromethane was distilled from calcium hydride. Tetrahydrofuran, diethyl ether, toluene and hexane were distilled from sodium-benzophenone ketyl. Methanol and ethanol were distilled from magnesium and iodine.

The compounds $Mn_2(CO)_{10}$ and $RuCl_3{\cdot}3H_2O$ were purchased from Strem. $Li(C_2H_5)_3BH$ was purchased from Aldrich. The complexes $Mn_2(CO)_8(PPh_3)_2$, [49] $Li^+[Mn(CO)_5]^-$ [50] and (η^5-C_5H_5)Ru(dppm)Cl [51, 52] were synthesized according to methods described in literature.

Epifluorohydrin, epichlorohydrin, styrene oxide, cyclohexene oxide, isobutylene oxide and 1,2-epoxyhexane were purchased from Acros. All substrates were used as received.

2.2.2 Instrumentation

Infrared spectra were obtained from a Bruker Vector 22 FT-IR spectrophotometer. ^{1}H NMR spectra were obtained from a Bruker DPX 400 spectrometer at 400.13 MHz. Chemical shifts (δ, ppm) were measured relative to the proton residue of the deuterated solvent ($CDCl_3$ δ 7.26 ppm, C_6D_6 δ 7.40 ppm.) $^{31}P\{^{1}H\}$ NMR spectra were taken on a Bruker DPX-400 spectrometer at 161.98 MHz. $^{31}P\{^{1}H\}$ NMR chemical shifts were externally referenced to 85% H_3PO_4 in D_2O (δ 0.0 ppm). Electrospray Ionization Mass Spectrometry was carried out with a Finnigan MAT 95S mass spectrometer by first dissolving the sample in CH_2Cl_2/MeOH. Elemental analyses were performed by M-H-W Laboratories, Pheonix, AZ, USA.

2.2.3 Substrates used for the CO_2/epoxide coupling reactions.

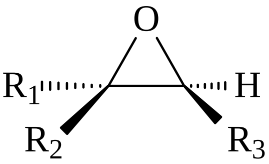

	R_1	R_2	R_3
Epifluorohydrin	CH_2F	H	H
Epichlorohydrin	CH_2Cl	H	H
Epibromohydrin	CH_2Br	H	H
Propylene oxide	CH_3	H	H
Styrene oxide	Ph	H	H
Butadiene monoxide	$CH=CH_2$	H	H
1,2-epoxyhexane	$CH_2CH_2CH_2CH_3$	H	H
Cyclohexene oxide	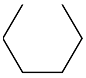		H
Isobutylene oxide	CH_3	CH_3	H

2.2.4 General procedures of preparation of complexes

Preparation of (η^5-C_5H_5)RuCO(μ-dppm)Mn$(CO)_4$ (1)

A THF (10mL) solution of LiMn$(CO)_5$ (0.060g, 29.5 mmol) was transferred with a cannular to a Schlenk flask equipped with a condenser and loaded with (η^5-C_5H_5)Ru(dppm)Cl (0.173g, 29.5 mmol). The solution was then heated at reflux for 16h. After cooling the solution to room temperature, the solvent was removed under vacuum to obtain a crude orange solid. The solid was extracted with toluene (8mL) and the extract was filtered through celite. The solvent of the filtrate was removed under vacuum, and the residue was washed with diethyl ether (1mL x 2) and hexane (2mL x 2), and dried under vacuum for 6h. Yield 0.22g (80%). Anal. Calcd for $C_{35}H_{27}O_5P_2RuMn$: C 56.39; H 3.65. Found: C 56.29; H 3.61. IR (KBr, cm^{-1}): υ(C≡O) 1710 (m), υ(C≡O) 1896 (s), υ(C≡O) 1938 (s), υ(C≡O) 2000 (s). ^{1}H-NMR (C_6D_6, 400.13 MHz, 25°C): δ 7.72-7.13 (m, phenyl protons of dppm), 5.02 (s, 5H of Cp ring), 2.90 (t, 2H of P-CH_2-P, J(HP) = 9.91Hz). ^{31}P{^{1}H}-NMR (C_6D_6, 161.98 MHz, 25°C): δ 54.9 [d, J(PP) = 91.16Hz], 56.5 [d, J(PP) = 91.16Hz]. ESI-MS (CH_2Cl_2-MeOH) *m/z*: 746 $[M]^+$

Preparation of $Li^+[Mn(CO)_4(PPh_3)]^-$ (2)

A sample of $Mn_2(CO)_8(PPh_3)_2$ (0.15g, 0.17 mmol) was dissolved in THF (10mL) in a 50mL Schlenk flask. To the solution, which was cooled to 0°C, excess $Li(C_2H_5)_3BH$ (0.1M solution in THF, 0.44mL, 0.44 mmol, 2.5 equiv) was added slowly using a needle and a syringe in a duration of 20 mins. The solution was allowed to stir for 2.5h, during which the temperature of the reaction mixture gradually increased to room temperature. The solvent was then removed under vacuum to afford a crude yellow solid, which was washed with diethyl ether (3mL x 2). The residue was then extracted with toluene (5mL). The solvent of the extract was removed under vacuum to yield a yellow solid; it was washed with hexane (5mL x 2) and dried in vacuo. Yield 0.10g (74%). IR (KBr, cm^{-1}): $\upsilon(C{\equiv}O)$ 1910 (s), 1932 (s) and 1950 (s), 1976 (s). ^1H NMR (400.13 MHz, THF-d_8, 25°C): δ 7.84 – 7.44 (m, H's of PPh_3). $^{31}P\{^1H\}$ NMR (161.98 MHz, THF-d_8, 25°C): δ 74.7 (s).

2.2.5 General Procedures

Coupling reaction of CO_2 with epoxide:

A typical experimental procedure for the carboxylation of epoxide with carbon dioxide is as follow: The catalyst (η^5-C_5H_5)Ru(CO)(μ-dppm)Mn$(CO)_4$ (0.0026g; 3.5μmol) or $Li^+[Mn(CO)_4(PPh_3)]^-$ (0.0015g; 3.5μmol) was added to the epoxide (~4.0mL; 9000equiv) in a stainless steel autoclave equipped with a magnet stirring bar. The solution was then heated with stirring under 40 bar of CO_2 at 100°C for 45h. The reactor was cooled rapidly in an ice bath and carefully vented. The yield of cyclic carbonate was determined by ^1H NMR spectroscopy. The set of three signals for the two methylene hydrogen atoms and the hydrogen on the substituted carbon of the substrate epoxide is well-separated from the set of three signals for the corresponding hydrogen atoms of the products cyclic carbonate. The yield of the cyclic carbonate can therefore be determined by comparing the sums of integration of these two sets of hydrogen atoms.

2.2.6 Crystallographic analysis for (η^5-C_5H_5)Ru(CO)(μ-dppm)Mn$(CO)_4$ (1)

Crystals of **1** suitable for X-ray diffraction studies was obtained by layering of hexane on CH_2Cl_2 solutions of the complexes. A suitable crystal of **1** was mounted on a Bruker CCD area detector diffractometer using Mo-Kα radiation (λ = 0.71073 Å) from generator operating at 50 kV and 30 mA. The intensity data of **1** was collected in the range of $2\theta = 3$ to 55º, with oscillation frames of φ and ω in the range 0-180º. 1321 Frames were taken in four shells. An empirical absorption correction of the SADABS (Sheldrick, 1996) program based on Fourier coefficient fitting was applied. The crystal structures were determined by the direct method, which yielded the positions of part of the non-hydrogen atoms, and subsequent difference Fourier syntheses were employed to locate all of the remaining non-hydrogen atoms which did not show up in the initial structure. Hydrogen atoms were located based on difference Fourier syntheses connecting geometrical analysis. All non-hydrogen atoms were refined anisotropically with weight function $w = 1/[\sigma^2(F_o^2) + 0.1000p]^2 + 0.0000p$, where $p = (F_o^2 + 2F_c^2)/3$ were refined. Hydrogen atoms were refined with fixed individual displacement parameters. All experiments and computations were performed on a Bruker CCD Area Detector Diffractometer and PC computer with program of Bruker Smart and Bruker SHELXTL packages.

2.2.7 Computational Details

Density functional theory calculations at the Becke3LYP (B3LYP) level [34] have been used to perform the geometry optimizations for all reactants, intermediates and transition states. Frequency calculations at the same level of theory have also been performed to identify all stationary points as minima (zero imaginary frequency) or transition states (one imaginary frequency). Calculations of intrinsic reaction coordinates (IRC) [53, 54] were also performed on transition states to confirm that such structures are indeed connecting two minima. The effective core potentials (ECPs) of Hay and Wadt with double-ζ valence basis set (LanL2DZ) [55-57] were used to describe Ru, Mn and P atoms. For all the other atoms, the standard 6-31G basis set [58, 59] was used. Polarization functions have been added for the Ru (ζ_f(Ru) = 1.235), Mn (ζ_f(Mn) = 2.195) and P (ζ_d(P) = 0.340). All calculations were performed with the use of the Gaussian 03 software package on PC Pentium IV computers.

2.3 Results and Discussion

2.3.3 Synthesis and Characterization of complex 1 and 2

The complex (η^5-C_5H_5)Ru(CO)(μ-dppm)Mn$(CO)_4$ **(1)** was synthesized by the typical metathetical method, via the reaction of (η^5-C_5H_5)Ru(dppm)Cl with LiMn$(CO)_5$ (**eq 2.1**). Refluxing a mixture of these two species in THF for 24h, the bimetallic complex **1** is obtained is 80% yield.

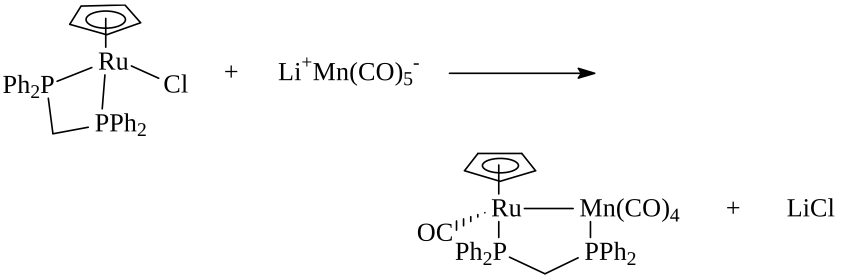

(2.1)

The $^{31}P\{^1H\}$ NMR spectrum of **1** shows a pair of doublets at δ 54.9 and 56.6 ppm (^2J(PP) = 91.2 Hz). The methylene protons of dppm are equivalent by coincidence, they appear as a triplet at δ 2.90 ppm (J(HP) = 9.91 Hz) in the ^1H NMR spectrum. Complex **1** shows three carbonyl peaks at 251.7 (m), 246.7 (s), and 225.9 (d, ^2J(PC) = 6.1 Hz) ppm in the ^{13}C NMR spectrum. The downfield multiplet probably results from overlapping signals. The carbonyl ligands in the complex probably do not scramble since their signals are sharp at room temperature. KBr IR spectrum of the complex shows, in addition to the bands at 1896, 1938, and 2000 cm^{-1} due to terminal carbonyl groups, a relatively low energy CO stretching frequency at 1710 cm^{-1}. The presence of the low CO stretching frequency indicates that a bridging or semi-bridging carbonyl group is present in the bimetallic complex.

The lithium salt $Li^+Mn(CO)_4(PPh_3)^-$ (**2**) is formed by reacting the dimeric species $[Mn_2(CO)_8(PPh_3)_2]$ with super hydride $[Li(C_2H_5)_3BH]$ in THF for 2.5h. The $^{31}P\{^1H\}$-NMR spectrum of **2** shows a single peak at δ 74.7ppm, it is due to the PPh_3 ligand on the Mn center. KBr IR spectrum of the complex shows four strong peaks that appear at 1910, 1932, 1950, and 1976 cm^{-1} due to the terminal carbonyl groups of Mn.

2.3.2 X-ray structural determination

The metal-metal-bonded bimetallic structure of **1** was confirmed by x-ray crystallographic study. The molecular structure of **1** is shown in **Fig. 2.1**. Crystal data and refinement details are given in **Table 2.1**. Selected bond distances and angles are given in **Table 2.2**. The Ru-Mn bond distance of 2.8524(7) Å in **1** is comparable with the metal-metal bond distances in other Ru-Mn bimetallic complexes containing bridging ligands, for example $[RuMn(\mu\text{-}H)(\mu\text{-}PPh_2)(\eta^5\text{-}C_5H_5)(CO)_5]$ in which the Ru-Mn bond distance is 2.894(1) Å; [60] it is, however, shorter than those of the Ru-Mn bimetallic complexes which have no bridging ligands, such as the α-diimine Ru-Mn bimetallic complex $[(CO)_5Mn\text{-}Ru(Me)(CO)_2(\alpha\text{-diimine})]$ (α-diimine = pyridine-2-carbaldehyde: N-isopropylimine (^{i}Pr-PyCa)), in which the Ru-Mn bond distance was found to be 2.9875(8) Å. [61] It is noticeable that in one of the carbonyl ligands attached to the manganese center, the Mn-C-O angle (Mn(1)-C(10)-O(5) = 167.3(4)°) deviates more from linearity than those of the other CO ligands on Mn. Moreover, the distance of the carbon atom of this less linear carbonyl ligand on Mn from the ruthenium center measures 2.656(4) Å, this relatively short distance is indicative of the presence of weak interaction between this CO and the ruthenium center. In a Zr-Ru bimetallic complex, the zirconium-bound CO, which is slightly bent (Zr-C-O 167°), semi-bridges the ruthenium center, the carbon atom of the bent

CO is 2.70 Å from the ruthenium center.[15] Moreover, in each of our recently reported Ru-M (M = Mo, W) bimetallic complexes, one of the M-bound CO ligands is a semi-bridging carbonyl, the M-C-O angle deviates significantly from linearity, and the distance of the carbon atom of this carbonyl ligand from the ruthenium center falls in the range 2.744 – 2.906 Å. [62]

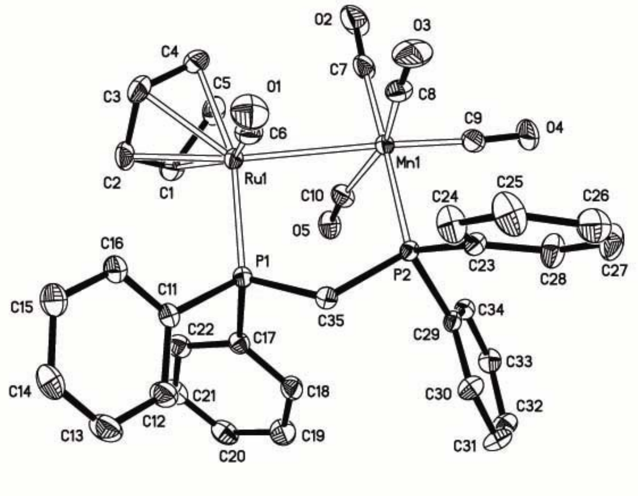

Figure 2.1: X-ray structure of η^5-$C_5H_5Ru(CO)(\mu$-dppm$)Mn(CO)_4$ (1)

Table 2.1: Crystal data and structure refinement for complexes 1

	1
Empirical formula	C35.5H28ClMnO5P2Ru
Formula weight	787.98
Temperature	294(2) K
Wavelength	0.71073 Å
Crystal system	Monoclinic
Space group	P2(1)/c
Unit cell dimensions	a = 18.813(3) Å = 90°
	b = 10.5259(14) Å = 90°
	c = 19.633(3) Å = 90°
Volume	3617.5(11) $Å^3$
Z	4
Density (calculated)	1.429 Mg/m^3
Absorption coefficient	0.955 mm^{-1}
F(000)	1588
Crystal size	0.22 x 0.20 x 0.14 mm^3
Theta range for data collection	2.11 to 27.54°
Index ranges	-23<=h<=24, -13<=k<=13, -25<=l<=10
Reflections collected	24254
Independent reflections	8410 [R(int) = 0.0363]
Completeness to theta = 27.64°	99.6 %
Absorption correction	Empirical
Max. and min. transmission	0.8779 and 0.8174
Refinement method	Full-matrix least-squares on F2
Data / restraints / parameters	8410 / 6 / 417
Goodness-of-fit on F2	1.032
Final R indices [I>2sigma(I)]	R1 = 0.0468, wR2 = 0.129
R indices (all data)	R1 = 0.0742, wR2 = 0.1439
Largest diff. peak and hole	0.858 and -0.436 e $Å^{-3}$

Table 2.2: Selected bond distances (Å) and angles (deg) for $(\eta^5\text{-}C_5H_5)Ru(CO)(dppm)Mn(CO)_4$ (1)

Interatomic distances (Å)

Ru (1) – Mn (1)	2.8524(7)	Ru (1) –P (1)	2.2842(10)
Mn (1) – P (2)	2.2894(11)	Ru (1) – C (6)	1.832(5)
Mn (1) – C (7)	1.801(5)	Mn (1) – C (8)	1.839(5)
Mn (1) – C (9)	1.793(5)	Mn (1) – C (10)	1.832(4)
O (1) – C (6)	1.158(6)	O (2) – C (7)	1.145(5)
O (3) – C (8)	1.130(5)	O (4) – C (9)	1.152(5)
O (5) – C (10)	1.157(5)		

Intramolecular angles (deg)

C (35) – P (1) – Ru (1)	112.32(12)	C (35) – P (2) – Mn (1)	113.75(12)
O (1) – C (6) – Ru (1)	171.7(4)	O (2) – C (7) – Mn (1)	176.0(6)
O (3) – C (8) – Mn (1)	176.3(5)	O (4) – C (9) – Mn (1)	176.1(4)
O (5) – C (10) – Mn (1)	167.3(4)		

2.3.3 Carbon dioxide/epoxide coupling reactions with 1 and 2

We found that the complexes (η^5-C_5H_5)Ru(CO)(μ-dppm)Mn(CO)$_4$ **(1)** and $Li^+[Mn(CO)_4(PPh_3)]^-$ **(2)** are able to catalyze the coupling reactions of epoxides with carbon dioxide (40 bar) to produce the cyclic carbonates at 100°C without any solvent and additives. The epoxides were converted to the corresponding cyclic carbonates with satisfactory yields. **Table 2.3** shows the results of the production of various cyclic carbonates from the **1-** and **2-** catalyzed coupling reactions. The catalytic reactions were carried out in neat epoxides, no CO_2/epoxide copolymer was formed in each of the reactions. After the removal of the product and the unreacted substrate of the catalytic reaction, ^{1}H and ^{31}P{^{1}H} NMR spectroscopy showed that the bimetallic complex was recovered unchanged.

Table 2.3: Catalytic coupling of CO_2 and epoxides catalyzed by 1 and 2[a]

Entry	Substrate	Catalyst	Yield (%)	TON[b]	TOF (h^{-1})[c]
1	Epifluorohydrin	**1**	96	8640	192
2	Epichlorohydrin	**1**	89	8000	178
3	Epibromohydrin	**1**	71	6450	143
4	Propylene oxide	**1**	16.6	1490	33
5[d]	Propylene oxide	**1**	Trace	—	—
6	Butadiene monoxide	**1**	50	2800	62
7	Styrene oxide	**1**	Trace	—	—
8	1,2-epoxyhexane	**1**	5.3	480	11
9	Cyclohexene oxide	**1**	Trace	—	—
10	Isobutylene oxide	**1**	nil	—	—
11	Epifluorohydrin	**2**	78	7020	156
12	Epichlorohydrin	**2**	60	5300	118
13	Epibromohydrin	**2**	48	4200	93
14	Propylene oxide	**2**	5.2	450	10
15	Butadiene monoxide	**2**	20.1	1795	40
16	Styrene oxide	**2**	Trace	—	—
17	1,2-epoxyhexane	**2**	Trace	—	—
18	Cyclohexene oxide	**2**	Trace	—	—
19	Isobutylene oxide	**2**	nil	—	—
20[d]	Propylene oxide	**2**	Trace	—	—
21[e]	Propylene oxide	**2**	Trace	—	—

[a]Typical reaction conditions: Catalyst: 3.5μmol (η^5-C_5H_5)Ru (CO)(μ-dppm)Mn(CO)$_4$ **(1)** and $Li^+[Mn(CO)_4(PPh_3)]^-$ **(2)**, substrates: 31.5mmol (S/C = 9000), CO_2 pressure

40 bar, 100°C, 45h. [b]Turnover numbers were determined by comparing the ratio of product to substrate in the ^{1}H NMR spectrum of an aliquot of the reaction mixture. [c]Moles of cyclic carbonates products per mole of catalyst per hour. [d]7.0μmol of CH_3CN added. [e]7.0μmol of 12-crown-4 added.

It is noteworthy that the presence of electron-withdrawing groups on the epoxides leads to higher conversions (**entries 1-4 Table 2.3**). Failure of styrene oxide and cyclohexene oxide to couple with CO_2 is probably due to steric reasons. We also studied the catalytic activity of the individual metallic moieties of **1** for the CO_2/epoxide coupling reactions. It was found that ruthenium complexes $[(\eta^5\text{-}C_5H_5)Ru(CO)(PPh_3)(CH_3CN)]^+OTf^-$ and $(\eta^5\text{-}C_5H_5)Ru(CO)(PPh_3)(Cl)/Ag^+OTf^-$ were inactive for the reactions.

2.3.4 Proposed mechanism for the catalytic CO_2/expoxide coupling reaction

It has been proposed that coupling of epoxides with carbon dioxide to yield cyclic carbonates probably require activation of both substrates; the former by a Lewis acid and the latter by a Lewis base. [17, 20, 21, 28] **Route I of Scheme 2.2** shows a possible mechanism for the **1**-catalyzed CO_2/epoxide coupling reactions. Heterolytic cleavage of the metal-metal bond generates the electrophilic ruthenium fragment and the nucleophilic manganese moiety. An epoxide molecule then coordinates to the Lewis acidic Ru center. On the other hand, the Lewis basic Mn center activates the carbon dioxide by forming the metallocarboxylate anion. Although not isolated, the manganese carboxylate $[Mn(CO)_4(PPh_3)(CO_2)]^-$ was believed to be the intermediate in the reaction of $K^+[CpFe(CO)(PPh_3)(CO_2)]^-$ with $[Mn(CO)_5(PPh_3)]BF_4$ followed by addition of CH_3I to afford $[CpFe(CO)_2(PPh_3)]BF_4$ and $Mn(CO)_4(PPh_3)(CH_3)$. [63] Nucleophilic ring-opening of the ruthenium-attached epoxide by the manganese carboxylate generates **A**, which then extrudes the cyclic carbonate by ring closure. It is widely accepted that coordination of an expoxide molecule to a Lewis acid facilitates nucleophilic ring opening of the former. [8, 9, 26, 33, 64, 65] The proposed epoxide complex and the ring-opened species in **Route I of Scheme 2.2** are probably transient intermediates because we have not been able to detect any one of these species in a NMR-monitored catalytic CO_2/propylene oxide coupling reaction carried out in a 10 mm sapphire high pressure NMR tube. We have also failed to isolate or detect any epoxide complex in independent studies involving the reactions of $[(\eta^5\text{-}C_5H_5)Ru(PPh_3)(CO)(CH_3CN)]^+$ and $(\eta^5\text{-}C_5H_5)Ru(PPh_3)(CO)(Cl)/Ag^+OTf^-$ with propylene oxide. The fact that addition of small amount of CH_3CN, which is a much better coordinating ligand to Ru than propylene oxide, completely quenches the catalytic reaction (**entry 5, Table 2.3**) lends support to the notion that activation of the epoxide by the electrophilic ruthenium center is crucial to the success of the coupling reaction.

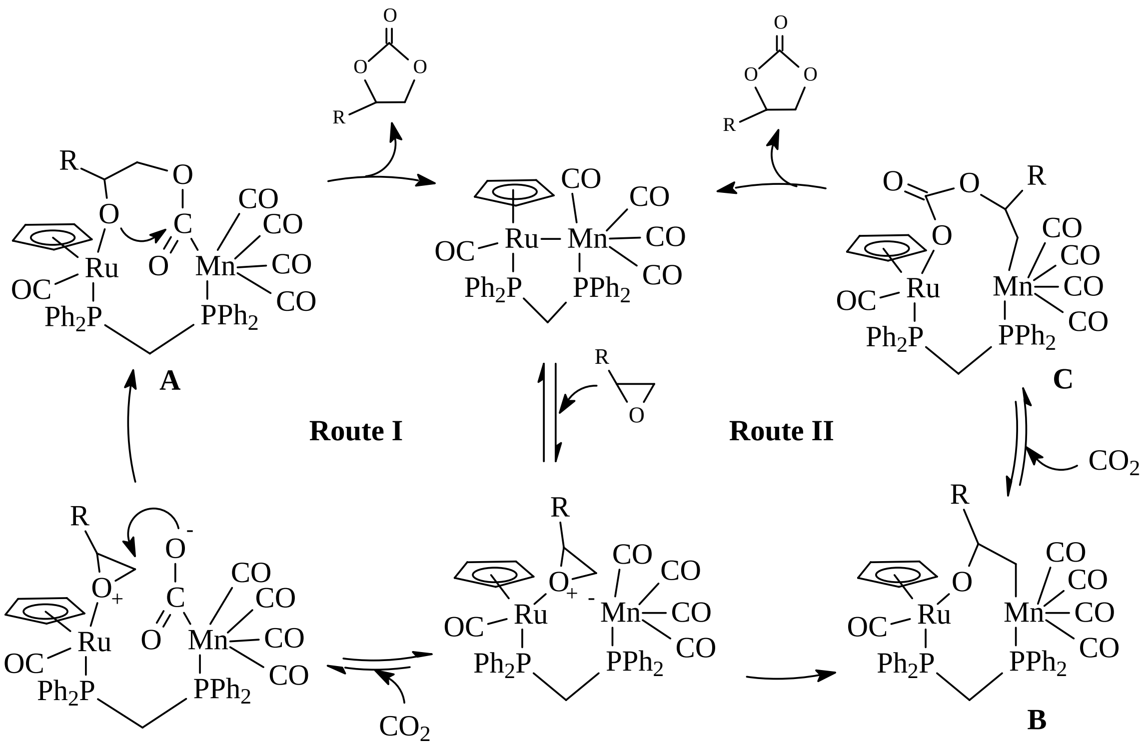

Scheme 2.2: Proposed mechanism for the production of cyclic carbonate catalyzed by 1

An alternative mechanism for the CO_2/epoxide coupling reaction is also proposed (**Route II, Scheme 2.2**). In this proposed mechanism, the manganese fragment, instead of forming the metallocarboxylate with CO_2, ring-opens the epoxide, which is activated via O-coordination to the ruthenium fragment, forming the cyclic alkoxide **B**, CO_2 then inserts into the Ru-O bond forming the cyclic metal carbonate **C**, which then extrudes the cyclic carbonate. Insertion of CO_2 into metal-alkoxide bond to form metal carbonate species is well-documented. [23, 66]

The lithium salt of the manganese tetracarbonylate anion $Li^+[Mn(CO)_4(PPh_3)]^-$ (**2**) was shown to be active catalyst for the coupling reactions, although, in general, its activity is lower than that of **1** (**Table 2.3**). The lithium cation of **2** is probably capable of activating the epoxide by attaching to the oxygen atom of the latter. The reaction pathway of the lithium salt 2-catalyzed coupling reactions is probably similar to those of **1-**catalyzed reactions (**Scheme 2.3**). The lithium cation is acting as electrophilic center in analogy to the ruthenium fragment of **1**. The fact that addition of acetonitrile (**Entry 20, Table 2.3**) or 18-crown-6 (**Entry 21, Table 2.3**), which is able to solvate or encapsulate Li^+, respectively, practically quenches the activity of **2** lends support to this notion. It has been reported that benzo-15-crown-5 acts as deactivator in the sodium halide-catalyzed CO_2/epoxide coupling reactions; the crown ether is a good host for the sodium cation. [19] The proximity of the metal centers in **1** is an advantage over **2**; the two metal centers in the latter are not linked together.

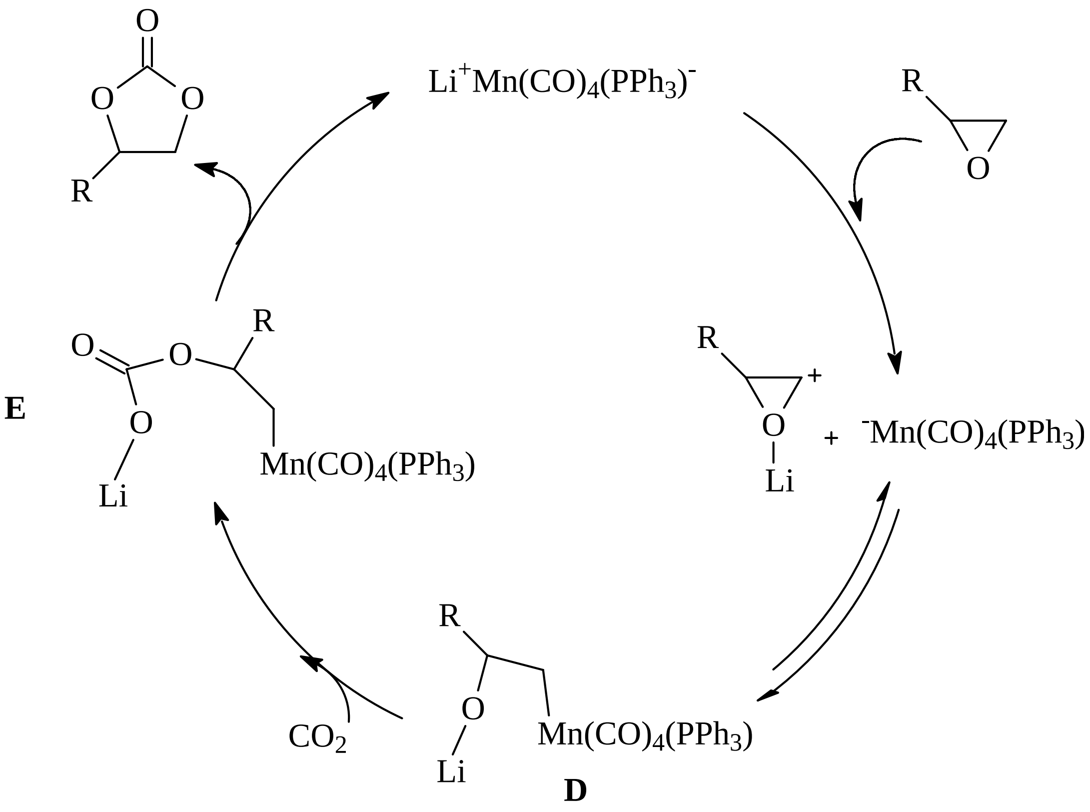

Scheme 2.3: Proposed mechanism for the production of cyclic carbonate catalyzed by 2

2.3.5 Theoretical study (carried out by K. C. Lam of the Department of Chemistry, The Hong Kong University of Science and Technology)

To understand the structural and energetic aspects of the possible reaction pathways proposed above for the carbon dioxide/epoxide coupling reactions catalyzed by Ru-Mn heterobimetallic complexes, theoretical calculations at the B3LYP level of density functional theory were carried out. In our calculations, model catalyst $(\eta^5\text{-}C_5H_5)Ru(CO)(\mu\text{-dppm})Mn(CO)_4$ was used in which the phenyl groups in the dppm ligand were replaced by H atoms. Two proposed reaction pathways (**Routes I and II in Scheme 2.2**) were studied here. For the convenience of our discussion, all calculated structures of intermediates, reactants and transition states are numbered. The transition states are labelled with **TS**.

Coupling reaction of carbon dioxide and ethylene oxide:

Figure 2.2 shows the two possible reaction pathways (**Routes I and II**) for the carbon dioxide/epoxide coupling reaction. In **Figure 2.2**, relative free energies are shown. Taking into account the effect of entropy, we used the free energies rather than the electronic energies for our discussion because two or more molecules are involved in the reactions studied here.

Both **Routes I and II** begin with a bimetallic complex **1**. After heterolytic cleavage of the Ru-Mn bond, an epoxide molecule coordinates to the electrophilic Ru center though the $O_{(epoxide)}$ atom to afford complex **2** via the transition state $\mathbf{TS_{1-2}}$. In **Route I**, carbon dioxide then coordinates to the nucleophilic Mn center through the electrophilic carbon atom to form complex **3**. Ring-opening of epoxide from **3** to **4** takes place via the transition state $\mathbf{TS_{3-4}}$. In this step, one of the two nucleophilic O atoms of carbon dioxide attacks one carbon atom of the coordinated epoxide ring, which behaves as an electrophile, to afford a relatively stable intermediate **4**. Intermediates **4** and **5** are rotational isomers, which differ in the O-C-C-O dihedral angles, being –72.5° and 59.3°, respectively. We were unable to locate the rotational transition states because of the flatness on the potential barriers should be small. From the rotational isomer **5**, ring closure occurs via $\mathbf{TS_{5-6}}$ to give **6** in which the product molecule (cyclic carbonate) coordinate to the Ru metal center. The last step is dissociation of the cyclic carbonate from the Ru center and regeneration of the catalyst via transition state $\mathbf{TS_{6-7}}$.

In **Route II**, after coordination of epoxide to the Ru center to give complex **2**, the nucleophilic Mn center attacks one C atom of the Ru-coordinated epoxide and opens the epoxide ring to afford a stable alkoxide intermediate **8** via transition state $\mathbf{TS_{2-8}}$. Carbon dioxide interacts with the O atom, which bonds to the Ru center to form **9**. Then, carbon dioxide inserts into the Ru-O bond to generate the cyclic metal carbonate **10** via the transition state **TS$_{9\text{-}10}$**. Intermediates **10** and **11** are rotational isomers with different Ru-O-C=O and O=C-O-C dihedral angles. The Ru-O-C=O dihedral angles of **10** and **11** are 139.9° and 13.4°, respectively. And the O=C-O-C dihedral angles of **10** and **11** are –7.2° and –173.4°, repectively. From **11**, ring closure occurs via **TS$_{11\text{-}6}$** to give **6** with a cyclic carbonate (the product molecule) coordinated to the Ru center through the O atom. Finally, dissociation of the cyclic carbonate from **6** and formation of the Ru-Mn bond regenerates the bimetallic catalyst.

Energetic aspects of Routes I and II:

On the basis of the energy profiles shown in **Figure 2.2**, we can see that **Route I** involves two major steps: 1) Coordination of epoxide to the Lewis acidic Ru center with heterolytic breaking of the Ru-Mn bond and metallocarboxylate-nucleophilic ring opening of epoxide. 2) Ring closure from intermediate **5** to yield the product molecule (cyclic carbonate) and regeneration of the catalyst. Coordination of epoxide to the Ru center and formation of the metallocarboxylate **3** occur sequentially in the first major step, leading to a significant decrease in the entropy. The Ru-Mn heterolytic cleavage creates a charge separation, giving Ru a formal charge of +1 and Mn of –1. The charge separation, entropy loss and opening of the epoxide ring, all together, contribute to the significantly large barrier (53.91 kcal/mol, **1** → **TS$_{3\text{-}4}$**) for the first major step. In the second major step, ring closure from **5** to yield the product molecule (cyclic carbonate) again creates a charge separation. This step (**5** → **TS$_{5\text{-}6}$**) has a barrier of 35.93 kcal/mol.

Route II involves three major steps 1) Coordination of epoxide to the Lewis acidic Ru center with heterolytic breaking of the Ru-Mn bond and Mn-nucleophilic ring opening of epoxide to give **8**. 2) Insertion of CO_2 into the Ru-O bond in **8** to give **10**. 3) Ring closure from **10** to yield cyclic carbonate and regeneration of the catalyst. The first major step has an overall barrier of 44.04 kcal/mol, which is smaller than the overall barrier calculated for the first major step of **Route I**. The energy required for coordination of epoxide with heterolytic cleavage of the Ru-Mn bond is the same as that in **Route I**. The smaller overall barrier here is a result of a smaller barrier for the Mn-nucleophilic ring opening as compared to the metallocarboxylate-nucleophilic ring opening in **Route I**. Examining the energy changes from **2** → **TS$_{2\text{-}8}$** and **2** → **TS$_{3\text{-}4}$**, we can conclude that the unfavorable metallocarboxylate-nucleophilic ring opening in **Route I** is mainly related to the entropy effect. In **Route II**, ring opening occurs immediately after the heterolytic Ru-Mn bond cleavage. However, the ring opening in **Route I** occurs after **2** takes one more molecule, CO_2. The CO_2 insertion from **8** in the second major step does not cost much energy with a barrier of 24.68 kcal/mol. In the third major step, ring closure from **10** to yield the product molecule (cyclic carbonate), similar to the second major step in **Route I**, has a large barrier of

43.55 kcal/mol (from **10** to **TS_{11-6}**). Again, formation of **6** creates a charge separation between the two metal centers, contributing to the large barrier. As the difference in the overall barriers between the first and third major steps is small, we expect that these two steps are important in determining the reaction rate.

Comparing the energetics of **Routes I and II** described above, one finds that **Route II** is favored over **Route I**. The experiments described in the preceding section show that the presence of electron-withdrawing groups on the epoxides leads to higher conversions (**Table 2.3**). It is expected that electron-withdrawing group, which increase the electrophilicity of the epoxide carbons, should reduce the barrier for the Mn-nucleophilic ring opening step in **Route II**. Electron-withdrawing groups should also facilitate the ring closure from **11** because this step is also related to the electrophilic attack of one of the epoxide carbons on the Ru-bonded oxygen in **11**.

It should be noted here that the reaction barrier calculated for both **Routes I and II** are substantially high. As mention above and will be discussed in more details below, the reaction paths involve heterolytic Ru-Mn bond cleavage, giving a charge separation. It is well recongnized that gas-phase calculations, which are now being commonly practiced in computational chemistry, for such charge separation processes always give very high reaction barriers. [67] Since we are interested in the comparison of **Routes I and II**, the relative barrier heights are more important than the absolute barriers. It should also be pointed out that intermediates **8-10** were predicted to be stable on the basis of the calculations. However, we did not observe these species experimentally. We suspect that the calculations might have overestimated the electrostatic interactions between Ru and O and between Mn and C in the Ru-O and Mn-C bonds of the intermediates, again due to the gas-phase models.

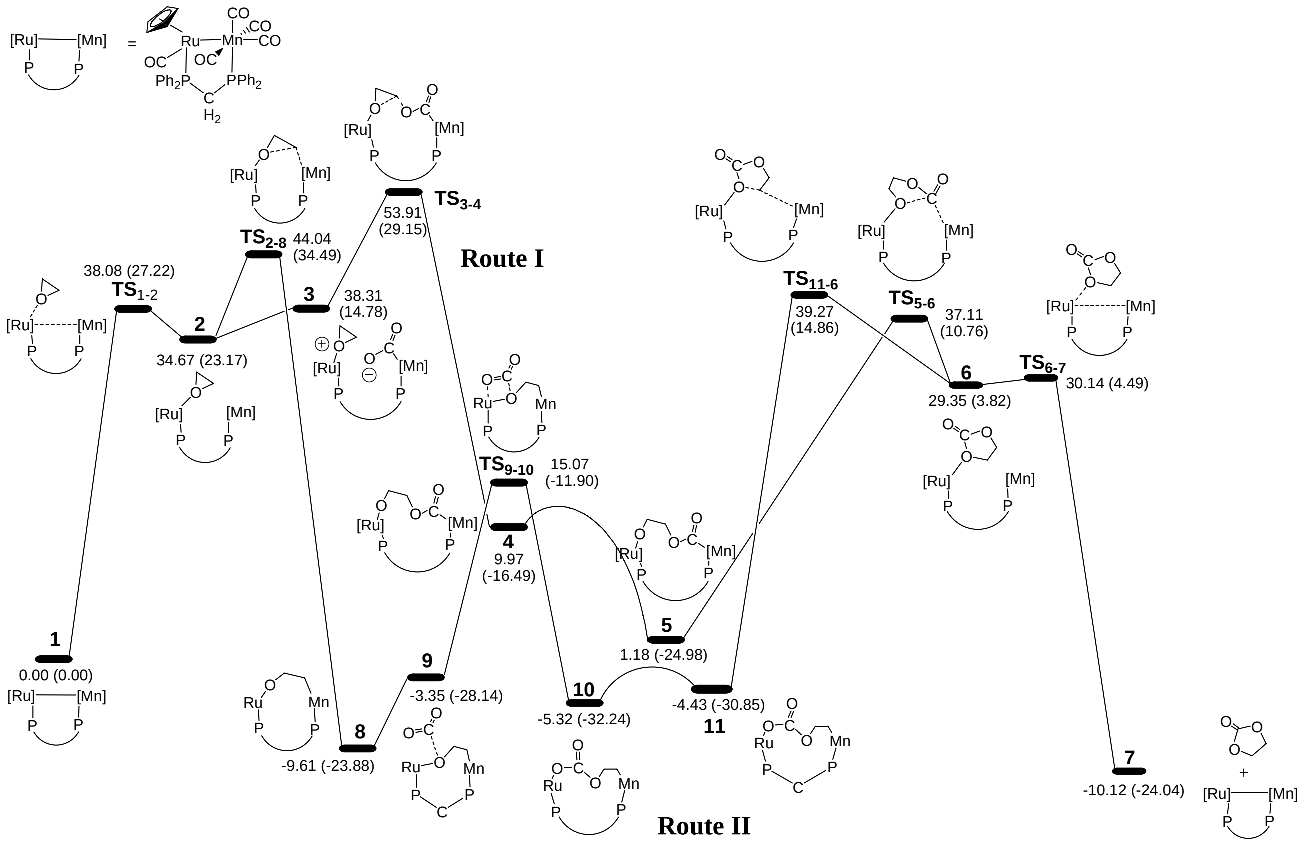

Figure 2.2: Schematic illustration of the two reaction pathways studied in the coupling reaction of carbon dioxide with ethylene oxide with calculated relative free energies (kcal/mol) for species involved in the reaction. The relative electronic energies are in parentheses. The relative energies of all species are given with respect to (η^5-C_5H_5)Ru(CO)(μ-dppm)Mn($CO)_4$, CO_2, and C_2H_4O.

Structures for the Species in Route II:

Structural details of the optimized intermediates and transition states for the favored route (**Route II**) are shown in **Figure 2.3**. The complex **1** can be described as being composed of a square pyramidal 18-electron, Mn(-1) d^8-ML_5 anion coordinated to a 16-electron Ru(+2) d^6-$CpML_2$ cation fragment via a dative Ru←Mn bond. The calculated bond length of Ru-Mn in **1** is 2.933Å which is slightly longer than the corresponding bond distance (2.852Å) of the X-ray crystal structure shown in **Table 2.2**. The metal-phosphine and metal-carbonyl distances were well reproduced. The calculated bond lengths and bond angles of **1** are in reasonably good agreement with the experimental values. In **2**, the Ru-Mn distance considerably lengthens to 4.803Å, indicating that the Ru-Mn bond is completely broken. The calculated NBO natural charges [68] of the Ru and Mn centers are 0.12 and -0.86, respectively, suggesting that **2** more closely resembles a Ru cation/Mn anion pair. Heterolytic bond cleavage in gas-phase requires huge amount of energy, therefore, the high activation barrier for the process **1→2** is reasonable. In the transition state $\mathbf{TS_{2\text{-}8}}$, the $O_{(epoxide)}$-$C_{(epoxide)}$ bond lengthens to 1.927Å and the $C_{(epoxide)}\cdots$Mn distance shortens to 3.700Å. These features indicate that $\mathbf{TS_{2\text{-}8}}$ is an early transition state. The Ru and Mn centers in **8** are bridged by an alkoxide group. In the transition state $\mathbf{TS_{9\text{-}10}}$, the $C_{(CO2)}$-$O_{(epoxide)}$ and

Ru-$O_{(CO2)}$ distances shortens to 1.486Å and 2.524Å, respectively. And the $C_{(CO2)}$-$O_{(CO2)}$ and Ru-$O_{(epoxide)}$ bonds lengthen to 1.290Å and 2.636Å, respectively. These geometrical features indicate that **$TS_{9\text{-}10}$** is a concerted four-center transition state. In the intermediate **10**, the Ru and Mn centers are bridged by the carbonate group. From **10** to **11**, the Ru-O-C=O dihedral angle changes from 139.9° to 13.4°, making the lone pairs of the oxygen which is bonded to Ru ready to interact with one of the epoxide carbons in the transition state **$TS_{11\text{-}6}$** in the ring closure process. In the transition state **$TS_{11\text{-}6}$**, the Mn-$C_{(epoxide)}$ distance lengthens to 3.112Å and the $C_{(epoxide)}$-$O_{(CO2)}$ distance shortens to 1.769Å, typical of a late transition state. In **6**, the Mn-$C_{(epoxide)}$ and Ru-Mn distances are 4.446Å and 4.804Å, respectively, indicating that there is no bonding interaction between the Ru and Mn fragments. The calculated NBO natural charges [68] of the Ru and Mn centers are 0.10 and -0.88, respectively. Similar to the process of **1** → **2**, a heterolytic bond cleavage for the process **11**→ **6** is found, requiring a high activation barrier. In the transition state **$TS_{6\text{-}7}$**, the Ru-Mn distance shortens to 4.493Å and the Ru-O distance lengthens to 2.545Å. This transition state is related to dissociation of the product molecule (cyclic carbonate) and regeneration of the catalyst.

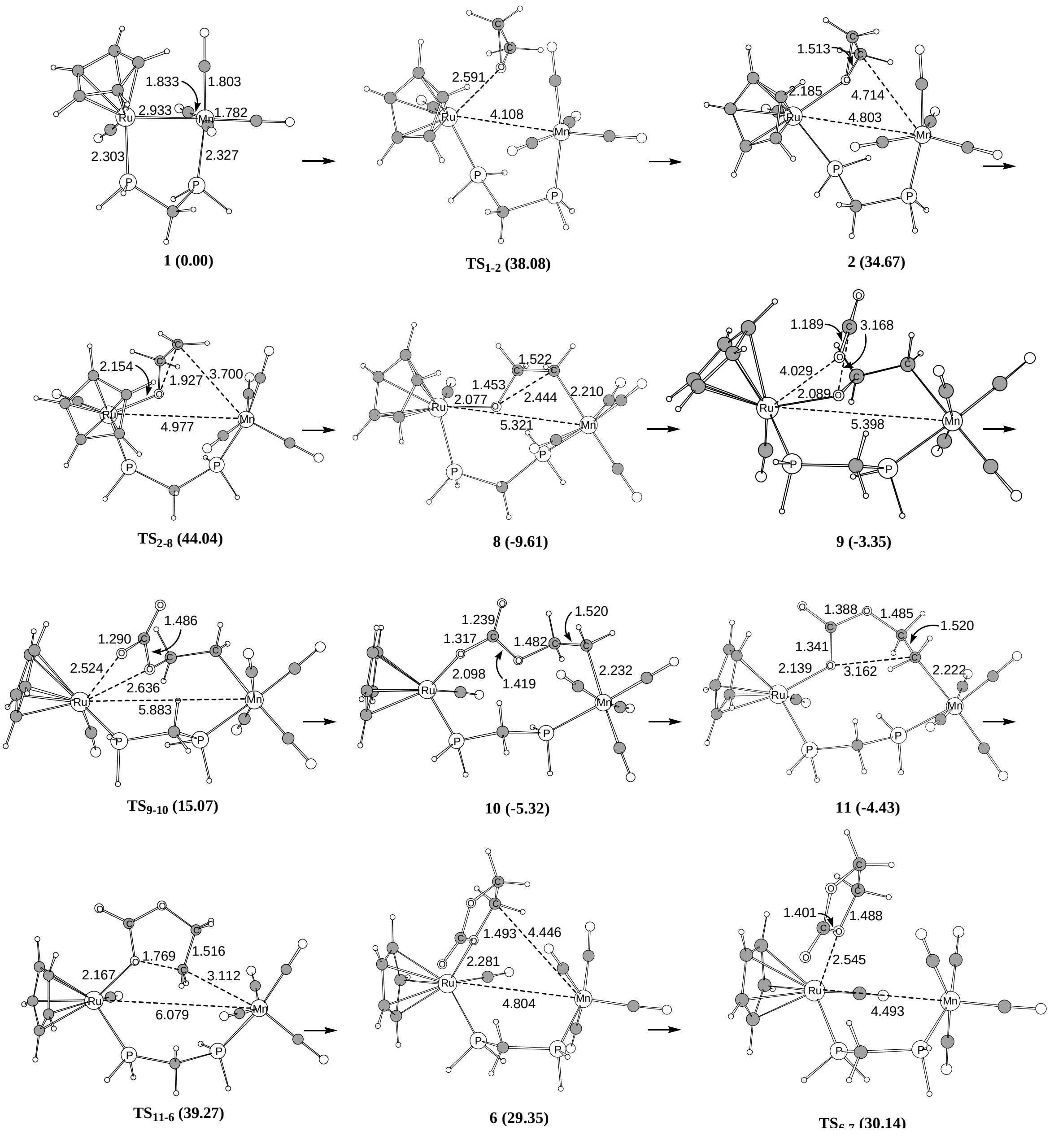

1 (0.00)

$TS_{1\text{-}2}$ (38.08)

2 (34.67)

$TS_{2\text{-}8}$ (44.04)

8 (-9.61)

9 (-3.35)

$TS_{9\text{-}10}$ (15.07)

10 (-5.32)

11 (-4.43)

$TS_{11\text{-}6}$ (39.27)

6 (29.35)

$TS_{6\text{-}7}$ (30.14)

Figure 2.3: B3LYP optimized structures for the species shown in Figure 2.2 (Route II). In parentheses are the free energies (kcal/mol) relative to the reactants. Bond lengths are given in angstroms.

2.4 Conclusion

This work represents an example of catalytic CO_2/epoxide coupling reactions with the well-defined heterobimetallic complex **1**. Our study indicates that cooperative participation of the metal centers of the complex in the catalysis is in operation. Theoretical calculations seem to support a reaction pathway involving heterolytic cleavage of the Ru-Mn bond and epoxide coordination to the Lewis acidic Ru center, ring-opening of the epoxide by the Lewis basic Mn center, followed by CO_2 insertions into the Ru-O bond to afford the carbonato intermediate, which then undergoes ring-closure to yield the cyclic carbonate product. The heterolytic metal-metal bond cleavage step and the ring-closure step, both of which create charge separations, have high energy barriers.

Chapter 3 Desulphurization of thiiranes catalyzed by the bimetallic complex [(η^5-C_5H_5)Ru(CO)(μ-dppm)Mn(CO)$_4$], and other complexes [(η^5-C_5H_5)Ru(CO)(PPh_3)(CH_3CN)]$^+$[BF_4]$^-$ and Li$^+$[Mn(CO)$_4$(PPh_3)]$^-$

3.1 Introduction

In Chapter 2, we studied the “cooperative reactivity” of bimetallic complexes in the CO_2/epoxide coupling reactions. Cooperative reactivity of multimetallic systems often leads to catalytic activity enhancement in comparison to the monometallic systems. We studied the catalytic activity of the bimetallic complex [(η^5-C_5H_5)Ru(CO)(μ-dppm)Mn(CO)$_4$] (**1**) and the lithium salt of the manganese carbonylate Li$^+$[Mn(CO)$_4$(PPh_3)]$^-$ (**2**) in the coupling reactions of epoxides and CO_2 to produce cyclic carbonates. The monometallic ruthenium systems like [(η^5-C_5H_5)Ru(PPh_3)$_2$(CH_3CN)]$^+$[BF_4]$^-$ and [(η^5-C_5H_5)Ru(CO)(PPh_3)(CH_3CN)]$^+$[BF_4]$^-$ were, however, found to be inactive, and it was learned that **1** has higher catalytic activity than **2**.

We reported in this chapter our attempt to use thiiranes, which are the sulfur analogues of epoxides to perform the coupling reactions with CO_2 in the presence of complex **1**. The CO_2/thiirane coupling reactions were, however, found to be unsuccessful; we therefore looked into the possibility of affecting the coupling reactions of CS_2 with thiiranes (the structure is as follows).

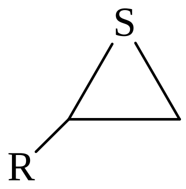

In our study of the CS_2/thiirane coupling reactions, we discovered that the bimetallic complex **1** was active catalyst for the reaction, producing five-membered cyclic trithiocarbonates; however, it was found that olefins were also produced as side products (**Scheme 3.1**). The generation of olefins in this reaction leads us to believe that complex **1** may be capable of catalyzing the desulphurization reactions of thiiranes. The five-membered cyclic trithiocarbonates are only produced at relatively high temperature (140°C). On the other hand, at low temperatures olefins are the dominant products, resulting from the desulfurization of thiiranes. We have focused our study at the desulfurization of thiiranes.

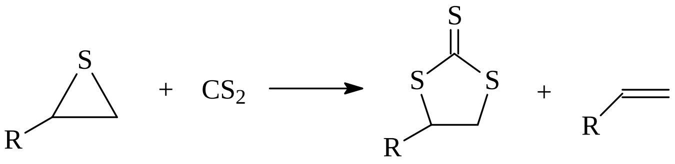

Scheme 3.1: The coupling reaction of thiiranes and CS_2 to produce five-membered cyclic carbonates and olefins

The catalytic desulfurization of thiiranes would become a more valuable reaction if it is possible to use a readily available thiirane as the sulfur source for the sulfurization of other olefins to produce more valuable thiiranes. We have tried the catalytic sulfur-transfer reaction using the readily available propylene sulfide as the sulfur source (eq 3.1). Unfortunately, we have found that **1**, **2**, and **3** are not active for the sulfur transfer reactions.

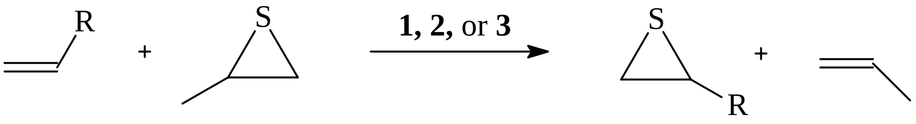

(3.1)

Over the last decade, there has not been any report of desulfurization reaction of thiiranes involving ruthenium complexes. The few examples using bimetallic catalysts, generated olefins in low yield. [42-45, 47, 48] In this chapter, we report our study on the desulfurization of thiiranes with the bimetallic complex **1**, $Li^+[Mn(CO)_4(PPh_3)]^-$ (**2**) and, $[(\eta^5\text{-}C_5H_5)Ru(CO)(PPh_3)(CH_3CN)]^+[BF_4]^-$ (**3**).

3.2 Experimental

3.2.1 Reagents

All reactions were carried out under a dry N_2 atmosphere using Schlenk techniques. All solvents were distilled and degassed prior to use. Dichloromethane was distilled from calcium hydride. Tetrahydrofuran, diethyl ether, toluene, and hexane were distilled from sodium-benzophenone ketyl. Methanol and ethanol were distilled from magnesium and iodine.

The compounds $Mn_2(CO)_{10}$ and $RuCl_3{\cdot}3H_2O$ were purchased from Strem. $Li(C_2H_5)_3BH$ was purchased from Aldrich. The complexes $Mn_2(CO)_8(PPh_3)_2$, [49] $Li^+Mn(CO)_5^-$,[50] $(\eta^5\text{-}C_5H_5)Ru(dppm)Cl$ [51, 52] and $(\eta^5\text{-}C_5H_5)Ru(CO)(PPh_3)Cl$ [69] were synthesized according to methods described in literature.

Ethylene sulfide and propylene sulfide were purchased from Acros, and they were used as received. The other episulfides were synthesized according to literature methods. [70, 71]

3.2.2 Instrumentation

Infrared spectra were obtained from a Bruker Vector 22 FT-IR spectrophotometre. ^{1}H NMR spectra were obtained from a Bruker DPX 400 spectrometer at 400.13 MHz. Chemical shifts (δ, ppm) were measured relative to the proton residues of the deuterated solvents ($CDCl_3$ δ 7.26 ppm, C_6D_6 δ 7.40 ppm.) $^{31}P\{^1H\}$ NMR spectra were taken on a Bruker DPX-400 spectrometer at 161.98 MHz. The $^{31}P\{^1H\}$ NMR chemical shifts were externally referenced to 85% H_3PO_4 in D_2O. (δ 0.00 ppm). Electrospray Ionization Mass Spectrometry was carried out with a Finnigan MAT 95S mass spectrometer by first dissolving the sample in CH_2Cl_2 / MeOH. Elemental analyses were performed by M-H-W Laboratories, Pheonix, AZ, USA.

3.2.3 Preparation of $[(\eta^5\text{-}C_5H_5)Ru(CO)(PPh_3)(CH_3CN)]^-[BF_4]^+$ (3)

A sample of $(\eta^5\text{-}C_5H_5)Ru(CO)(PPh_3)Cl$ (0.10g, 0.23mmol) was weighed into a Schlenk flask equipped with a condenser and containing a solution of $Ag^+BF_4^-$

(0.091g, 0.47mmol, 2 equiv) in the mixed solvents (THF 20mL; CH_3CN 3mL). The resulting mixture was then heated at reflux for 24h. After cooling the mixture to room temperature, the solution was filtered through celite, the solvent of the filtrate was removed under vacuum, and the residue thus obtained was washed with diethyl ether (2mL x 2) and hexanes (4mL x 2) and dried under vacuum. Yield 0.88g (72%). IR (KBr, cm^{-1}): $\upsilon(C \equiv O)$ 1983 (s). ^1H NMR (400.13 MHz, THF-d_8, 25°C) δ7.51-7.34 (m, 15H of PPh_3), 4.93 (s, 5H of Cp ring), 1.55 (s, 3H, CH_3CN). $^{31}P\{^1H\}$ NMR (161.98 MHz, THF-d_8, 25°C) δ 54.0 (s, P of PPh_3)

3.2.4 General Procedures

Desulfurization of thiiranes:

A typical experimental procedure for the desulfurization of thiiranes is as follow: The catalyst $(\eta^5\text{-}C_5H_5)RuCO(\mu\text{-dppm})Mn(CO)_4$ (0.0040g, 0.0054mmol), or $Li^+[Mn(CO)_4(PPh_3)]^-$ (0.0025g, 0.0057mmol), or $[(\eta^5\text{-}C_5H_5)Ru(CO)(PPh_3)(CH_3CN)]^-[BF_4]^+$ (0.0030g, 0.0051mmol) was added to the thiirane (~4mL; ~9000equiv) in 1,4-dioxane (~4mL) in a 35mm thick-walled tube equipped with a magnetic stirring bar. The tube was then sealed and heated with stirring at 100°C. At the end of the required length of time, the tube was cooled rapidly. The yield of corresponding olefin was determined by ^{1}H-NMR spectroscopy. The set of three signals for the two methylene hydrogen atoms and the hydrogen on the substituted carbon of the substrate thiirane are well-separated from the set of three signals for the corresponding hydrogen atoms of the product olefin. The yield of the olefin can therefore be determined by comparing the sums of integration of these two sets of hydrogen signals.

3.2.5 Thiiranes used for the desulphurization reactions

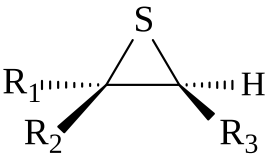

Substrate	R_1	R_2	R_3
Ethylene sulfide	H	H	H
Propylene sulfide	H	CH_3	H
Isobutylene sulfide	CH_3	CH_3	H
1,2-Episulfidehexane	H	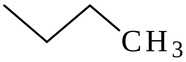	H
Styrene sulfide	H	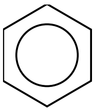	H
Cyclohexene sulfide	H	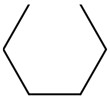	
Butadiene sulfide	H	$CH_2{=}CH$	H
Phenyl methoxy sulfide	H	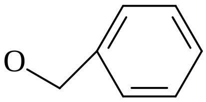	H
Phenyl propylene sulfide	H	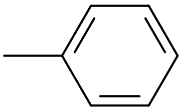	H

3.3 Results and Discussion

3.3.1 Thiiranes desulphurization reactions with 1, 2, and 3

The three complexes [(η^5-C_5H_5)Ru(CO)(μ-dppm)Mn(CO)$_4$] **(1)**, Li^+[Mn(CO)$_4$(PPh$_3$)]$^-$ **(2)**, and [(η^5-C_5H_5)Ru(CO)(PPh$_3$)(CH$_3$CN)]$^+$[BF$_4$]$^-$ **(3)** are able to catalyze the desulphurization reactions of thiiranes to produce the corresponding olefins in high yields at 100ºC in 1,4-dioxane without any additive. The results of the **1-**, **2-**, and **3-**catalyzed desulfurization reactions are shown in **Tables 3.1**, **3.2**, and **3.3**, respectively.

Table 3.1: **Desulphurization reactions of thiiranes catalyzed by complex 1 to produce the corresponding olefins**[a]

Entry	Substrate	Time(h)	% yield [b]	Total TON [c]	TOF (h^{-1}) [d]
1	Styrene sulfide	3	96	8640	2880
2	Butadiene sulfide	5	78	7020	1404
3	Cyclohexene sulfide	13	71	6390	492
4	Phenyl methoxy sulfide	33	96	8640	262
5	Phenyl propylene sulfide	>100	Trace	—	—
6 [e]	Phenyl propylene sulfide	100	90	8100	81
7	Ethylene sulfide	40	100	9000	225
8	Propylene sulfide	45	100	9000	200
9	Isobutylene sulfide	50	94	8460	169
10	1,2-Episulfidehexane	>65	Trace	—	—
11 [e]	1,2-Episulfidehexane	65	86	7740	119

[a] Typical reaction conditions: Catalyst: 3.8µmol, substrates: 34.5mmol (S/C = 9000), reaction temperature 100°C, THF: 4mL. [b] Determined by comparing the ratio of product to substrate in the ^{1}H NMR spectrum of an aliquot of the reaction mixture. [c] Turnover number (TON) = no. of mole of product/no. of mole of catalyst. [d] TOF = TON/reaction time. [e] reaction temperature 120°C.

Table 3.2: **Desulphurization reactions of thiiranes catalyzed by complex 2 to produce the corresponding olefins**[a]

Entry	Substrate	Time(h)	% yield [b]	Total TON[c]	TOF (h^{-1}) [d]
1	Styrene sulfide	3	39	3510	1170
2[f]	Styrene sulfide	3	19	1710	570
3	Butadiene sulfide	5	52	4680	936
4	Cyclohexene sulfide	13	52	4680	360
5	Phenyl methoxy sulfide	33	40	3600	109
6	Phenyl propylene sulfide	50	Trace	—	—
7[e]	Phenyl propylene sulfide	100	49	4410	44
8	Ethylene sulfide	40	58	5220	131
9	Propylene sulfide	45	53	4770	106
10	Isobutylene sulfide	50	52	4680	94
11	1,2-Episulfidehexane	>50	Trace	—	—
12[e]	1,2-Episulfidehexane	65	52	4680	72
13[g]	Styrene sulfide	3	42	3780	1260

[a]Typical reaction conditions: Catalyst: 3.8μmol, substrates: 34.5mmol (S/C = 9000), reaction temperature 100°C, THF: 4mL. [b]Determined by comparing the ratio of product to substrate in the ^{1}H NMR spectrum of an aliquot of the reaction mixture. [c]Turnover number (TON) = no. of mole of product/no. of mole of catalyst. [d]TOF = TON/reaction time. [e] reaction temperature 120°C. [f]7.6 μmol of 12-crown-4 added. [g]catalyst: **2** and **3** (3.8μmol each), substrates: 34.5mmol (S/C = 9000).

Table 3.3: **Desulphurization reactions of thiiranes catalyzed by complex 3 to produce the corresponding olefins**[a]

Entry	Substrate	Time(h)	% yield[b]	Total TON[c]	TOF (h^{-1})[d]
1	Styrene sulfide	3	34	3060	1020
2	Butadiene sulfide	5	48	4320	864
3	Cyclohexene sulfide	13	55	4950	381
4	Phenyl methoxy sulfide	33	46	4140	125
5	Phenyl propylene sulfide	>100	Trace	—	—
6[e]	Phenyl propylene sulfide	100	54	4860	49
7	Ethylene sulfide	40	56	5040	126
8	Propylene sulfide	45	52	4680	104
9	Isobutylene sulfide	50	50	4500	90
10	1,2-Episulfidehexane	>65	Trace	—	—
11[e]	1,2-Episulfidehexane	65	57	5130	79

[a]Typical reaction conditions: Catalyst: 3.8μmol, substrates: 34.5mmol (S/C = 9000), reaction temperature 100°C, THF: 4mL. [b]Determined by comparing the ratio of product to substrate in the ^{1}H NMR spectrum of an aliquot of the reaction mixture. [c]Turnover number (TON) = no. of mole of product/no. of mole of catalyst. [d]TOF = TON/reaction time. [e] reaction temperature 120°C.

3.3.2 Proposed mechanism for the desulphurization reaction of thiiranes

In Chapter 2, we report that the heterobimetallic complex **1** is able to catalyze the CO_2/epoxide coupling reactions. The first step of our proposed mechanism for the reaction is the heterolytic cleavage of the metal-metal bond to generate the electrophilic ruthenium fragment and the nucleophilic manganese moiety. An epoxide molecule is activated by coordination to the Lewis acidic Ru center. Therefore, it is envisioned that the bimetallic complex **1** can activate the thiiranes in a similar manner in the desulphurization reactions.

A mechanism for the **1-**catalyzed desulphurization reactions of thiiranes is depicted in **Scheme 3.2**. We propose that the metal-metal bond of complex **1** is cleaved with the coordination of nucleophilic thiirane to the Ru center to form species **A**, which we have not been able to isolate. Wilson and co-workers proposed that $(\eta^5\text{-}C_5H_5)Ru(PPh_3)_2OTf$ reacted with thiirane to produce the thiirane-coordinated complex $[(\eta^5\text{-}C_5H_5)Ru(PPh_3)_2(SC_2H_4)]OTf$; the thiirane is the sulphur source for the generation of the sulfur-containing complex $[(\eta^5\text{-}C_5H_5)Ru(PPh_3)_2S]^+$. [72] The nucleophilic Mn moiety attacks the less hindered β-carbon of thiirane, leading to ring-opening of the thiirane molecule to form species **B**. The relatively electron-rich sulphur atom then attacks the Mn center to afford the olefin and the Ru–S–Mn complex (species **C**). Komiya and co-workers have reported a highly regio- and stereocontrolled ring-opening reaction of thiiranes. [48] The reaction of thiiranes with organoplatinum-manganese complex (dppe)RPtMn(CO)$_5$ giving the heterodinuclear complex (dppe)RPtSCR$_1$R$_2$CR$_3$R$_4$Mn(CO)$_5$ from which stereoselective desulfurization occurs to afford the olefin and a Pt-S-Mn type complex (species **X**) (**Scheme 3.3**).

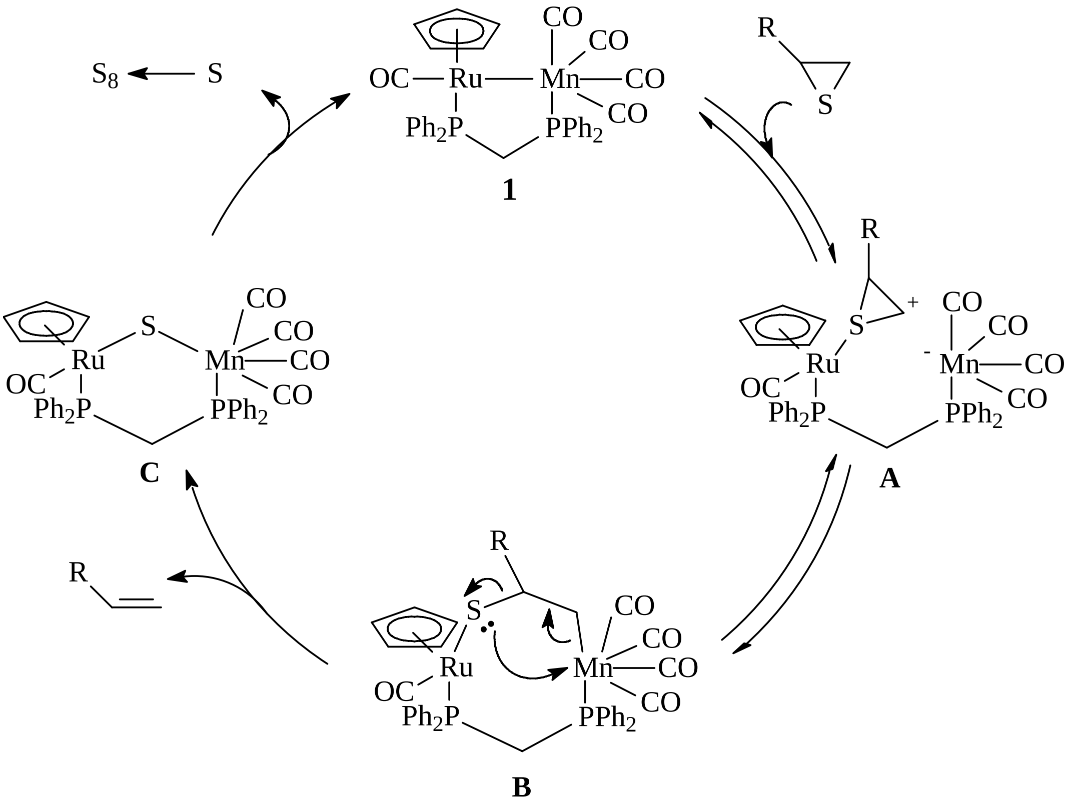

Scheme 3.2: Desulphurization of thiiranes catalyzed by complex 1

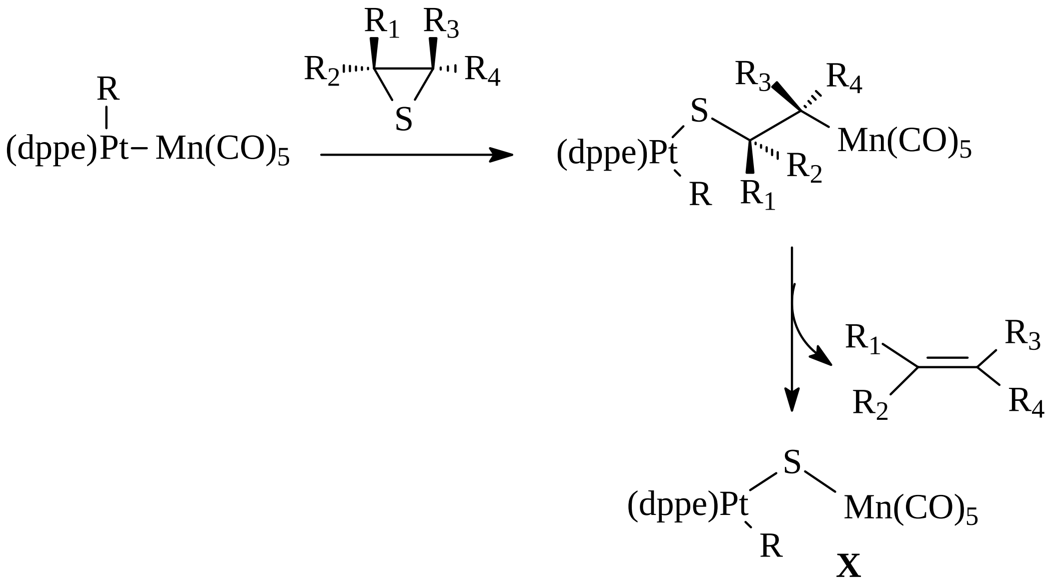

R = Me, R_1 = Me or H, R_2 = H or Me, R_3 = R_4 = H

Scheme 3.3: The ring-opening reaction of thiiranes with Pt-Mn complex forming the corresponding olefins and sulphur-bridged (Pt-S-Mn) complexes

In independent studies, it was found by ^1H and $^{31}P\{^1H\}$ NMR spectroscopy that after heating a THF-*d₈* solution of **1** and styrene sulfide or propylene sulfide in an NMR tube 100°C for 45h, **1** remained unchanged.

Studying and comparing the catalytic activities of the monometallic components of the bimetallic complex might sometime provide indirect evidence supporting the presence cooperative reactivity of the bimetallic complexes in chemical reactions. Therefore, the activities of the monometallic fragments of $[(\eta^5\text{-}C_5H_5)Ru(CO)(\mu\text{-dppm})Mn(CO)_4]$ **(1)** in thiirane desulphurization, were studied. It was found that the lithium salt of the manganese carbonylate $Li^+[Mn(CO)_4(PPh_3)]^-$ **(2)** and the monometallic species $[(\eta^5\text{-}C_5H_5)Ru(CO)(PPh_3)(CH_3CN)]^+[BF_4]^-$ **(3)** are capable of catalyzing the desulphurization reactions of thiiranes. However, the activities of these individual metal fragments are lower than that of complex **1**. The **2-** and **3-**catalyzed desulphurization reactions produced olefins and different sulfur compounds; the former yielded S_8 and the **3-**catalyzed reaction gave the cyclic polydisulfides. The results of **2-** and **3**-catalyzed desulphurization of thiiranes are shown in **Tables 3.2** and **3.3**, respectively.

The mechanisms of the desulphurization reaction of thiiranes by complexes **2** and **3** are shown in **Scheme 3.4 and 3.5** respectively. As proposed in **Scheme 3.4**, the interaction of the thiirane molecule with Li^+ increases the electrophilicity of the β-carbon of the former. The Mn fragment $[Mn(CO)_4(PPh_3)]^-$ then attacks the electrophilic β-carbon of the thiirane to form species **H**. The sulphur atom then attack the Mn center to produce a Li-S-Mn type complex and the olefin. Finally, the sulphur is eliminated and the manganese complex is regenerated.

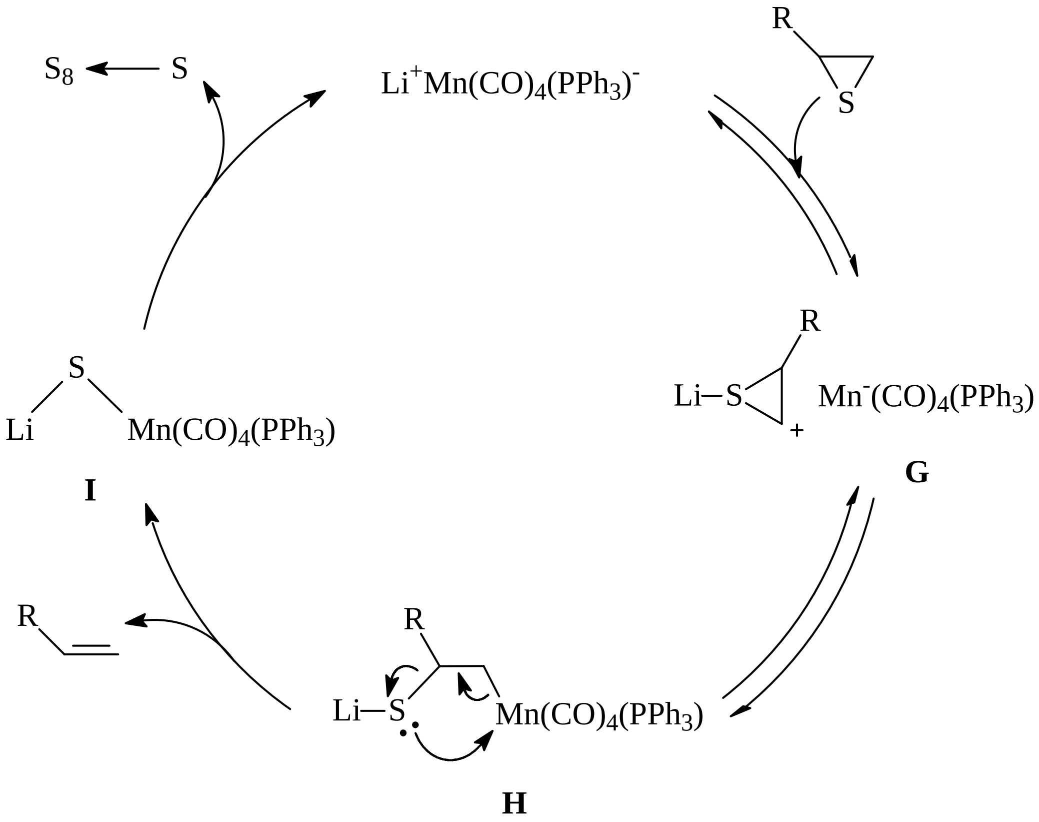

Scheme 3.4: Desulphurization of thiiranes catalyzed by complex 2

In **Scheme 3.5**, it is proposed that the thiirane first substitutes the acetonitrile ligand on the Ru center. An additional thiirane molecule attaches to the β-carbon of coordinated thiirane ligand and open the ring, forming **A**. Eliminate of CH_2=CHR from species **A** would generate a SCH_2CH_2S ruthenium complex **B**. Finally, the coordinated SCH_2CH_2S ligand, which is displaced by acetonitrile, form the oligomeric speices **X**.

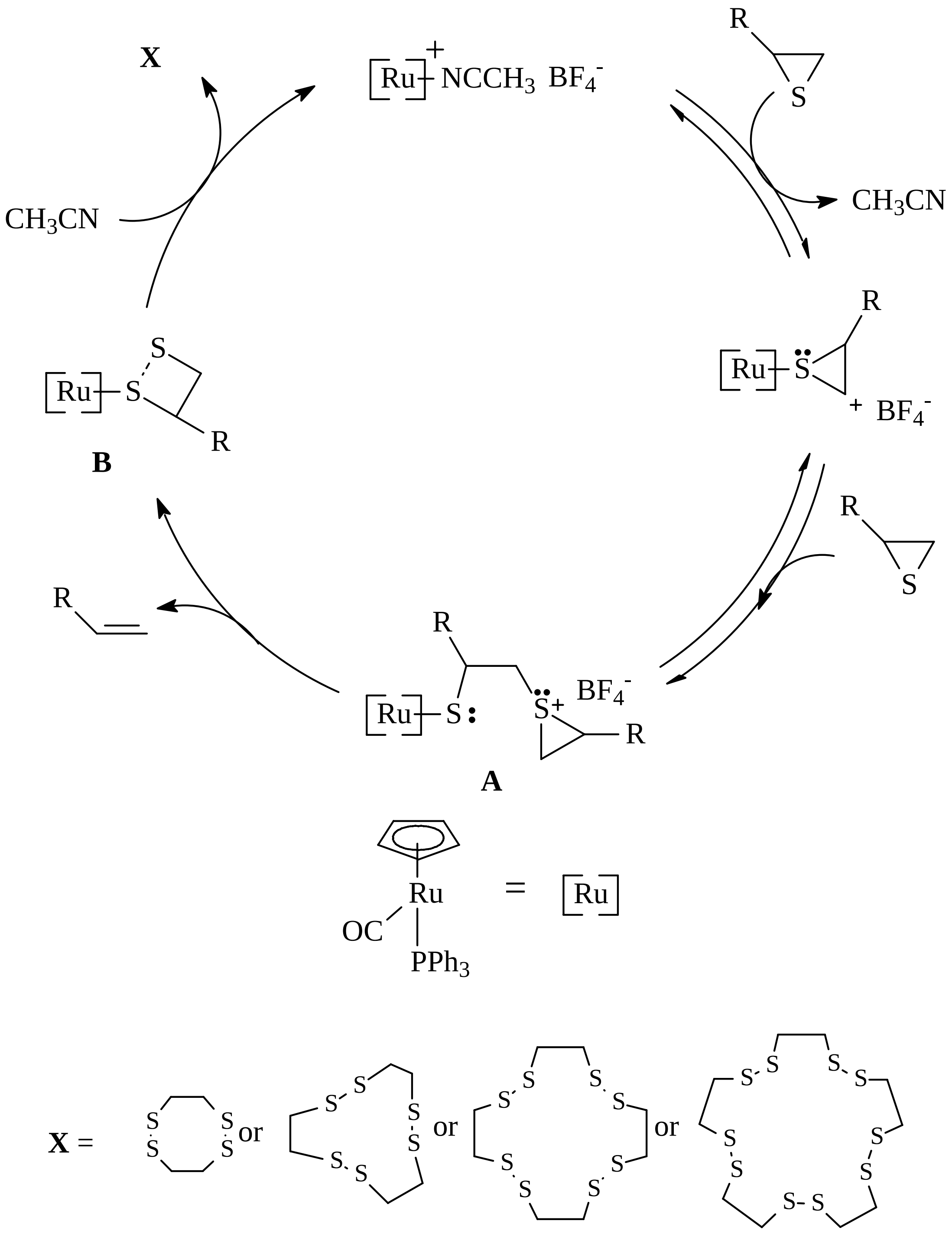

Scheme 3.5: Desulphurization of thiiranes catalyzed by complex 3

The mechanisms of the **2-**catalyzed desulphurization of thiirane is similar to that of the **1**-catalyzed reaction, both producing the corresponding olefin and sulphur (S_8). However, the mechanism of complex **3-**catalyzed desulphurization of thiirane is different from those of the reactions catalyzed by **1** and **2**. The sulfur-containing products of the **3-**catalyzed reactions are the cyclic polydisulfides in stead of S_8.

The bimetallic complex $[(\eta^5\text{-}C_5H_5)Ru(CO)(\mu\text{-dppm})Mn(CO)_4]$ (**1**) shows higher catalytic activity than $Li^+[Mn(CO)_4(PPh_3)]^-$ (**2**), and the monometallic complex $[(\eta^5\text{-}C_5H_5)Ru(CO)(PPh_3)(CH_3CN)]^+[BF_4]^-$ (**3**). The synergistic effect in the complex **1** probably results from the proximity of the two metal centers, enabling them to act cooperatively, and therefore giving rise to a higher catalytic activity.

In one of the experiments (**Entry 12, Table 3.3**), a (**2** + **3**) catalytic system was used. It was, however, found that the yield of olefin in this experiment was much lower than that of the **1-**catalyzed reaction (**Entry 1, Table 3.1**). That complex **1** having a higher catalytic activity than a combination of the individual complexes **2** and **3** demonstrates that this catalytic system with the two metal centers linked together by a bridging ligand is more active. In another experiment, the addition of 12-crown-4 (**Entry 24, Table 3.3**), which is able to solvate Li^+, quenches the activity of complex **2**. The result supports the notion that the Li^+ cation plays an important role in this reaction.

The ring opening of thiirane is believed to be affected not only by the steric hindrance of the substrate, but also by the electronic property of the β-carbon atom of the coordinated thiirane. The substrates having electron-withdrawing groups give higher yields of olefins than those that do not containing these groups. For example: styrene sulfide and butadiene sulfide (Entries **1, 2** in **Table 3.1,** Entries **1, 3** in **Table 3.2,** Entries **1, 2** in **Table 3.3**) give higher yields of the corresponding olefins than propylene sulfide (Entry **8** in **Table 3.1**, Entry **9** in **Table 3.2**, Entry **8** in **Table 3.3**). Since ring opening of the thiirane is achievable via nucleophilic attack at the β-carbon of the former, it is therefore not unexpected that substrates containing electron-withdrawing group would render this ring-opening step more facile.

The sterically bulky substrates (**Entries 9, 10, 11** in **Table 3.1**, **Entries 10, 11, 12** in **Table 3.2**, **Entries 9, 10, 11** in **Table 3.3**) show relatively low conversions. Comparing the yields of the olefinic products of the phenyl methoxy sulfide (**Entry 4** in **Table 3.1**, **Entry 5** in **Table 3.2**, **Entry 4** in **Table 3.3**) and phenyl propylene sulfide desulfurization reactions (**Entries 5, 6 in Table 3.1**, **Entries 6, 7 in Table 3.2**, **Entries 5, 6 in Table 3.3**), we can find that the yield of the product from the former is much higher than that of the latter, it is probably due to the fact that the highly bulky phenyl propylene group is not able to rotate freely.

3.4 Conclusion

The heterbimetallic complex η^5-$C_5H_5Ru(CO)(\mu\text{-dppm})Mn(CO)_4$ (**1**), $Li^+[Mn(CO)_4(PPh_3)]^-$ (**2**) and $[\eta^5\text{-}C_5H_5Ru(CO)(PPh_3)(CH_3CN)]^+[BF_4]^-$ (**3**) are found to be able to catalyze the desulphurization reactions of thiiranes to afford corresponding olefins with satisfactory yields. The bimetallic complex **1** was found to show higher catalytic activity than the monometallic species **2** and **3**.

Chapter 4 PPN salts-catalyzed coupling reactions of CO_2 with neat epoxides to yield cyclic carbonates

4.1 Introduction

As described in Chapter 2, we have successfully used the bimetallic complex $[(\eta^5\text{-}C_5H_5)Ru(CO)(\mu\text{-dppm})Mn(CO)_4]$ (**1**) and the complex $Li^+Mn(CO)_4(PPh_3)^-$ (**2**) to catalyze the coupling reactions of epoxides and CO_2 to produce five-membered cyclic carbonates. To see if the Li^+ cation in complex **2** is important to the success of the coupling reaction, we study the catalytic activity of $PPN^+Mn(CO)_4(PPh_3)^-$ (**6**) (PPN = bis(triphenylphosphine)immium) in the CO_2/epoxide coupling reactions. The results of the **1-**, **2-**, and **6-**catalyzed CO_2/propylene oxide coupling reactions are shown in **Table 4.1**.

Interestingly, it was found that $PPN^+Mn(CO)_4(PPh_3)^-$ (**6**) gave a higher yield and turnover number of cyclic carbonate than the bimetallic complex **1** and $Li^+Mn(CO)_4(PPh_3)^-$ (**2**) in the coupling reactions. We suspect that the PPN^+ cation might play an important role in the catalytic processes.

Table 4.1: The catalytic reactivity of bimetallic complex, Li complex and PPN complex in coupling reaction of propylene oxide and CO_2[a]

Catalyst	Yield (%)	Total TON[b]
$(\eta^5\text{-}C_5H_5)Ru(CO)(\mu\text{-dppm})Mn(CO)_4$	16.6	1490
$Li^+Mn(CO)_4(PPh_3)^-$	5.2	450
$PPN^+Mn(CO)_4(PPh_3)^-$	36	3240

[a] Typical reaction conditions: Catalyst: 3.5 μmol, substrates: 31.5mmol propylene oxide (S/C = 9000), CO_2 pressure 40 bar, 100°C, 45h. [b] turnover numbers were determined by comparing the ratio of product to substrate in the ^1H NMR spectrum of an aliquot of the reaction mixture.

The bis(triphenylphosphine)immium (PPN) cation is well-known for imparting a high degree of stability to air-sensitive anions, and has therefore been extensively used as counterion for anionic mono- and polynuclear metal carbonyls. [73-75] Ruff *et al* reported that the PPN^+ cation enables the isolation of $M_2(CO)_{10}SR^-$ (M = Cr, Mo, W, R = CH_3, C_6H_5, $C_6H_5CH_2$) anion as the PPN salts, which are orange to yellow solids. [76] In 1972, Schlientz and co-workers reported on the use of the PPN^+ cation as the counterion for isolating mononuclear mercaptide derivatives. [77]

The PPN^+ cation is readily available as halide salts and simple salts bearing inorganic anions such as cyanate, thiocyanate, azide and nitrate. X-ray photoelectron spectroscopic (ESCA) study on PPN salts implied that the phosphorous atoms in PPN^+ carry a degree of positive charge, while the nitrogen atom is largely negative in character, suggesting that the ionic structure (**Figure 4.1**) is the more appropriate description of PPN^+. [78]

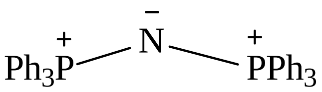

Figure 4.1: The ionic structure of PPN^+ cation

We reported in this chapter our study on the catalytic activity of some PPN salts (PPN^+Cl^-, $PPN^+Mn(CO)_5^-$, $PPN^+Mn(CO)_4(PPh_3)^-$) in the CO_2/epoxide coupling reactions to form cyclic carbonates.

4.2 Experimental

4.2.1 Reagents

All preparative reactions were carried out under a dry N_2 atmosphere using Schlenk techniques. All solvents were distilled and degassed prior to use. Dichloromethane was distilled from calcium hydride. Tetrahydrofuran, diethyl ether, toluene and hexane were distilled from sodium-benzophenone ketyl. Methanol and ethanol were distilled from magnesium and iodine.

(PPN)Cl (**4**) and $Li(C_2H_5)_3BH$ was purchased from Aldrich. $Mn_2(CO)_{10}$ was purchased from Strem. $Mn_2(CO)_8(PPh_3)_2$ [49] and $Li^+Mn(CO)_5^-$ [50] were prepared according to published procedures.

Epifluorohydrin, epichlorohydrin, epibromohydrin, styrene oxide, butadiene monoxide, isobutylene oxide and 1,2-epoxyhexane were purchased from Acros. All substrates were used as received.

4.2.2 Instrumentation

Infrared spectra were obtained from a Bruker Vector 22 FT-IR spectrophotometer. ^{1}H NMR spectra were obtained from a Bruker DPX 400 spectrometer at 400.13 MHz. Chemical shifts (δ, ppm) were measured relative to the proton residue of the deuterated solvent ($CDCl_3$-δ 7.26 ppm). $^{31}P\{^1H\}$ NMR spectra were taken on a Bruker DPX-400 spectrometer at 161.98 MHz. $^{31}P\{^1H\}$ NMR chemical shifts were externally referenced to 85% H_3PO_4 in D_2O (δ 0.00 ppm).

4.2.3 General procedures for the preparation of complexes

Preparation of $[PPN^+][Mn(CO)_5^-]$ (5):

A sample of $Mn_2(CO)_{10}$ (0.15g, 0.38 mmol) added to a Schlenk flask was dissolved in THF (10mL). $Li(C_2H_5)_3BH$ (0.1m, 0.96mL, 0.96 mmol, 2.5 equiv) was added slowly to the solution at 0°C. The reaction mixture was allowed to warm to room temperature and stir for 2.5h. A CH_2Cl_2 (10mL) solution of [PPN][Cl] (0.44g, 0.76 mmol) was transferred with a cannular to the Schlenk flask. The resulting solution was allowed to stir overnight at room temperature and then filtered through celite; the solvent of the filtrate was removed under vacuum. The residue was washed with diethyl ether (5mL) and then extracted with 10mL of toluene. The extract was brought to dryness to afford a yellow solid, which was washed with diethyl ether (2 x 5mL) and dried in vacuum. Yield 0.42g 0.57mmol (75%). IR (KBr, cm^{-1}): υ(C ≡ O) 1941 (m), 1962 (s), 1993 (s), 2008 (s). ^{1}H-NMR ($CDCl_3$, 400.13 MHz, 25°C): δ 7.83-7.27 (m, H's PPN). ^{31}P{^{1}H}-NMR ($CDCl_3$, 161.98 MHz, 25°C): δ 15.6 (s, 2P's of PPN). ^{13}C{^{1}H}-NMR ($CDCl_3$, 100.061 MHz, 25°C): δ 213.6 (CO), δ 215.9 (CO), δ 233.8 (CO), δ 237.6 (CO), δ 250.4 (CO).

Preparation of [PPN][$Mn(CO)_4PPh_3$] (6):

A sample of $Mn_2(CO)_8(PPh_3)_2$ (0.33g, 0.38 mmol) added to a Schlenk flask was dissolved in THF (10mL). $Li(C_2H_5)_3BH$ (1.0M, 0.96mL, 0.96 mmol, 2.5 equiv) was added slowly to the reaction mixture at 0°C. The solution was allowed to warm to room temperature and stir for 2.5h. A CH_2Cl_2 (10mL) solution of [PPN][Cl] (0.44g, 0.76 mmol) was transferred with a cannular to the Schlenk flask. The solution was allowed to stir overnight at room temperature and then filtered through celite, and the solvent of the filtrate was removed under vacuum. The residue was washed with diethyl ether (5mL) and then extracted with 10mL of toluene. The extract was brought to dryness to afford a yellow solid, which was washed with diethyl ether (2 x 5mL) and dried in vacuum. Yield 0.51g 0.53mmol (70%). IR (KBr, cm^{-1}): υ(C ≡ O) 1911 (s), 1931 (s), 1947 (s), 1977 (s). ^{1}H-NMR ($CDCl_3$, 400.13 MHz, 25°C): δ 7.45-7.76 (m, H's of PPN and PPh_3). $^{31}P\{^1H\}$-NMR ($CDCl_3$, 161.98 MHz, 25°C): δ 22.3 (s, 2P's of PPN), δ 77.3 (s, 1P of PPh_3). $^{13}C\{^1H\}$-NMR ($CDCl_3$, 100.061 MHz, 25°C): δ 189.9 (CO), δ 195.8 (CO), δ 201.6 (CO), δ 230.8 (CO).

Preparation of $PPN^+BF_4^-$ (7):

Samples of PPNCl (0.80g, 1.39mmol) and $Na^+BF_4^-$ (0.15g, 1.39mmol) were dissolved in THF (10mL), and the reaction mixture was stirred at room temperature for 24h. At the end of the reaction, the mixture was filtered through celite and the remaining solvent was dried under vacuum. Yield 0.63g 1.39mmol (72%). ^{1}H-NMR ($CDCl_3$, 400.13 MHz, 25°C): δ 7.70-7.35 (m, H's of PPN). $^{31}P\{^1H\}$-NMR ($CDCl_3$, 161.98 MHz, 25°C): δ 15.5 (s, P of PPN).

Preparation of PPN^+OTf^- (8):

Samples of PPNCl (0.80g, 1.39mmol) and Ag^+OTf^- (0.36g, 1.39mmol) were dissolved in THF (10mL), and the reaction mixture was stirred at room temperature for 24h. At the end of the reaction, the mixture was filtered through celite and the remaining solvent was dried under vacuum. Yield 0.73g 1.39mmol (76%). ^{1}H-NMR ($CDCl_3$, 400.13 MHz, 25°C): δ 7.75-7.30 (m, H's of PPN). $^{31}P\{^1H\}$-NMR ($CDCl_3$, 161.98

MHz, 25°C): δ 15.8 (s, P of PPN).

4.2.4 General Procedures for the CO_2/epoxide coupling reaction

Coupling reaction of CO_2 with epoxide:

Typical experimental procedures for the coupling reaction of epoxide with carbon dioxide are as follow: The catalyst [PPN][Cl] (0.0082g; 0.014mmol), [PPN][$Mn(CO)_5$] (0.0105g; 0.014mmol), or [PPN][$Mn(CO)_4PPh_3$] (0.0138g; 0.014mmol) was added to the epoxide (~1.0mL; 1000 equiv no of mole) in a 10 mL stainless steel autoclave equipped with a magnet stirring bar. The solution was heated with stirring under 5 bar of CO_2 at 100°C. At the end of the required length of time, the autoclave was cooled rapidly and vented carefully. The yield of cyclic carbonate was determined by ^{1}H-NMR spectroscopy. The set of three signals for the two methylene hydrogen atoms and the hydrogen on the substituted carbon of the substrate epoxide is well-separated from the set of three signals for the corresponding hydrogen atoms of the products cyclic carbonate. The yield of the cyclic carbonate can therefore be determined by comparing the sum of integration of one set of hydrogen atoms with that of the other set. To identify the cyclic carbonate, at the conclusion of the catalytic reaction, the unreacted epoxide, which has a much lower boiling point than the cyclic carbonate, was easily removed under reduced pressure, and the cyclic carbonate that remained was identified by comparing its ^{1}H NMR spectrum with that of the authentic sample.

4.2.5 Epoxides used for the CO_2/epoxide coupling reactions

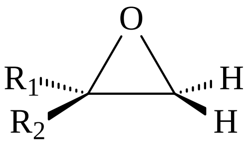

Substrates	R_1	R_2
Epifluorohydrin	CH_2F	H
Epichlorohydrin	CH_2Cl	H
Epibromohydrin	CH_2Br	H
Styrene oxide	Ph	H
Propylene oxide	CH_3	H
Butadiene monoxide	$CH=CH_2$	H
1,2-epoxyhexane	$CH_2CH_2CH_2CH_3$	H
Isobutylene oxide	CH_3	CH_3

4.3 Results and Discussion

4.3.1 Synthesis and characterization of complex 6

$PPN^+Mn(CO)_4(PPh_3)^-$ (**6**) is formed by reacting $Li^+Mn(CO)_4(PPh_3)^-$ with PPN^+Cl^- in CH_2Cl_2 overnight. The $^{31}P\{^1H\}$ NMR spectrum of **6** shows two singlets at δ 22.3 and 77.3 ppm, due to the P atom of the PPN^+ cation and the PPh_3 ligand coordinated to Mn center, respectively. In the infrared spectrum, the four peaks appeared at 1911 (m), 1931 (s), 1947 (s), and 1977 (s) cm^{-1} that are due to the terminal carbonyl groups of Mn. The singlets at δ 189.9, 195.8, 201.6, and 230.8 ppm in the $^{13}C\{^1H\}$ NMR spectrum are due to the carbonyl groups.

4.3.2 Carbon dioxide/epoxide coupling reactions with 4, 5 and 6

The readily available salt PPN^+Cl^- **(4)** and the complexes $PPN^+Mn(CO)_5^-$ **(5)** and $PPN^+Mn(CO)_4(PPh_3)^-$ **(6)** are able to catalyze the coupling reactions of epoxides with CO_2 to produce the corresponding cyclic carbonates at 80°C or 100°C under 5bar of CO_2 without solvent and additives. The epoxides were converted to the corresponding cyclic carbonates with satisfactory yields and no side products were formed. The results of CO_2/epoxide coupling reaction catalyzed by **4**, **5** and **6** are shown in **Table 4.2**. All three PPN salts are active at lower temperature (80°C), the TON and TOF are however much lower than those obtained at 100°C. It can be seen that the epihalohydrins which contain electron-withdrawing groups, show higher reactivity. (**Entries 1─6, 8─10, 31-39 Table 4.2**)

Table 4.2: Coupling of epoxides with CO_2 catalyzed by PPN salts[a]

Entry	Substrate	Temperature (°C)	Time (h)	Catalyst	TON[b]	TOF (h^{-1})[c]
1	Epifluorohydrin	100	1	**4**	867	867
2	Epifluorohydrin	100	1	**5**	876	876
3	Epifluorohydrin	100	1	**6**	847	847
4	Epichlorohydrin	100	1	**4**	846	846
5	Epichlorohydrin	100	1	**5**	853	853
6	Epichlorohydrin	100	1	**6**	809	809
7	Epichlorohydrin	100	1	**3**	23	23
8	Epibromohydrin	100	1	**4**	828	828
9	Epibromohydrin	100	1	**5**	846	846
10	Epibromohydrin	100	1	**6**	808	808
11	Epibromohydrin	100	1	**3**	19	19
12	Styrene oxide	100	6	**4**	790	132
13	Styrene oxide	100	6	**5**	772	129
14	Styrene oxide	100	6	**6**	783	131
15	Propylene oxide	100	6	**4**	665	111
16	Propylene oxide	100	6	**5**	669	112
17	Propylene oxide	100	6	**6**	624	104
18	Propylene oxide	100	6	**3**	60	10
19[d]	Propylene oxide	100	6	**3**	nil	nil
20	Propylene oxide	100	24	**7**	nil	nil
21	Propylene oxide	100	24	**8**	nil	nil
22	Butadiene monoxide	100	6	**4**	638	106

23	Butadiene monoxide	100	6	**5**	624	104
24	Butadiene monoxide	100	6	**6**	642	107
25	1,2-epoxyhexane	100	6	**4**	646	108
26	1,2-epoxyhexane	100	6	**5**	628	105
27	1,2-epoxyhexane	100	6	**6**	634	106
28	Isobutylene oxide	100	6	**4**	668	111
29	Isobutylene oxide	100	6	**5**	653	109
30	Isobutylene oxide	100	6	**6**	627	105
31	Epifluorohydrin	80	2	**4**	867	867
32	Epifluorohydrin	80	2	**5**	876	876
33	Epifluorohydrin	80	2	**6**	847	847
34	Epichlorohydrin	80	2	**4**	846	846
35	Epichlorohydrin	80	2	**5**	853	853
36	Epichlorohydrin	80	2	**6**	809	809
37	Epibromohydrin	80	2	**4**	828	828
38	Epibromohydrin	80	2	**5**	846	846
39	Epibromohydrin	80	2	**6**	808	808
40	Styrene oxide	80	24	**4**	790	132
41	Styrene oxide	80	24	**5**	772	129
42	Styrene oxide	80	24	**6**	783	131
43	Propylene oxide	80	24	**4**	665	111
44	Propylene oxide	80	24	**5**	669	112
45	Propylene oxide	80	24	**6**	624	104
46	Butadiene monoxide	80	24	**4**	638	106
47	Butadiene monoxide	80	24	**5**	624	104
48	Butadiene monoxide	80	24	**6**	642	107

49	1,2-epoxyhexane	80	24	**4**	646	108
50	1,2-epoxyhexane	80	24	**5**	628	105
51	1,2-epoxyhexane	80	24	**6**	634	106
52	Isobutylene oxide	80	24	**4**	668	111
53	Isobutylene oxide	80	24	**5**	653	109
54	Isobutylene oxide	80	24	**6**	627	105

[a]Typical reaction conditions: Catalyst: 3.5μmol [PPN][Cl] **(4)**, [PPN][Mn(CO)$_5$] **(5)**, [PPN][Mn(CO)$_4$(PPh$_3$)] **(6)**, [79][Mn(CO)$_4$(PPh$_3$)] **(3)**, [PPN][BF$_4$] **(7)**, [PPN][OTf] **(8)** substrate: 3.5mmol (S/C = 1000), CO$_2$ pressure 5 bar. [b]Turnover numbers were determined by comparing the ratio of product to substrate in the ^{1}H NMR spectrum of an aliquot of the reaction mixture. [c]Moles of cyclic carbonates products per mole of catalyst per hour. [d]7.0μmol of 12-crown-4 added.

4.3.3 Proposed mechanism for the catalytic CO_2/expoxide coupling reaction

The catalytic reactions were carried out in neat epoxides. No CO_2/epoxide copolymer was formed in each of the reactions. We monitored the **4-**, **5-**, and **6**-catalyzed CO_2/ propylene oxide coupling reactions by high pressure ^{31}P NMR spectroscopy. It was found that in each case the PPN cation was the only phosphorus-containing species throughout the experiment.

A possible mechanism for the PPN salt-catalyzed coupling reactions is proposed and shown in **Scheme 4.1**. Coordination of the epoxide to the phosphorus atom of PPN^+ activates the former towards nucleophilic ring opening by Y^- (Y^- = Cl^-, $Mn(CO)_5^-$, or $Mn(CO)_4(PPh_3)^-$). It is widely accepted that coordination of an epoxide to a Lewis acid facilitates nucleophilic ring-opening of the former. For example, it has been shown by Jacobsen, *et al.* that coordination of the epoxide to the (salen)Cr(III) complex is a necessary step to activate the former towards nucleophilic ring-opening by the (salen)Cr(III)-azide complex (**Scheme 4.2**). [9] In **Scheme 4.1**, insertion of CO_2 into **A** then gives the carbonato species **B**. Although **A** is not exactly a metal-alkoxy complex, its reactivity towards CO_2 is expected to be similar to that of metal alkoxides. Insertion of CO_2 into a metal-alkoxy bond to form metal carbonate species is well documented. [66, 80] Finally, the S_N2-type ring-closing step gives the cyclic carbonate product. A similar mechanism has been proposed for the CO_2/epoxide coupling reaction with other catalyst systems. [19, 26, 31, 79, 81-83] It was learned that in the coupling reactions catalyzed by various salts M^+X^- (M^+ = Na^+, Li^+ or $PhCH_2N^+Me_3$), only the halide salts (Br^-, Cl^-, and I^-) showed considerable activity. The salts with nonnucleophilic anions, such as *p*-toluenesulfonate and perchlorate, and salts with higher nucleophilic anions such as acetate, cyanide, phenolate, and thiophenolate showed very low activity. The activity of the halide salts is attributable to the halide ions possessing nucleophicity high enough to ring-open the epoxide and good leaving ability essential to the ring-closure, which is a S_N2-type reaction on sp^3 carbon. [19]

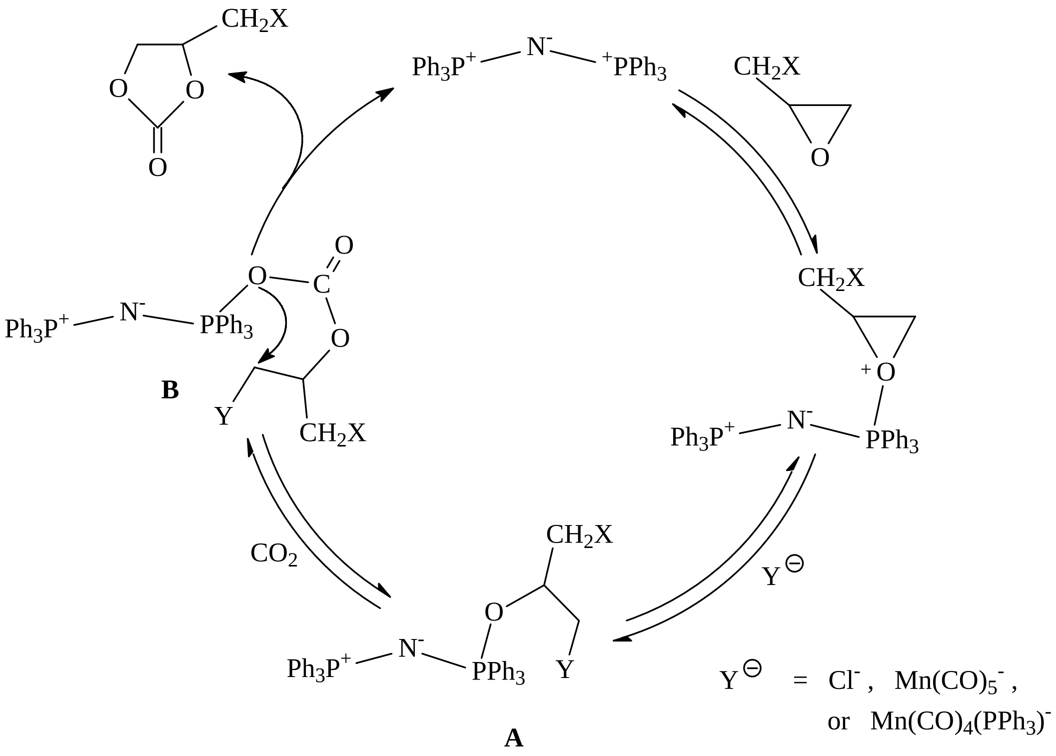

Scheme 4.1: PPN salt-catalyzed the coupling reaction of CO_2 and epoxide

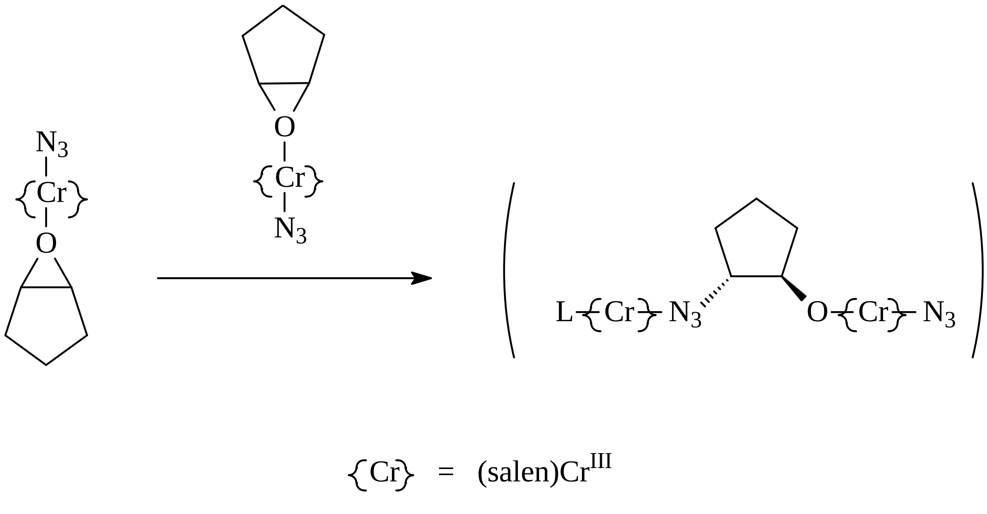

Scheme 4.2: Epoxide activate and ring-opening by Cr complexes proposed by Jacobsen

An alternative mechanism involving parallel Lewis-acid-activation of epoxide and Lewis-base-activation of CO_2 is shown in **Scheme 4.3**. This pathway also begins with PPN-activation of the epoxide molecule. In the second step, it is proposed that the anion, instead of ring-opening the epoxide, activates the carbon dioxide molecule by forming the manganese formate (**eq 4.1**) or the chloroformate (**eq 4.2**). Gibson *et al.* have proposed that the mangenese carboxylate $[Mn(CO)_4(PPh_3)(CO_2)]^-$, which has not been isolated, to be the intermediate in the reaction of $K^+[CpFe(CO)(PPh_3)(CO_2)]^-$ with $[Mn(CO)_5(PPh_3)]^+BF_4^-$ followed by addition of CH_3I to afford $[CpFe(CO)_2(PPh_3)]^+BF_4^-$ and $Mn(CO)_4(PPh_3)(CH_3)$. [63] Moreover, since the catalytic reactions were performed in neat substrates, it is conceivable, in the absence of solvating solvent, that the chloride anion (in the case of PPN^+Cl^-) might possess greatly enhanced nucelophilicity. It would react with carbon dioxide to generate the chloroformate anion. The manganese formate or chloroformate opens the expoxide forming **C**, and finally ring-closure gives the product. A similar mechanism involving haloformate anion opening up the epoxide has been proposed. [19]

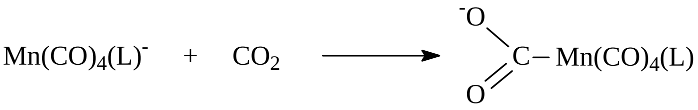

$$Mn(CO)_4(L)^- + CO_2 \longrightarrow {}^-O_2C{-}Mn(CO)_4(L) \qquad (4.1)$$

L = CO , PPh_3

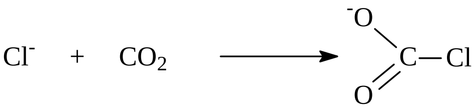

$$Cl^- + CO_2 \longrightarrow {}^-O_2C{-}Cl \qquad (4.2)$$

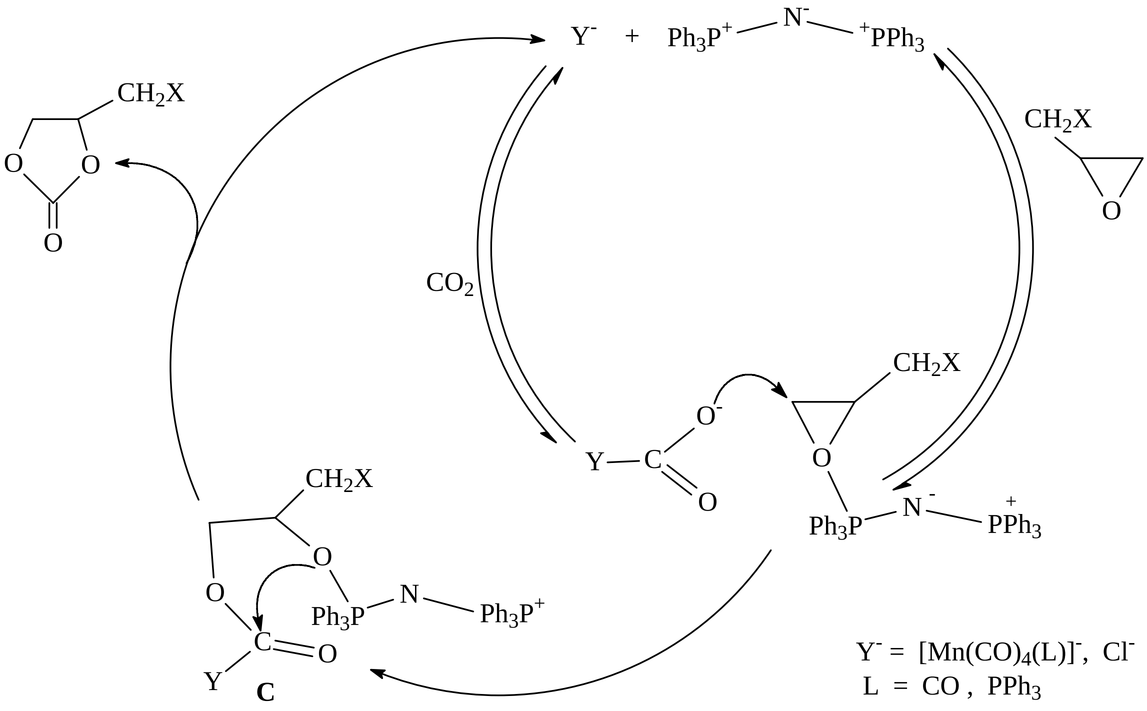

Scheme 4.3: PPN manganese carbonates-catalyzed the coupling reaction of CO_2 and epoxide

At this stage, we are not able to favor one mechanism over the other one. More works would have to be done to elucidate the mechanistic details of the catalytic reactions. It is observable that the epihalohydrins react faster than the other epoxides (Entries **1-6, 8-10, Table 4.2**). A possible explanation for the enhanced activity of the epihalohydrins might lies on the greater electrophilicity of the epoxide carbons of these compounds facilitating the ring-closure step (**Scheme 4.1**) or ring-opening step (**Scheme 4.3**) in two mechanisms that we proposed. Paddock and Nguyen have found the epichlorohydrin to be the most active epoxide among the aromatic and aliphatic epoxides in the Cr(III)salen complex – catalyzed CO_2/epoxide coupling reactions. [28]

4.4 Conclusion

We have shown that the PPN manganese carbonyls and more interestingly the off-the-shelf reagent PPN^+Cl^- are good catalysts for the coupling reactions of CO_2 (5 bar) with epoxides to yield cyclic carbonates. The reactions are clean with no polycarbonate contamination, and are performed in neat substrates with no need of organic solvents. Works aimed at elucidating the mechanistic details of the catalytic reactions are now in progress.

Chapter 5 Conclusion

We found that the heterobimetallic complex η^5-$C_5H_5Ru(CO)(\mu\text{-dppm})Mn(CO)_4$ (**1**) and the complex $Li^+[Mn(CO)_4(PPh_3)]^-$ (**2**) catalyzed the coupling reactions of CO_2 and epoxides to afford the corresponding cyclic carbonates with satisfactory yields. We studied and compared the reactivities of complexes **1** and **2**, and found that the latter, in which the two metal centers are not linked, showed lower reactivity than the former. Our study indicates that cooperative participation of the metal centers of the complexes is in operation during catalysis. Mechanisms of the **1**-, and **2**-catalyzed CO_2/epoxide coupling reaction have been proposed.

Theoretical calculations support a reaction pathway involving a heterolytic cleavage of the Ru-Mn bond with the epoxide coordinating to the Lewis acidic Ru center, the Lewis basic Mn center then ring-open the epoxide; subsequent CO_2 insertion into the Ru-O bond affords the alkoxide intermediate, which then undergoes ring-closure to yield the cyclic carbonate product.

The heterbimetallic complex η^5-$C_5H_5Ru(CO)(\mu\text{-dppm})Mn(CO)_4$ (**1**), $Li^+[Mn(CO)_4(PPh_3)]^-$ (**2**) and $[\eta^5\text{-}C_5H_5Ru(CO)(PPh_3)(CH_3CN)]^+[BF_4]^-$ (**3**) are found to be able to catalyze the desulphurization reactions of thiiranes to afford corresponding olefins with satisfactory yields. The bimetallic complex **1** was found to show higher catalytic activity than the monometallic species **2** and **3**. Mechanisms with the thiirane coordinating to the metal center as the first step are proposed for the **1**-, **2**-, and **3**-catalyzed thiirane desulphurization reactions.

We showed that the off-the-shelf reagent PPN^+Cl^- (**4**) is a good catalyst for the coupling reactions of CO_2 (5 atm) with epoxides to yield cyclic carbonates. We have studied and compared the catalytic reactivities of **4** with the PPN-manganese carbonylate complexes $[PPN]^+[Mn(CO)_5]^-$ (**5**) and $[PPN]^+[Mn(CO)_4(PPh_3)]^-$ (**6**). These PPN salts show very similar catalytic activity. The reactions are clean with no polycarbonate contamination, and are performed in neat substrates with no need of organic solvents. Works aimed at elucidating the mechanistic details of the catalytic reactions are now in progress.

Reference

1. Broussard, M.E., Juma, B., Train, S. G., Peng, W.-J., Laneman, S. A., and Stanley, G. G., *A Bimetallic Hydroformylation Catalyst: High Regioselectivity and Reactivity Through Homobimetallic Cooperativity.* Science, 1993. **260**: p. 1784-1788.

2. Matthews RC, H.D., Peng WJ, Train SG, Treleaven WD, Stanley GG, *Bimetallic hydroformylation catalysis: In situ characterization of a dinuclear rhodium(II) dihydrido complex with the largest Rh-H NMR coupling constant.* Angewandte Chemie, International Edition in English, 1996. **35**: p. 2253-2256.

3. Torres, F., Sola, E., Elduque, A., Martinez, A. P., Lahoz, F. J., and Oro, L. A., *Evidence for a Dinuclear Mechanism in Alkyne Hydrogenations Catalyzed by Pyrazolate-Bridged Diiridium Complexes. Chemistry, a European Journal*, 2000. **6**: p. 2120-2128.

4. Ishii Y, M.K., Kamita K, Hidai M, *Selective hydroformylation of internal acetylenes by PdCl2(PCy3)(2): Remarkable synergistic effect of cobalt.*

Journal of the American Chemical Society, 1997. **119**: p. 6448-6449.

5. Trepanier SJ, S.B., McDonald R, Cowie M, *Selective coupling of methylene units in a Rh/Os complex to give either C-3 or C-4 fragments.* Journal of the American Chemical Society, 1999. **121**: p. 2613-2614.

6. Gao Y, K.J., Yap GPA, Puddephatt RJ, *An efficient binuclear catalyst for decomposition of formic acid.* Chemical Communications, 1998. **21**: p. 2365-2366.

7. Gao Y, K.J., Jenkins HA, Puddephatt RJ, Yap GPA, *The interconversion of formic acid and hydrogen/carbon dioxide using a binuclear ruthenium complex catalyst.* Journal of Chemical Society, Dalton Transactions, 2000. **18**: p. 3212-3217.

8. Mahadevan, V., Getzler, Y. D. Y. L., and Coates, G. W., *[Lewis acid]+[CO(CO)(4)](-) complexes: A versatile class of catalysts for carbonylative ring expansion of epoxides and aziridines. Angewandte Chemie, International Edition in English*, 2002. **41**: p. 2781-2784.

9. Hansen, K.B.L., J. L.; Jacobsen, E. N.; *On the Mechanism of Asymmetric Nucleophilic Ring-Opening of Epoxides Catalyzed by (Salen)CrIII Complexes.*

Journal of the American Chemical Society, 1996. **118**: p. 10924-10925.

10. Leitner, W., *The coordination chemistry of carbon dioxide and its relevance for catalysis: A critical study. Coordination Chemistry Reviews*, 1996. **155**: p. 257-284.

11. Arakawa H, A.M., Armor JN, Barteau MA, Beckman EJ, Bell AT, Bercaw JE, Creutz C, Dinjus E, Dixon DA, Domen K, DuBois DL, Eckert J, Fujita E, Gibson DH, Goddard WA, Goodman DW, Keller J, Kubas GJ, Kung HH, Lyons JE, Manzer LE, Marks TJ, Morokuma K, Nicholas KM, Periana R, Que L, Rostrup-Nielson J, Sachtler WMH, Schmidt LD, Sen A, Somorjai GA, Stair PC, Stults BR, Tumas W, *Catalysis research of relevance to carbon management: Progress, challenges, and opportunities. Chemical Reviews*, 2001. **101**: p. 953-996.

12. Behr, A., *Carbon-dioxide as an alternative C1 synthetic unit-activation by transition-metal complexes. Angewandte Chemie, International Edition in English*, 1988. **27**: p. 661-678.

13. Behr, A., *Use of carbon dioxide in industrial organic syntheses.* Chemical Engineering and Technology, 1987. **10**: p. 16-27.

14. Denise, B., and Sneeden, R. P. A., *Hydrogenate CO2. CHEMTECH*, 1982: p. 108-112.

15. Shaikh, A.-A.G., and Sivaram, S., *Organic carbonates. Chemical Reviews*, 1996. **96**: p. 951-976.

16. Inoue, S.K., H. and Tsuruta, T, J. Polym Sci, 1969. **B7**: p. 287.

17. Darensbourg, D.J., Holtcamp, M. W., *Catalysts for the reactions of epoxides and carbon dioxide. Coordination Chemistry Reviews*, 1996. **153**: p. 155-174.

18. Ratzenhofer, M., Kisch, H., *Metal-catalyzed synthesis of cyclic carbonates from carbon-dioxide and oxiranes. Angewandte Chemie, International Edition in English*, 1980. **19**: p. 317-318.

19. Kihara, N., Hara, N., Endo, T., *Catalytic activity of various salts in the reaction of 2,3-epoxypropyl phenyl ether and carbon-dioxide under atmospheric-pressure. Journal of Organic Chemistry*, 1993. **58**: p. 6198-6202.

20. Yano, T., Matsui, H., Koiki, T., Ishiguro, H., Fujihara, H., Yoshihara, M., Maeshima, T., *Magnesium oxide-catalysed reaction of carbon dioxide with an epoxide with retention of stereochemistry. Chemical Communication*, 1997. **12**: p. 1129-1130.

21. Yamaguchi, K., Ebitani, K., Yoshida, T., Yoshida, H., Kaneda, K., *Mg-Al mixed oxides as highly active acid-base catalysts for cycloaddition of carbon dioxide to epoxides. Journal of the American Chemical Society*, 1999. **121**: p. 4526-4527.

22. Iwasaki, T., Kihara, N., Endo, T., *Reaction of various oxiranes and carbon dioxide. Synthesis and aminolysis of five-membered cyclic carbonates. Bulletin of the Chemical Society of Japan*, 2000. **3**: p. 713-719.

23. Tsuda, T., Chujo, Y., and Saegusa, T., *Copper (I) cyanoacetate as a carrier of activated carbon dioxide. Journal of Chemical Society, Chemical Communications*, 1976: p. 415-416.

24. Karlsson, J.-E.B.a.O., *Stereochemistry of copper- and nickel-catalyzed insertion of carbon dioxide into epoxides. A microwave study. Tetrahedron Letters*, 1980. **21**: p. 4985-4988.

25. Fujinami T, S.T., Kamiya M, Fukuzawa S, Sakkai S, *Palladium catalyzed reaction of butadiene monoxide with carbon-dioxide. Chemical Letters*, 1985: p. 199-200.

26. Hoon Sik Kim, J.J.K., Byung Gwon Lee, Ok Sang Jung, Ho Gyeom Jang,

Sang Ook Kang, *Isolation of a Pyridinium Alkoxy Ion Bridged Dimeric Zinc Complex for the Coupling Reactions of CO2 and Epoxides. Angewandte Chemie International Edition*, 2000. **39**: p. 4096-4098.

27. Kruper W. J, D.D.V., *Cataltic formation of cyclic carbonates from epoxides and CO2 with chromium metalloporphyrinates. Journal of Organic Chemistry*, 1995. **60**: p. 725-727.

28. Paddock, R.L.a.N., S. T, *Chemical CO2 Fixation: Cr(III) Salen Complexes as Highly Efficient Catalysts for the Coupling of CO2 and Epoxides. Journal of the American Chemical Society*, 2001. **123**: p. 11498-11499.

29. Kasuga K, K.N., *The fixation of carbon dioxide with 1,2-epoxypropane catalyzed by alkali-metal halide in the presence of a crown ether. Inorganica Chimica Acta*, 1997. **257**: p. 277-278.

30. Aida, T., and Inoue, S., *Activation of carbon dioxide with aluminum porphyrin and reaction with epoxide. Studies on (tetraphenylporphinato)aluminum alkoxide having a long oxyalkylene chain as the alkoxide group. Journal of the America Society*, 1983. **104**: p. 1304-1309.

31. Calo V, N.A., Monopoli A, Fanizzi A, *Cyclic carbonate formation from*

carbon dioxide and oxiranes in tetrabutylammonium halides as solvents and catalysts. Organic Letters, 2002. **15**: p. 2561-2563.

32. Tascedda P, D.E., *Novel electrochemical reactivity of Ni(cyclam)Br2-catalytic carbon-dioxide incorporation into epoxides. Journal of Chemical Society Chemical Communications*, 1995. **1**: p. 43-44.

33. Tascedda P, W.M., Dinjus E, et al., *Nickel-catalyzed electrochemical carboxylation of epoxides: mechanistic aspects. Applied Organometallic Chemistry*, 2001. **15**: p. 141-144.

34. Super M, B.E., Costello C, Beckman E, *Copolymerization of 1,2-epoxycyclohexane and carbon dioxide using carbon dioxide as both reactant and solvent. Macromolecules*, 1997. **30**: p. 368-372.

35. Kawanami H, I.Y., *Chemical fixation of carbon dioxide to styrene carbonate under supercritical conditions with DMF in the absence of any additional catalysts. Chemical Communications*, 2000. **21**: p. 2089-2090.

36. Yasuda H, H.L., Sakakura T, *Cyclic carbonate synthesis from supercritical carbon dioxide and epoxide over lanthanide oxychloride. Journal of Catalysis*, 2002. **209**: p. 547-550.

37. Yang, H.Z., Gu, Y., Deng, Y., and Shi, F., *Electrochemical activation of carbon dioxide in ionic liquid: synthesis of cyclic carbonates at mild reaction conditions. Chemical Communications*, 2002: p. 274-275.

38. Sander, M., *Thiiranes.* Chemical Reviews, 1966. **66**: p. 297-339.

39. Kendall JD, S.N., *Rhodium catalysed S- and SO-transfer: Novel syntheses of norbornane episulfoxides and episulfides.* SYNLETT, 1998. **4**: p. 391-392.

40. Dittmer, D.C., *Thiiranes and Thiirenes.* Pergamon, Oxford, 1984. **7**.

41. Torres M, L. E., Gunning H. E., Strausz O. P., *4n-pi-electron antiaromatic heterocycles.* Pure and Applied chemistry, 1980. **52**: p. 1623-1643.

42. Jacob, J.E., J. H., *Stereospecific rhenium catalyzed desulfurization of thiiranes.* Chemical Communications, 1999: p. 1003-1004.

43. Adams, R.D.Q., J. A.; Yamamoto, J. H., *Catalytic Transformations of Thiiranes by the W(CO)5 Grouping. A New Route to Cyclic Polydisulfides.* Journal of the American Chemical Society, 1996. **118**: p. 10674-10675.

44. Adams, R.D.Y., J. H.; Holmes, A.; Baker, B. J., *Catalytic Transformations of Thiiranes by (Thiirane)W(CO)5 Complexes.* Organometallics, 1997. **16**: p. 1430-1439.

45. Adams, R.D.P., J. L., *Catalytic Transformations of Vinylthiiranes by Tungsten Carbonyl Complexes. A New Route to 3,6-Dihydro-1,2-dithiins.* Journal of the American Chemical Society, 1999. **121**: p. 3984-3991.

46. Alper, H., Paik, H. N., *New effective desulfurization reagents.* The Journal of Organic Chemistry, 1977. **42**: p. 3522-3524.

47. Fasi, A.G., A. Palinko, I and Kiricsi, I, *Cyclodimerisation and Cyclotrimerisation During the Ring-Opening Reactions of Ethylene Sulfide (Thiirane) over Acidic Molecular Sieves and Alumina.* Catalysis Letters, 2001. **76**: p. 95-98.

48. Komiya, S.M., S. Furuya, M. and Hirano, M., *Regio- and Stereoselective Insertion Reactions of Thiiranes into Pt-Mn (or Re) Bond in Organoplatinum-Manganese or -Rhenium Heterodinuclear Complexes as Intermediates toward Desulfurization Reaction.* Journal of the American Chemical Society, 2000. **122**: p. 170-171.

49. Drew, D.D., D. J. Darensbourg, M. Y., *Synthesis, spectral properties, and reactions of manganese and rhenium pentacarbonyl phosphine and phosphite cation derivatives and related complexes.* Inorganic Chemistry, 1975. **14**: p.

1579-1584.

50. Gladysz, J.A.W., G. M. Tam, W. Johnson, D. L. Parker, D. W. Selover, J. C., *Synthesis of metal carbonyl monoanions by trialkylborohydride cleavage of metal carbonyl dimers: a convenient one-flask preparation of metal alkyls, metal acyls, and mixed-metal compounds.* Inorganic Chemistry, 1979. **18**: p. 553-558.

51. Bruce, M.I.H., C. Swincer, A. G. and Wallis, R. C., *some η5-cyclopentadienylruthenium (II) complexes containing triphenylphosphine.* Inorganic Synthesis, 1982. 2**1:** p. 78-84.

52. King, R.B.a.S., F. G. A., C*yclopentadienyl metal carbonyls and some derivatives.* Inorganic Synthesis, 1963. 7**:** p. 99-115.

53. Fukui, K., A *formulation of reaction coordinate.* Journal of physical chemistry, 1970. 7**4:** p. 4161-4163.

54. Fukui, K., T*he path of chemical-reactions-the irc approach.* Accounts of chemical research, 1981. 1**4:** p. 363-368.

55. Hay P. J., W.W.R., A*binitio effective core potentials for molecular calculations-potentials for the transition-metal atoms Sc to Hg.* Journal of

chemical physics, 1985. 8**2:** p. 270-283.

56. Wadt W. R., H.P.J., A*binitio effective core potentials for molecular calculations-potentials for main group elements Na to Bi.* Journal of chemical physics, 1985. 8**2:** p. 284-298.

57. Hay P. J., W.W.R., A*binitio effective core potentials for molecular calculations-potentials for K to Au including the outermost core orbitals.* Journal of chemical physics, 1985. 8**2:** p. 299-310.

58. Gordon, M.S., T*he isomers of silacyclopropane.* Chemical Physics Letters, 1980. 7**6:** p. 163-168.

59. Harihara P. C., P.J.A., I*nfluence of polarization functions on molecular-orbital hydrogenation energies.* Theoretica chimica acta, 1973. 2**8:** p. 213-222.

60. Caffyn A. J. M., M.M.J., Raithby P. R., S*ynthesis of Phosphido-Bridged Ruthenium Manganese Complexes - X-Ray Crystal-Structures of (RuMn(Mu-H)(Mu-PPH2)-(ETA-5-C5H5)(CO)5), (Ru2(Mu-H)(Mu-PPH2)(ETA-5-C5H5)2(CO)2) and (RuMn2(Mu-H)(MU-PPH2)2(ETA-5-C5H5)(CO)9).* Journal of the Chemical Society-Dalton Transactions, 1991. 9**:** p. 2**349-2356.**

61. Nieuwenhuis H. A., V.A., Moraal M. A., Stufkens D. J., Oskam A., Goubitz K, S*ynthesis, structure and spectroscopic properties of novel metal-metal bonded Manganese-Ruthenium complexes with alpha-diimine ligands-X-ray structure of [(CO)(5)Mn-Ru(Me)(CO)(2)(Sigma(N),Sigma(N')-IPR-PYCA)](IPR-PYCA=Pyridine-2-Carbaldehyde-N-Isopropylimine).* Inorganica Chimica Acta, 1995. 2**32:** p. 19-25.

62. Man ML, Z.Z., Ng SM, Lau CP, S*ynthesis, characterization and reactivity of heterobimetallic complexes (eta(5)-C5R5)Ru(CO)(mu-dppm)M(CO)(2)(eta(5)-C5H5) (R = H, CH3; M = Mo, W). Interconversion of hydrogen/carbon dioxide and formic acid by these complexes.* Dalton Transactions, 2003. 1**9:** p. 3727-3735.

63. Gibson, D.H.a.O., T. S., S*ynthesis and reactions of anionic metallocarboxylates of iron.* Journal of the American Chemical Society, 1987. 1**09:** p. 7191-7193.

64. Martinez, L.E.L., J. L. Carsten, D. H. Jacobsen, E. N., H*ighly Enantioselective Ring Opening of Epoxides Catalyzed by (salen)Cr(III) Complexes.* Journal of the American Chemical Society, 1995. 1**17:** p. 5897-5898.

65. Hoon Sik Kim, J.J.K., Sang Deuk Lee, Myoung Soo Lah, Dohyun Moon, Ho Gyeom Jang, N*ew Mechanistic Insight into the Coupling Reactions of CO2 and Epoxides in the Presence of Zinc Complexes.* Chemistry - A European Journal, 2003. 9**:** p. 678-686.

66. Darensbourg, D.J.H., M. W.; Struck, G. E.; Zimmer, M. S.; Niezgoda, S. A.; Rainey, P.; Robertson, J. B.; Draper, J. D.; Reibenspies, J. H., C*atalytic Activity of a Series of Zn(II) Phenoxides for the Copolymerization of Epoxides and Carbon Dioxide.* Journal of the American Chemical Society, 1999. 1**21:** p. 107-116.

67. Cordaro, J.G.B., R. G., D*issociation of Carbanions from Acyl Iridium Compounds: An Experimental and Computational Investigation.* Journal of the American Chemical Society, 2004. 1**26:** p. 16912-16929.

68. Weihold, E.D.G.A.E.R.J.E.C.F., N*BO.* V**ersion 3.1.**

69. Humphries, A.P.K., S. A. R., R*eaction of Cyclopentadiene with Carbonyl-Ruthenium and Carbonyl-Osmium Complexes.* Journal of the Chemical Society-Dalton Transactions, 1975. 1**6:** p. 1710-1714.

70. Yadav, J.S.R., B. V. S.; Reddy, Ch. S.; Rajasekhar, K., [*Bmim]PF6: A Novel*

and Recyclable Ionic Liquid for Conversion of Oxiranes to Thiiranes in Aqueous Media. The Journal of Organic Chemistry, 2003. 6**8:** p. 2525-2527.

71. Iranpoor, N.a.K., F., S*tereospecific formation of S(?) styrene sulfide: Efficient conversion of epoxides to thiiranes catalysed with Ru(III).* Tetrahedron, 1997. 5**3:** p. 11377-11382.

72. Amarasekera, J., Rauchfuss, T. B., Wilson, S. R., S*ynthesis and structure of [CpRu(PPh3)2(SC2H4)]OSO2CF3. A transition-metal analog of an episulfonium salt.* Journal of the American Chemical Society, 1988. 1**10:** p. 2332-2334.

73. Ruff, J.K., C*hemistry of the dinuclear carbonyl anions. III. Halogen-bridged anions.* Inorganic Chemistry, 1968. 7**:** p. 1821-1825.

74. Ruff, J.K., C*hemistry of the dinuclear carbonyl anions. II. Mixed-metal derivatives.* Inorganic Chemistry, 1968. 7**:** p. 1818-1821.

75. Ruff, J.K., L*ewis adducts of the Fe(CO)42- and Co(CO)4-.* Inorganic Chemistry, 1968. 7**:** p. 1499-1503.

76. Ruff, J.K.a., R. B., C*hemistry of the dinuclear carbonyl anions. V. Sulfur-bridged derivatives.* Inorganic Chemistry, 1969. 8**:** p. 180-181.

77. Schlientz, W.J.a.R., J. K., C*hemistry of dinulcear carbonly anions. VII. Anionic metal carbonyl mercaptides.* Inorganic Chemistry, 1972. 1**1:** p. 2265-2267.

78. Swartz, W.E.R., J. K. and Hercules, D. M., X*-ray photoelectron spectroscopic study of some bis(triphenylphosphine)iminium salts.* Journal of the American Chemical Society, 1972. 9**4:** p. 5227 - 5229.

79. Li, F.X., L. Xia, C. Hu, B., C*hemical fixation of CO2 with highly efficient ZnCl2/[BMIm]Br catalyst system.* Tetrahedron Letters, 2004. 4**5:** p. 8307-8310.

80. Tsuda, T.S., S. Ueda, K and Saegusa, T, A *new reversible carbon dioxide carrier. (tert-Butylcarbonato)tris(tert-butyl isocyanide)copper(I), t-BuOCO2Cu(CN-t-Bu)3.* Inorganic Chemistry, 1976. 1**5:** p. 2329-2332.

81. Shen, Y.-M.D., W.-L.; Shi, M., C*hemical Fixation of Carbon Dioxide Catalyzed by Binaphthyldiamino Zn, Cu, and Co Salen-Type Complexes.* Journal of Organic Chemistry, 2003. 6**8:** p. 1559-1562.

82. Shi, J.-W.H.a.M., C*hemical Fixation of Carbon Dioxide by NaI/PPh3/PhOH.* Journal of Organic Chemistry, 2003. 6**8:** p. 6705-6709.

83. Shen, Y.-M., Duan, W-L, Shi , M, C*hemical Fixation of Carbon Dioxide Co-Catalyzed by a Combination of Schiff Bases or Phenols and Organic Bases.* European Journal of Organic Chemistry, 2004: p. 3080-3089.

Appendix

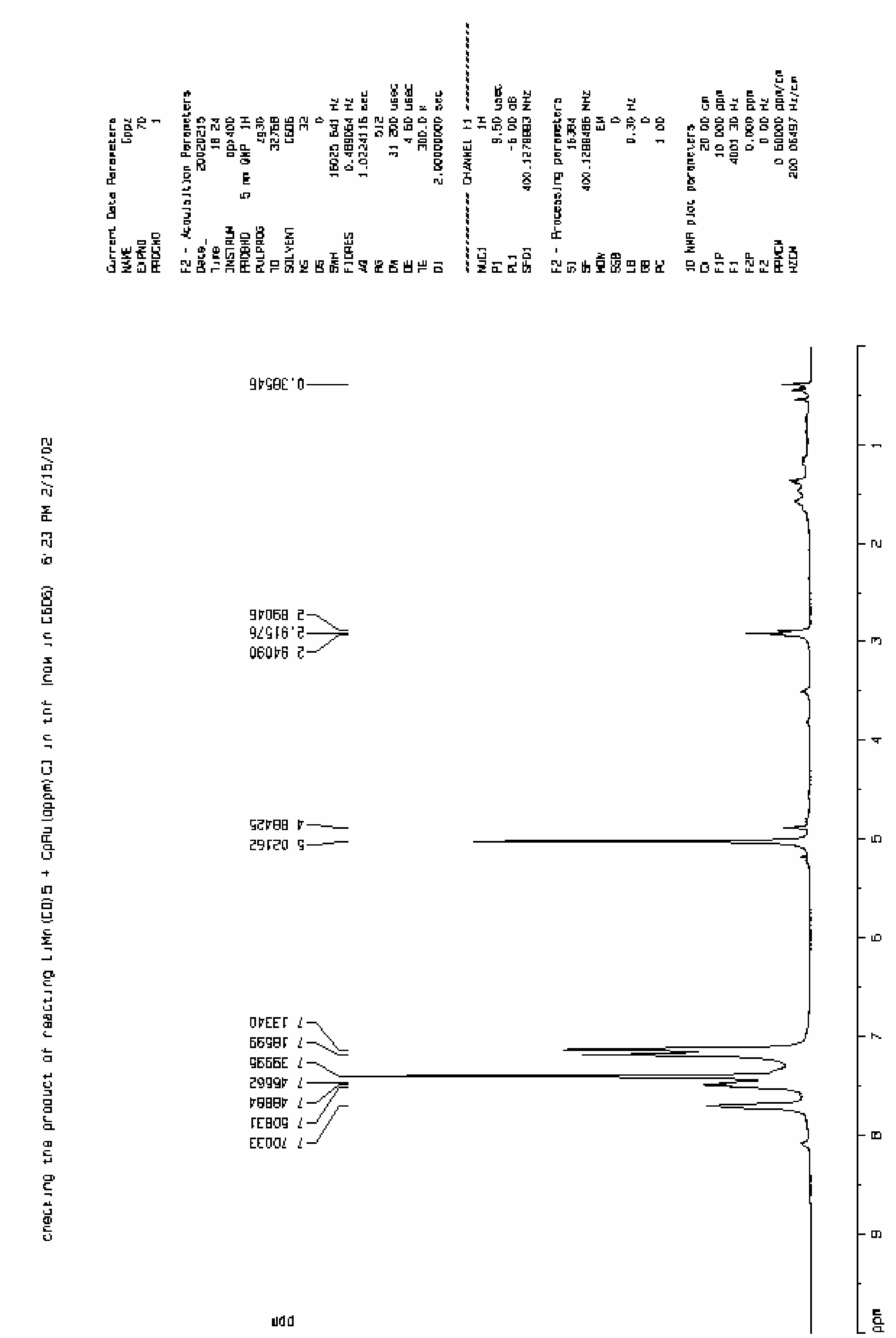

Figure 1: 400.13 MHz ^{1}H-NMR spectrum of $(\eta^5\text{-}C_5H_5)Ru(CO)(\mu\text{-dppm})Mn(CO)_4$ (1).

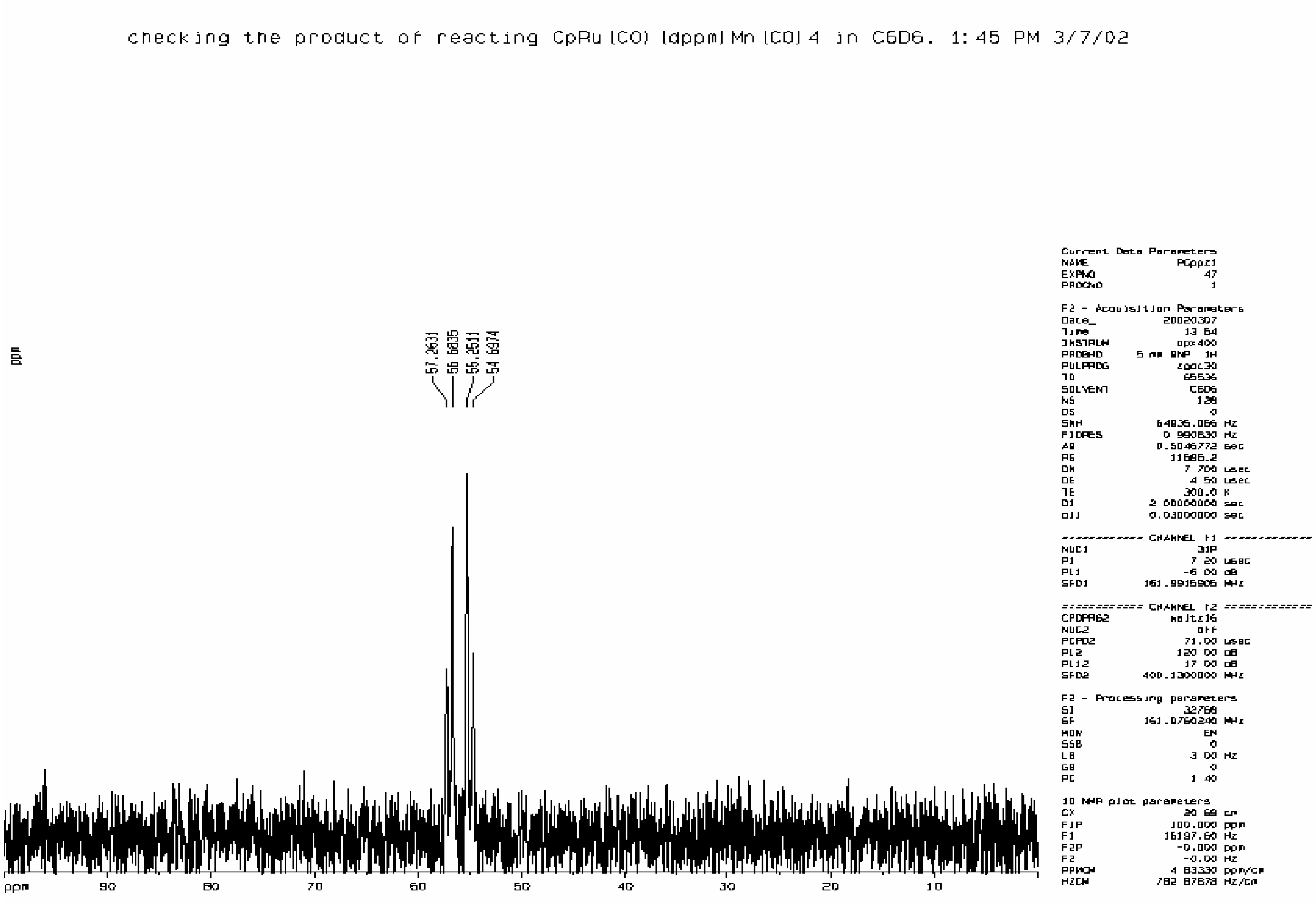

```
Current Data Parameters
NAME              PCppz1
EXPNO                 47
PROCNO                 1

F2 - Acquisition Parameters
Date_           20020307
Time               13.54
INSTRUM           spect400
PROBHD      5 mm BBO 1H
PULPROG           zgpg30
TD                 65536
SOLVENT             C6D6
NS                   128
DS                     0
SWH            64935.066 Hz
FIDRES          0.990830 Hz
AQ             0.5046772 sec
RG               11585.2
DW                 7.700 usec
DE                  4.50 usec
TE                 300.0 K
D1            2.00000000 sec
d11           0.03000000 sec

============ CHANNEL f1 ============
NUC1                 31P
P1                  7.20 usec
PL1                -6.00 dB
SFO1         161.9915905 MHz

============ CHANNEL f2 ============
CPDPRG2          waltz16
NUC2                 off
PCPD2              71.00 usec
PL2               120.00 dB
PL12               17.00 dB
SFO2         400.1300000 MHz

F2 - Processing parameters
SI                 32768
SF           161.9760240 MHz
WDW                   EM
SSB                    0
LB                  3.00 Hz
GB                     0
PC                  1.40

1D NMR plot parameters
CX                 20.69 cm
F1P              100.000 ppm
F1              16197.60 Hz
F2P               -0.000 ppm
F2                 -0.00 Hz
PPMCM            4.83330 ppm/cm
HZCM           782.87878 Hz/cm
```

Figure 2: 161.98 MHz $^{31}P\{^1H\}$-NMR spectrum of (η^5-C_5H_5)Ru(CO)(μ-dppm)Mn$(CO)_4$ (1).

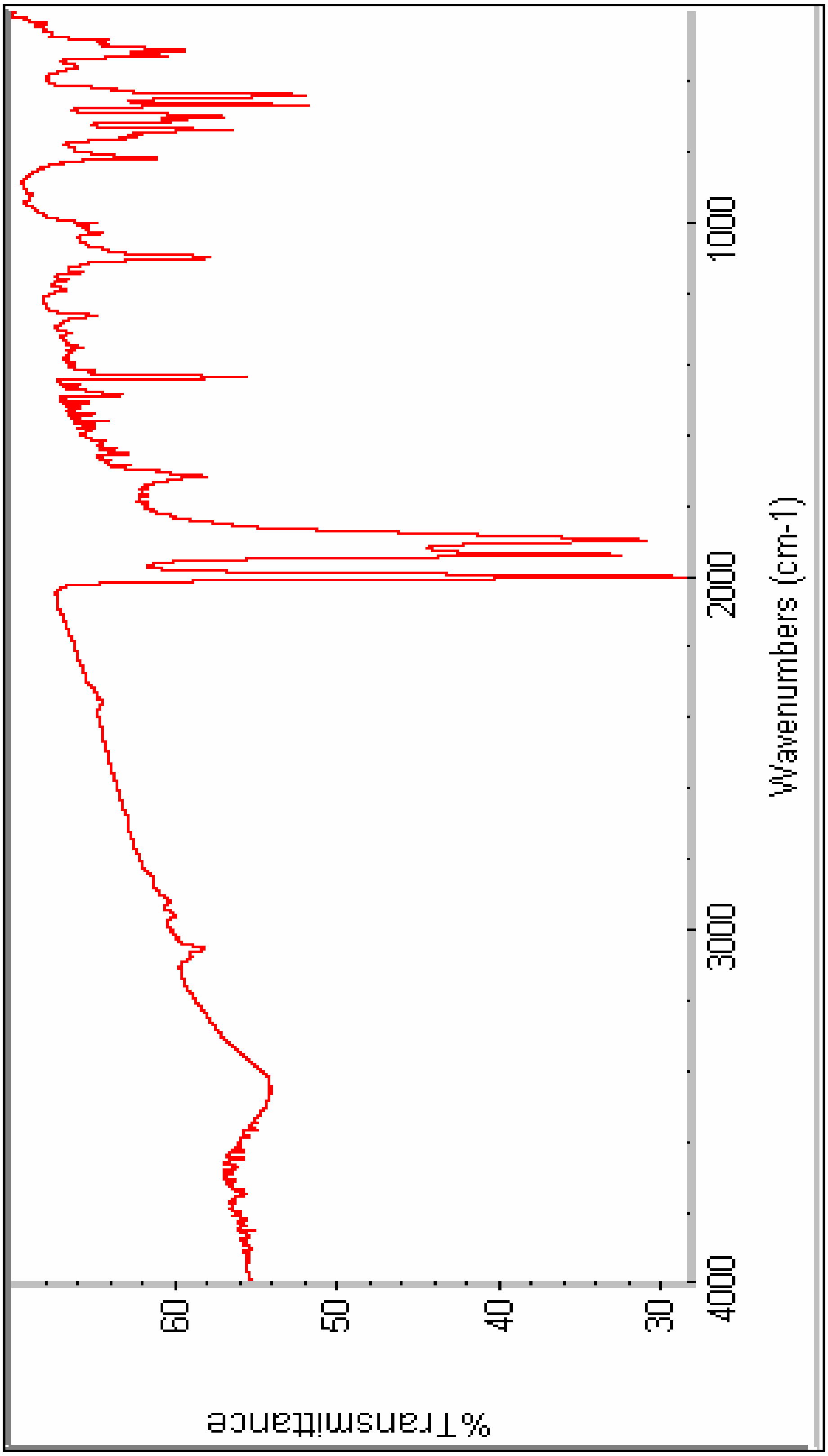

Figure 3: Infra-red spectrum of (η^5-C_5H_5)Ru(CO)(μ-dppm)Mn(CO)$_4$ (1).

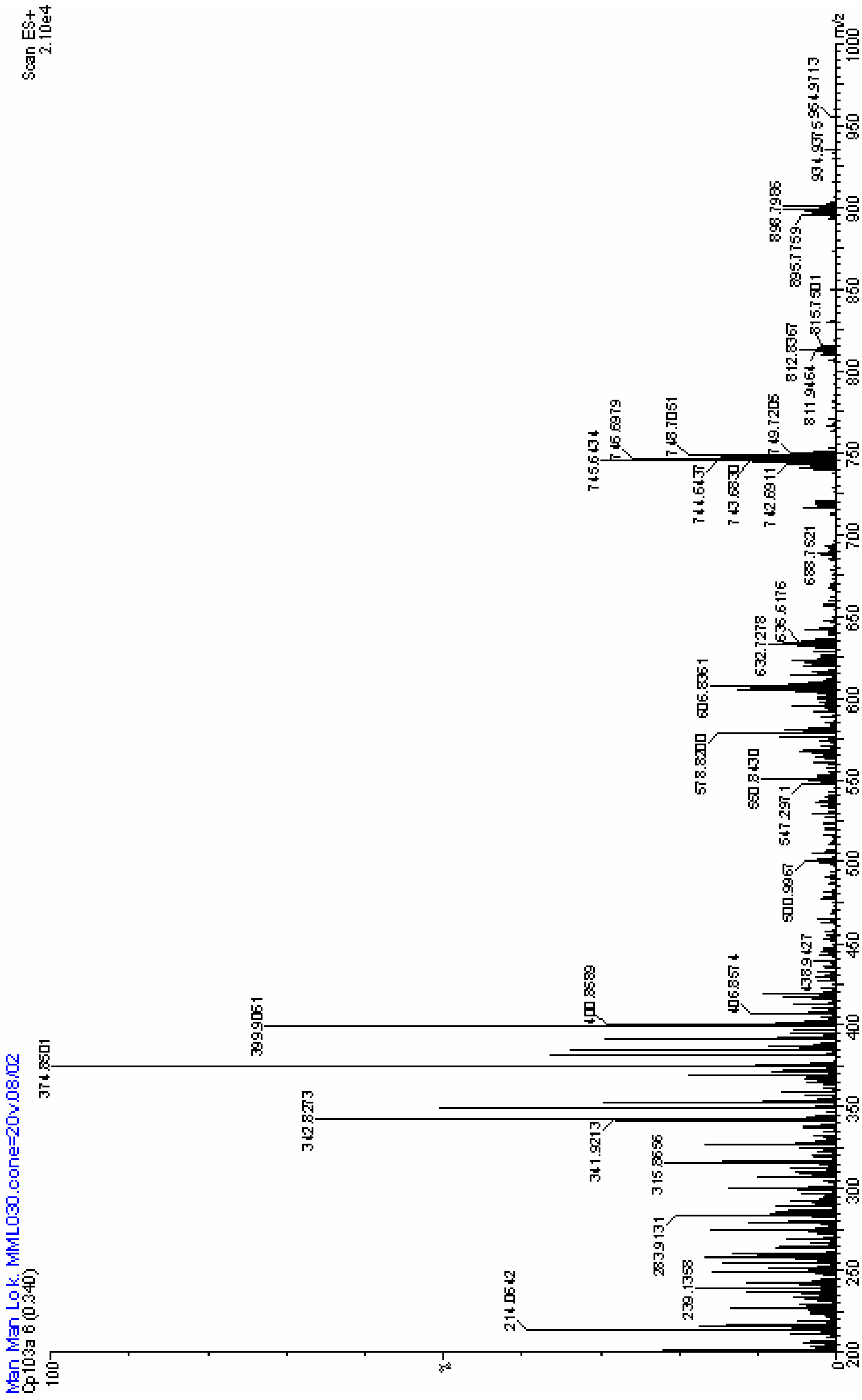

Figure 4: Mass spectrum of (η^5-C_5H_5)Ru(CO)(μ-dppm)Mn(CO)$_4$ (1).

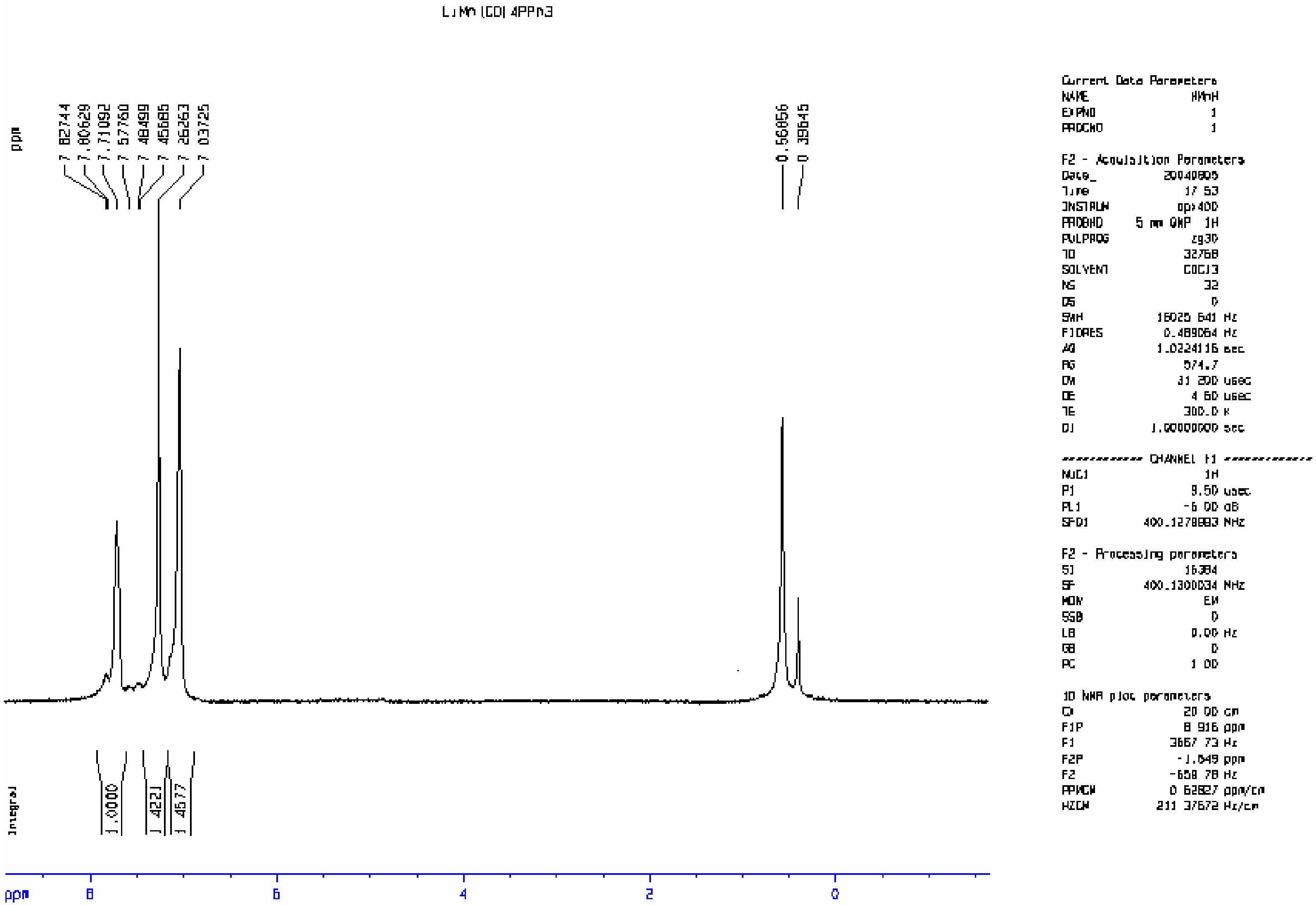

```
Current Data Parameters
NAME               HMnH
EXPNO                 1
PROCNO                1

F2 - Acquisition Parameters
Date_          20040805
Time              17.53
INSTRUM           dpx400
PROBHD     5 mm QNP  1H
PULPROG            zg30
TD                32768
SOLVENT           CDCl3
NS                   32
DS                    0
SWH          16025.641 Hz
FIDRES        0.489064 Hz
AQ           1.0224116 sec
RG                574.7
DW               31.200 usec
DE                 4.60 usec
TE                300.0 K
D1           1.00000000 sec

============ CHANNEL f1 =============
NUC1                 1H
P1                 9.50 usec
PL1               -6.00 dB
SFO1        400.1278883 MHz

F2 - Processing parameters
SI                16384
SF          400.1300034 MHz
WDW                  EM
SSB                   0
LB                 0.00 Hz
GB                    0
PC                 1.00

1D NMR plot parameters
CX                20.00 cm
F1P               8.916 ppm
F1              3567.73 Hz
F2P              -1.649 ppm
F2              -659.78 Hz
PPMCM           0.52827 ppm/cm
HZCM          211.37672 Hz/cm
```

Figure 5: 400.13 MHz ^{1}H-NMR spectrum of $Li^+[Mn(CO)_4(PPh_3)]^-$ (2).

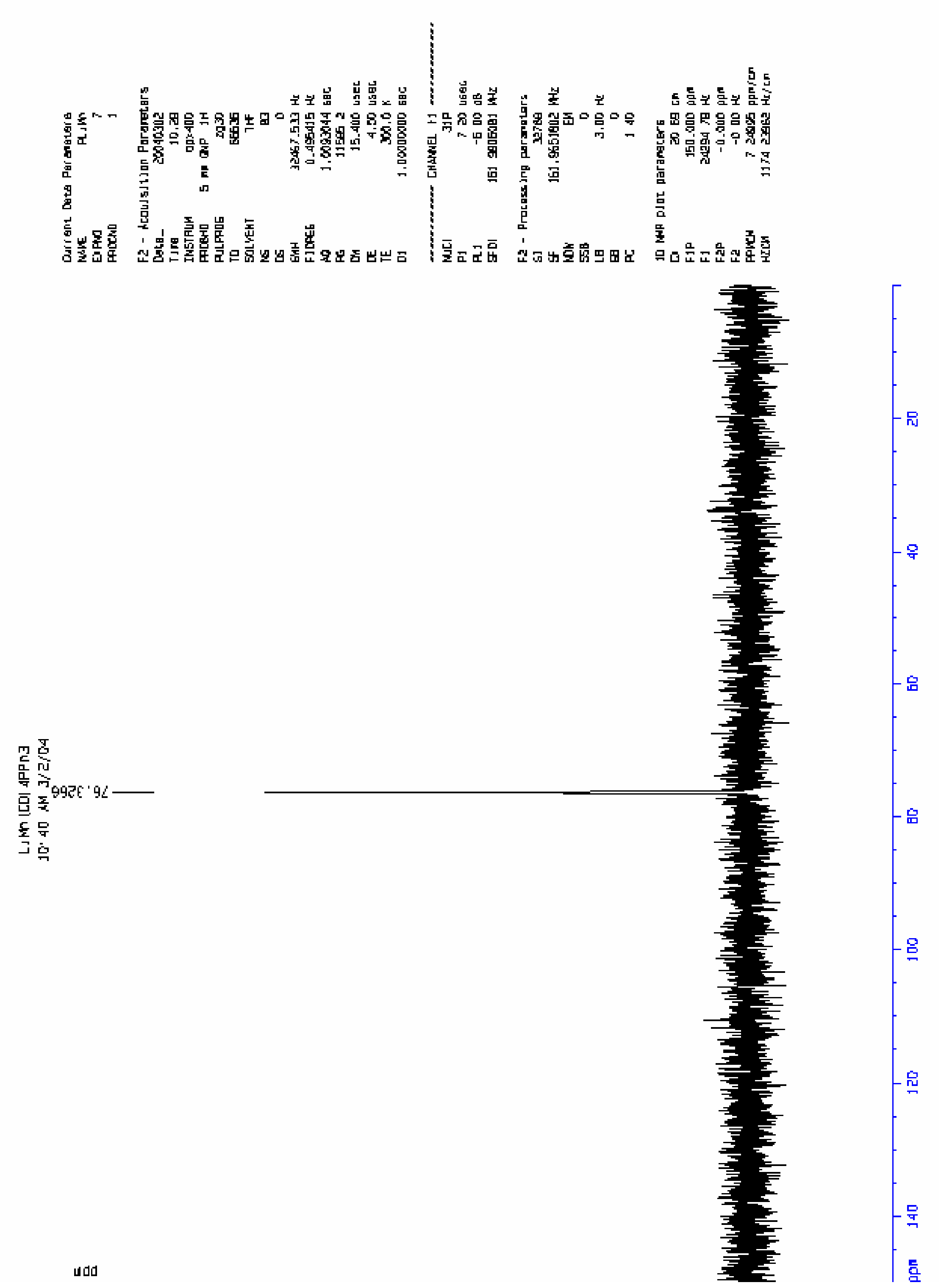

```
Current Data Parameters
NAME             PLiMn
EXPNO                7
PROCNO               1

F2 - Acquisition Parameters
Date_         20040302
Time             10.28
INSTRUM         dpx400
PROBHD    5 mm QNP 1H
PULPROG           zg30
TD               65536
SOLVENT            THF
NS                  83
DS                   0
SWH         32467.533 Hz
FIDRES       0.495415 Hz
AQ          1.0093044 sec
RG             11585.2
DW              15.400 usec
DE                4.50 usec
TE               300.0 K
D1          1.00000000 sec

======== CHANNEL f1 ========
NUC1               31P
P1                7.20 usec
PL1              -6.00 dB
SFO1       161.9806081 MHz

F2 - Processing parameters
SI               32768
SF         161.9651802 MHz
WDW                 EM
SSB                  0
LB                3.00 Hz
GB                   0
PC                1.40

1D NMR plot parameters
CX               20.69 cm
F1P            150.000 ppm
F1            24294.78 Hz
F2P             -0.000 ppm
F2               -0.00 Hz
PPMCM          7.24988 ppm/cm
HZCM        1174.23962 Hz/cm
```

Figure 6: 161.98 MHz $^{31}P\{^1H\}$-NMR spectrum of $Li^+[Mn(CO)_4(PPh_3)]^-$ (2).

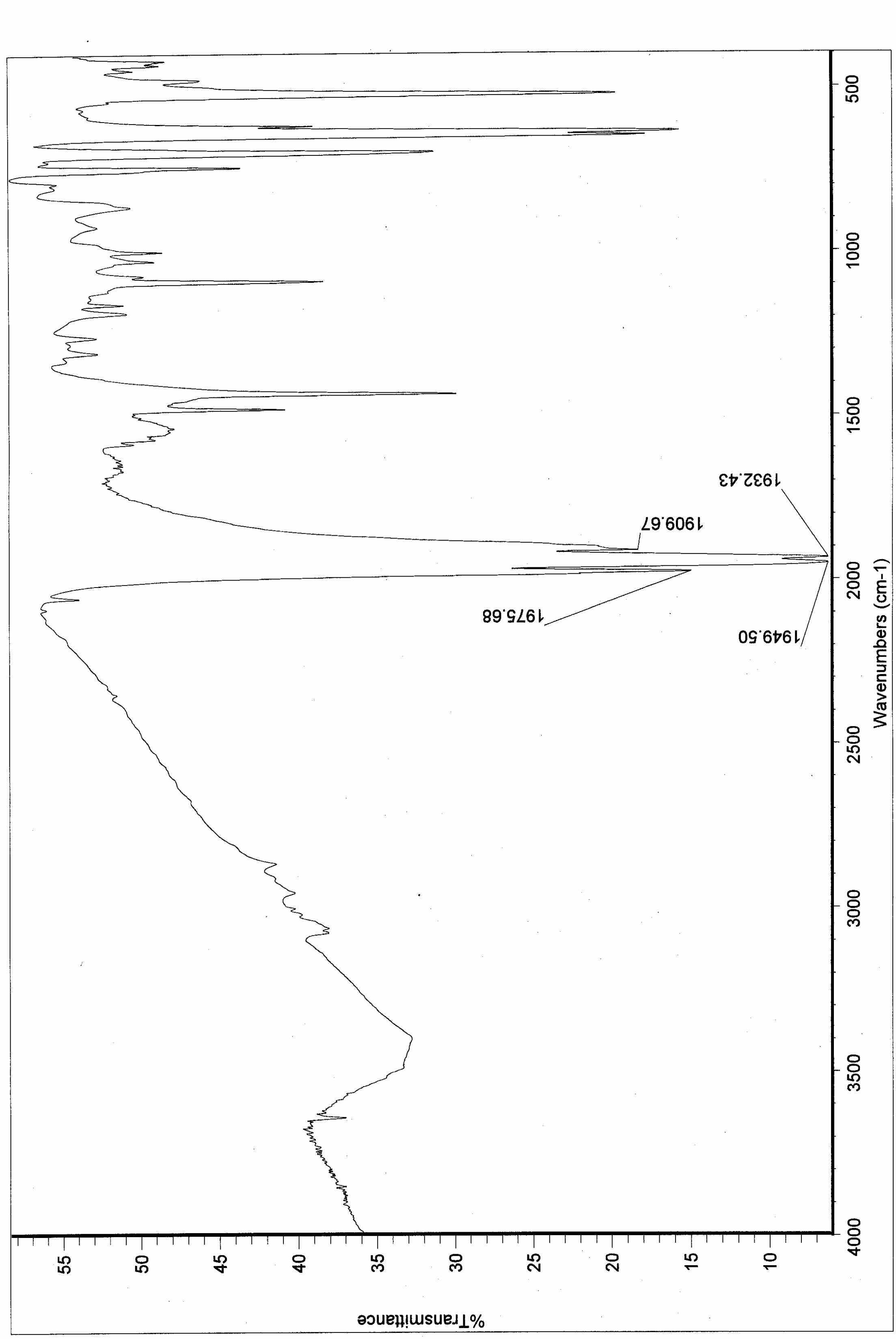

Figure 7: Infra-red spectrum of $Li^{+}[Mn(CO)_4(PPh_3)]^{-}$ (2).

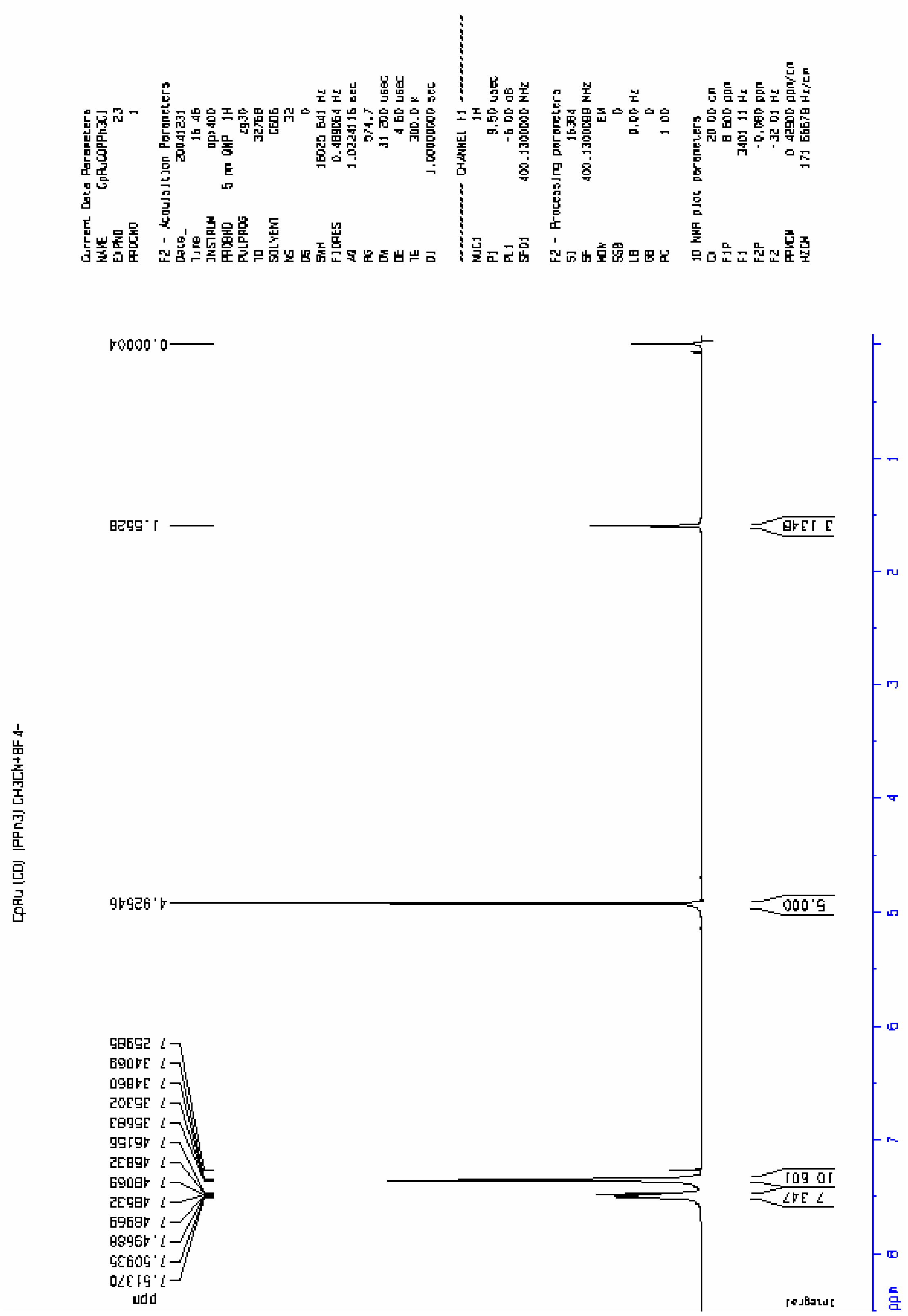

```
Current Data Parameters
NAME        CpRuCOPPh3CJ
EXPNO                 23
PROCNO                 1

F2 - Acquisition Parameters
Date_           20041231
Time               16 46
INSTRUM           dpx400
PROBHD      5 mm QNP  1H
PULPROG             zg30
TD                 32768
SOLVENT             C6D6
NS                    32
DS                     0
SWH           16025 641 Hz
FIDRES         0.489064 Hz
AQ            1.0224116 sec
RG                 574.7
DW               31 200 usec
DE                 4 60 usec
TE                300.0 K
D1           1.00000000 sec

============ CHANNEL f1 ============
NUC1                  1H
P1                  9.50 usec
PL1                -6 00 dB
SFO1         400.1300000 MHz

F2 - Processing parameters
SI                 16384
SF           400.1300088 MHz
WDW                   EM
SSB                    0
LB                  0.00 Hz
GB                     0
PC                  1 00

1D NMR plot parameters
CX                 20 00 cm
F1P                8 600 ppm
F1               3401 11 Hz
F2P               -0.080 ppm
F2                -32 01 Hz
PPMCM            0 42900 ppm/cm
HZCM           171 66678 Hz/cm
```

Figure 8: 400.13 MHz ^{1}H-NMR spectrum of [η^5-$C_5H_5Ru(CO)(PPh_3)(CH_3CN)]^+[BF_4]^-$ (3).

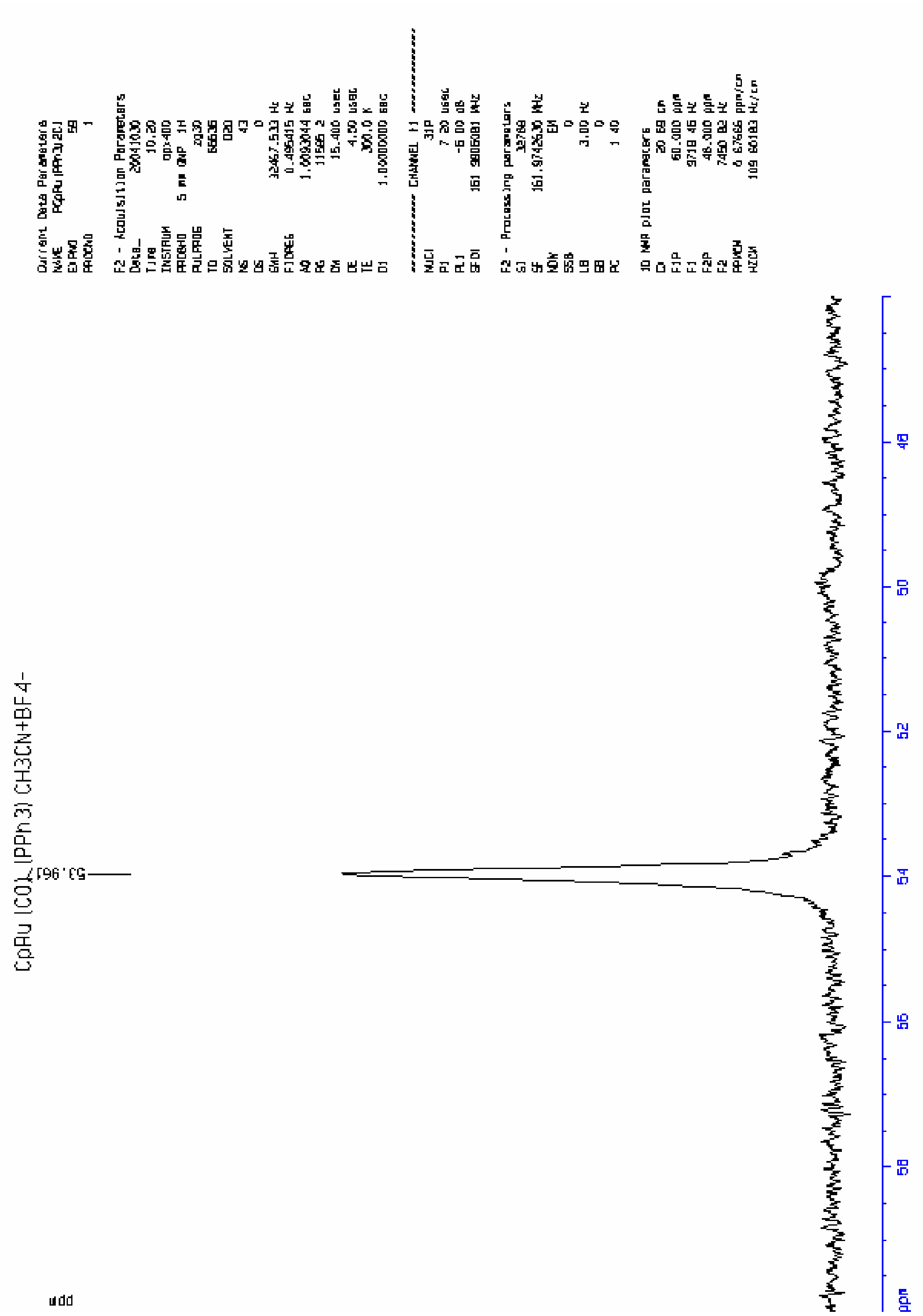

Figure 9: 161.98 MHz $^{31}P\{^{1}H\}$-NMR spectrum of $[\eta^{5}\text{-}C_5H_5Ru(CO)(PPh_3)(CH_3CN)]^{+}[BF_4]^{-}$ (3).

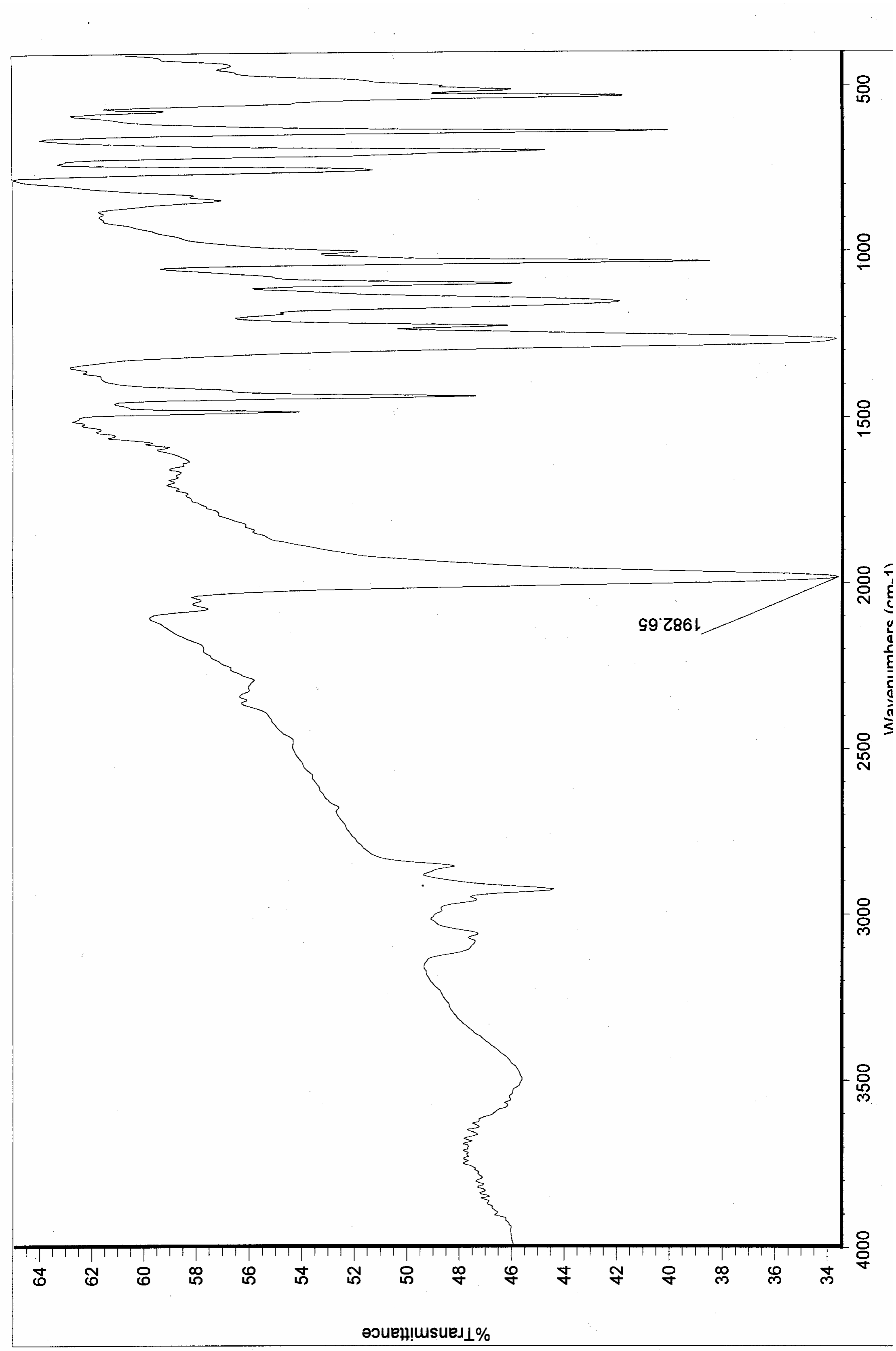

Figure 10: Infra-red spectrum of [η^5-C_5H_5Ru(CO)(PPh_3)(CH_3CN)]$^+$[BF_4]$^-$ (3).

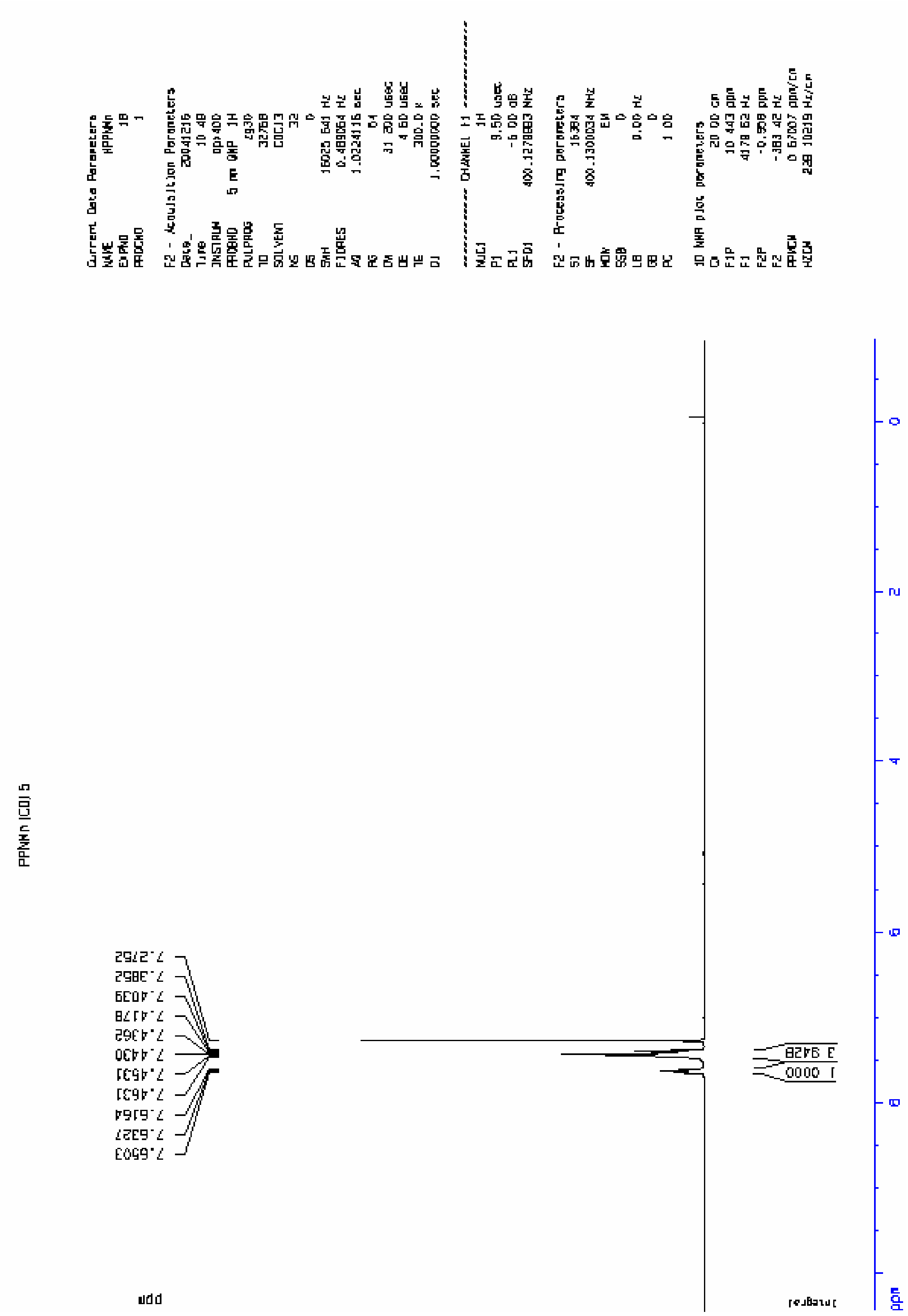

```
Current Data Parameters
NAME             HPPNMn
EXPNO                18
PROCNO                1

F2 - Acquisition Parameters
Date_          20041216
Time              10.48
INSTRUM          dpx400
PROBHD     5 mm QNP  1H
PULPROG            zg30
TD                32768
SOLVENT           CDCl3
NS                   32
DS                    0
SWH           16025.641 Hz
FIDRES         0.489064 Hz
AQ            1.0224116 sec
RG                   64
DW               31.200 usec
DE                 4.60 usec
TE                300.0 K
D1           1.00000000 sec

============ CHANNEL f1 ============
NUC1                 1H
P1                 9.50 usec
PL1               -6.00 dB
SFO1        400.1278883 MHz

F2 - Processing parameters
SI                16384
SF          400.1300034 MHz
WDW                  EM
SSB                   0
LB                 0.00 Hz
GB                    0
PC                 1.00

1D NMR plot parameters
CX                20.00 cm
F1P              10.443 ppm
F1              4178.62 Hz
F2P              -0.958 ppm
F2              -383.42 Hz
PPMCM           0.67007 ppm/cm
HZCM          268.10219 Hz/cm
```

Figure 11: 400.13 MHz ^{1}H-NMR spectrum of [PPN$^+$][Mn(CO)$_5$$^-$] (5).

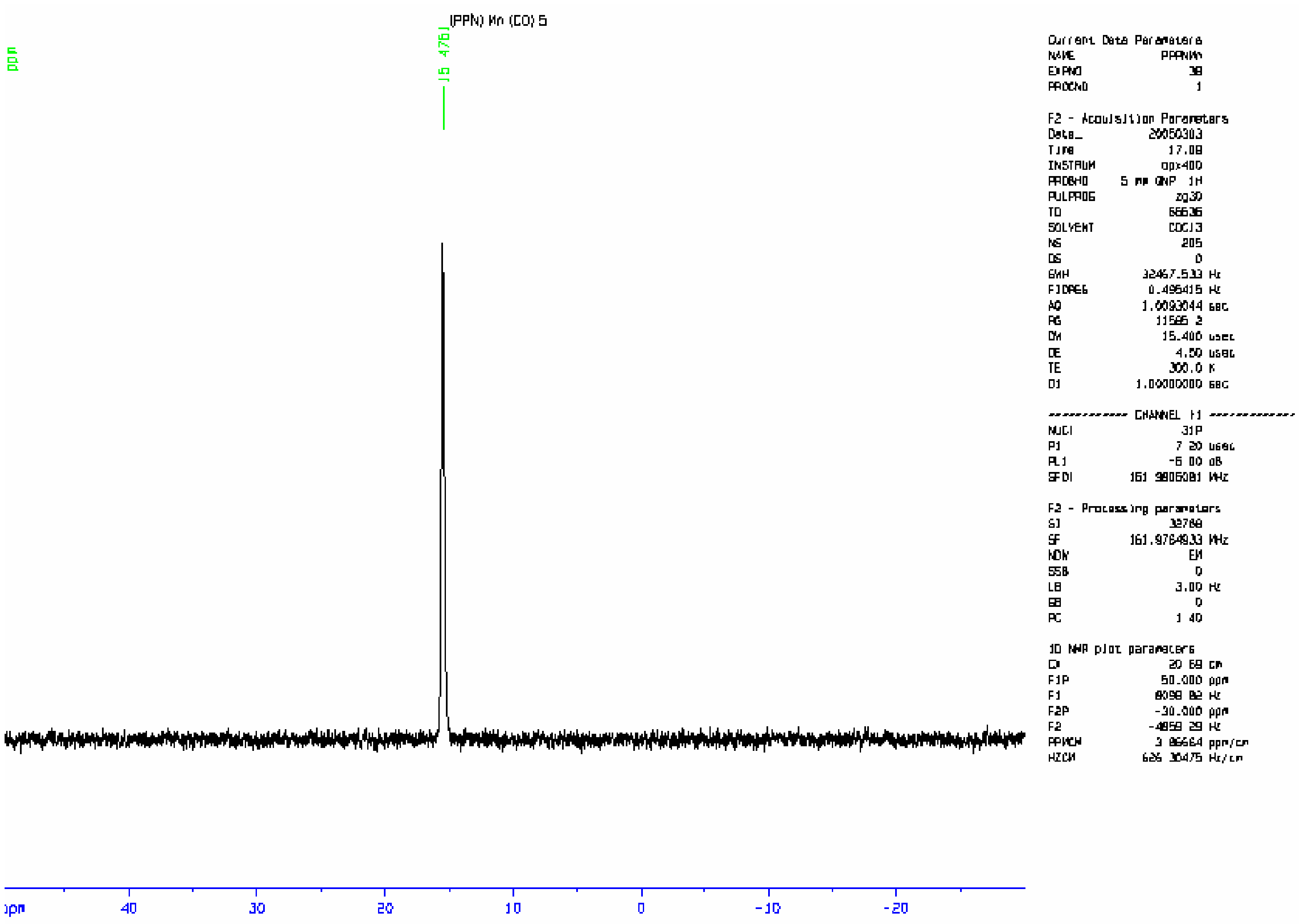

Figure 12: 161.98 MHz $^{31}P\{^1H\}$-NMR spectrum of $[PPN^+][Mn(CO)_5^-]$ (5).

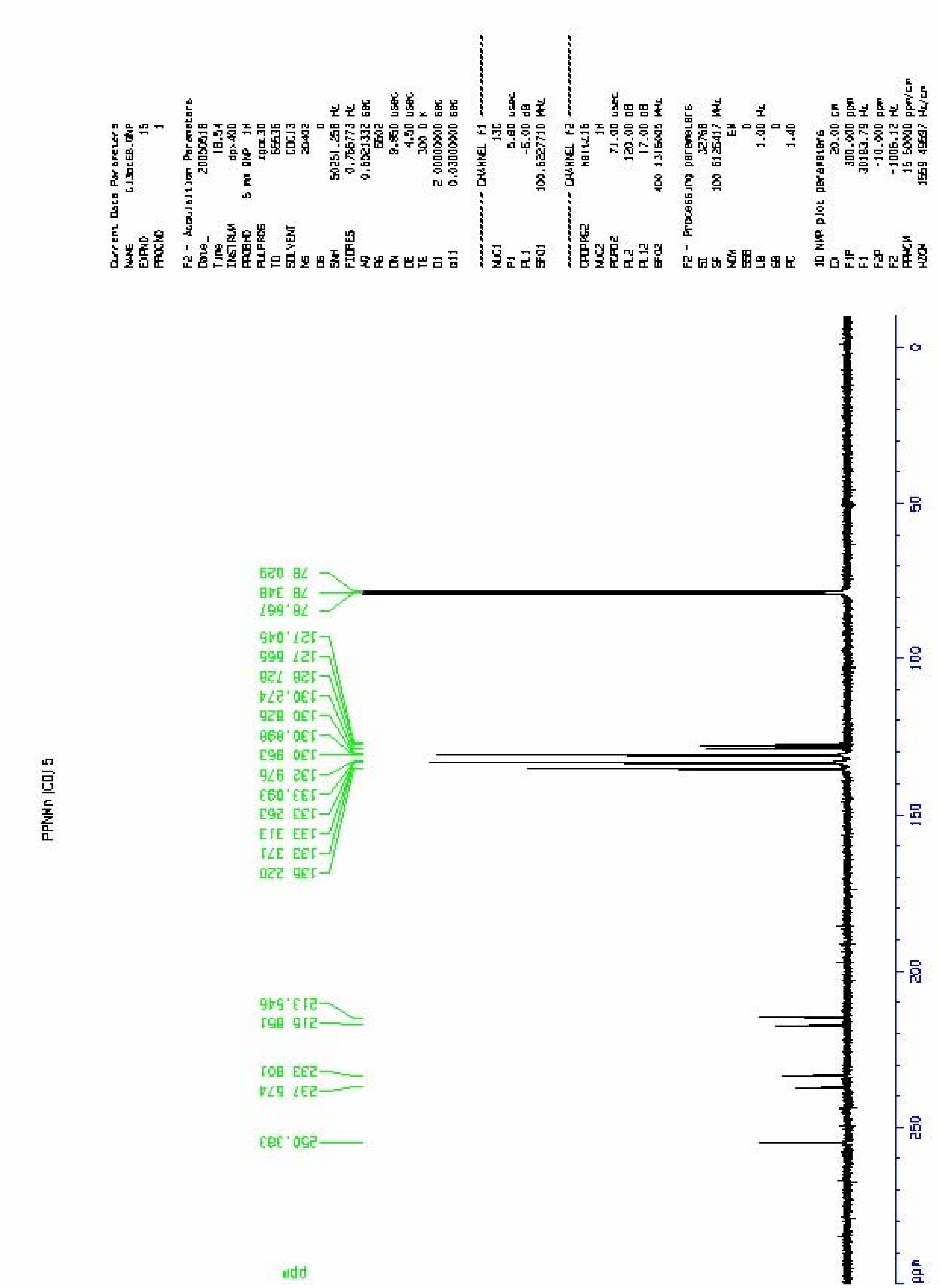

Figure 13: 100.061MHz $^{13}C\{^{1}H\}$-NMR spectrum of $[PPN^{+}][Mn(CO)_5^{-}]$ (5).

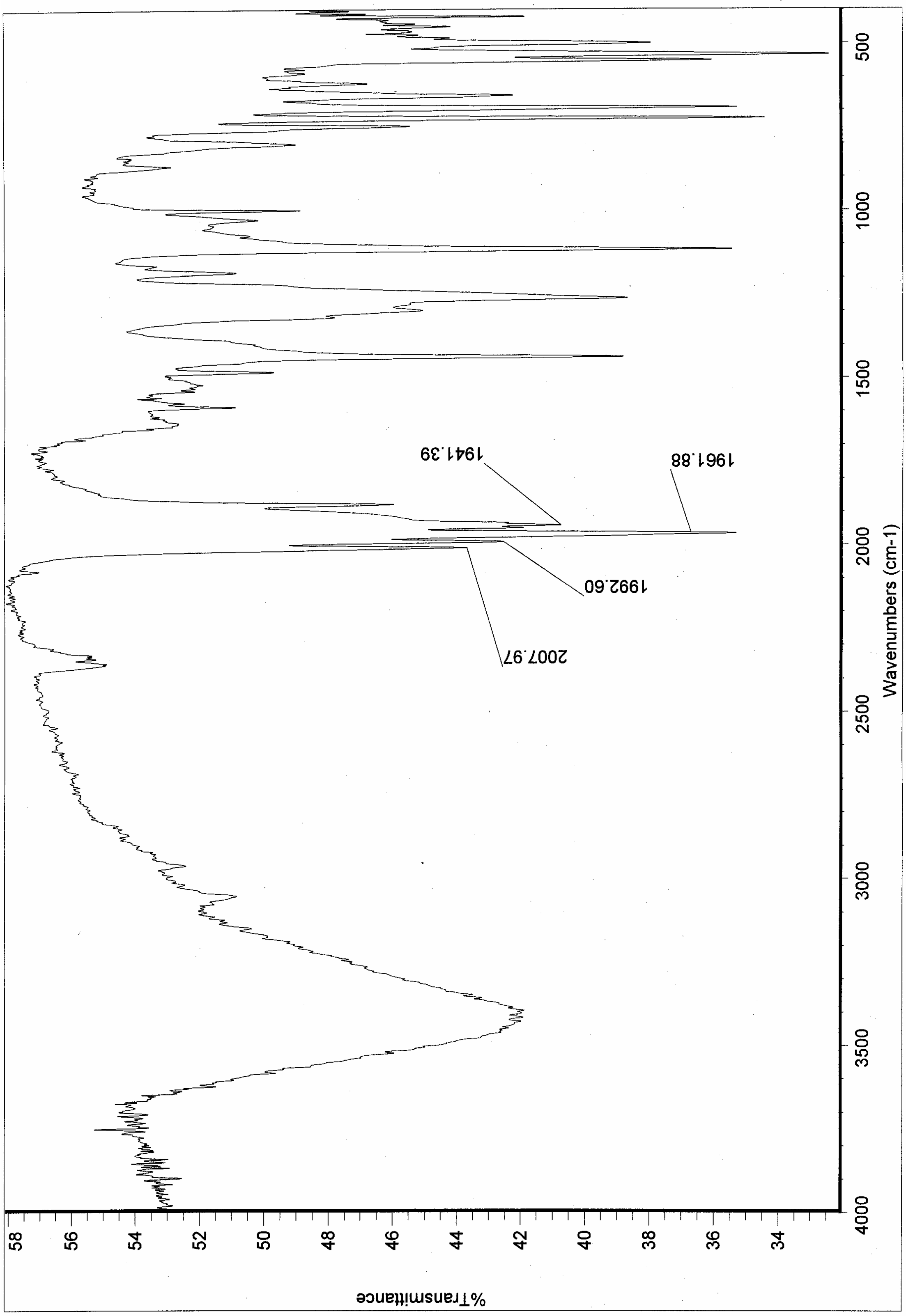

Figure 14: Infra-red spectrum of [PPN$^+$][Mn(CO)$_5^-$] (5).

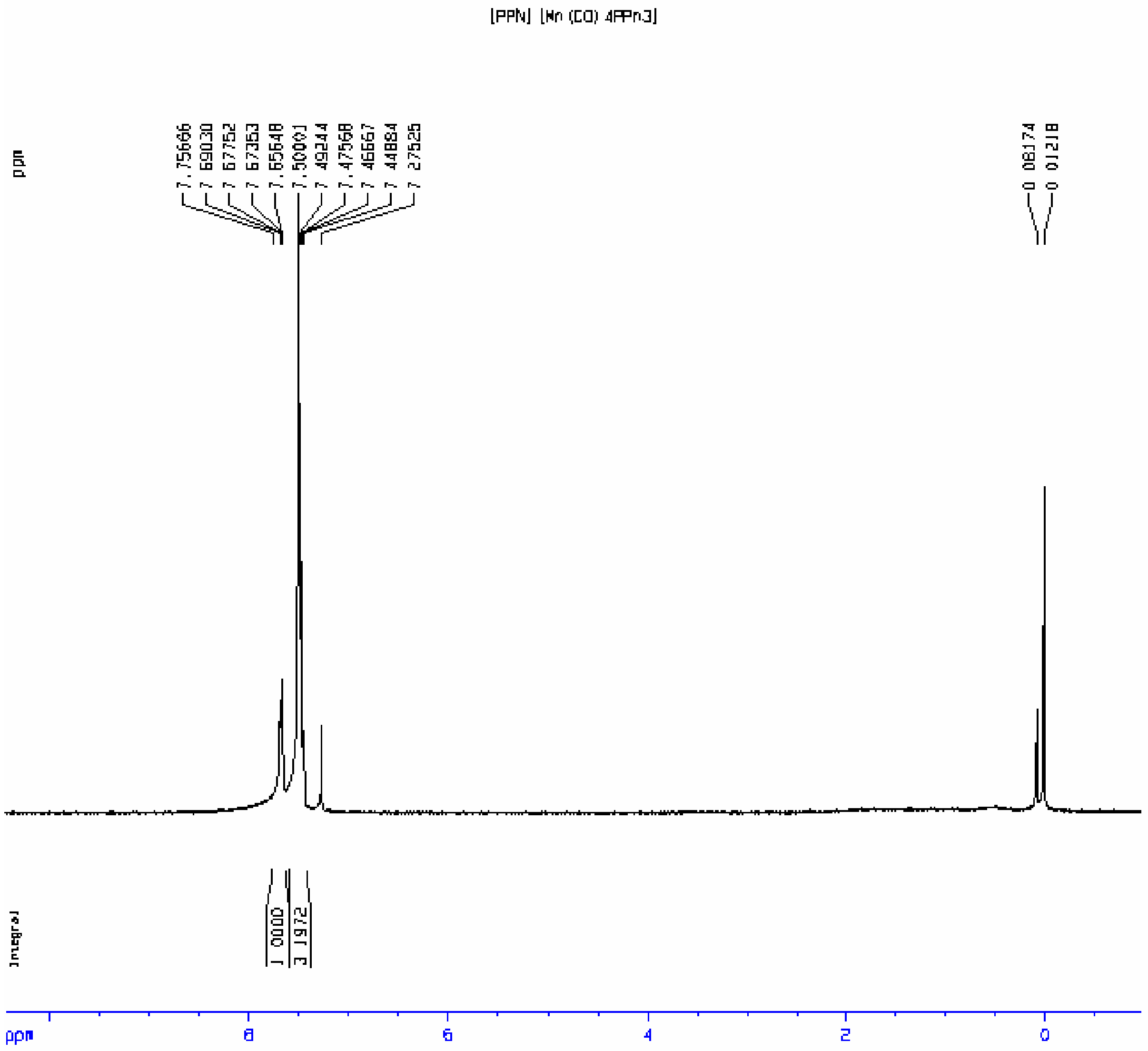

```
Current Data Parameters
NAME              HPPNMn
EXPNO                 21
PROCNO                 1

F2 - Acquisition Parameters
Date_           20050203
Time               16 07
INSTRUM           spx400
PROBHD     5 mm QNP  1H
PULPROG             zg30
TD                 32768
SOLVENT            CDCl3
NS                    32
DS                     0
SWH           16025 641 Hz
FIDRES         0.489064 Hz
AQ            1.0224116 sec
RG                1448.2
DW                31 200 usec
DE                  4 60 usec
TE                 300.0 K
D1            1.00000000 sec

============ CHANNEL f1 =============
NUC1                  1H
P1                  9.50 usec
PL1                -6 00 dB
SFO1         400.1278883 MHz

F2 - Processing parameters
SI                 16384
SF           400.1300034 MHz
WDW                   EM
SSB                    0
LB                  0.00 Hz
GB                     0
PC                  1 00

1D NMR plot parameters
CX                 20 00 cm
F1P               10 443 ppm
F1               4178 62 Hz
F2P               -0.958 ppm
F2               -383 42 Hz
PPMCM            0 67007 ppm/cm
HZCM           268 10219 Hz/cm
```

Figure 15: 400.13 MHz ^{1}H-NMR spectrum of [PPN][Mn(CO)$_4$PPh$_3$] (6).

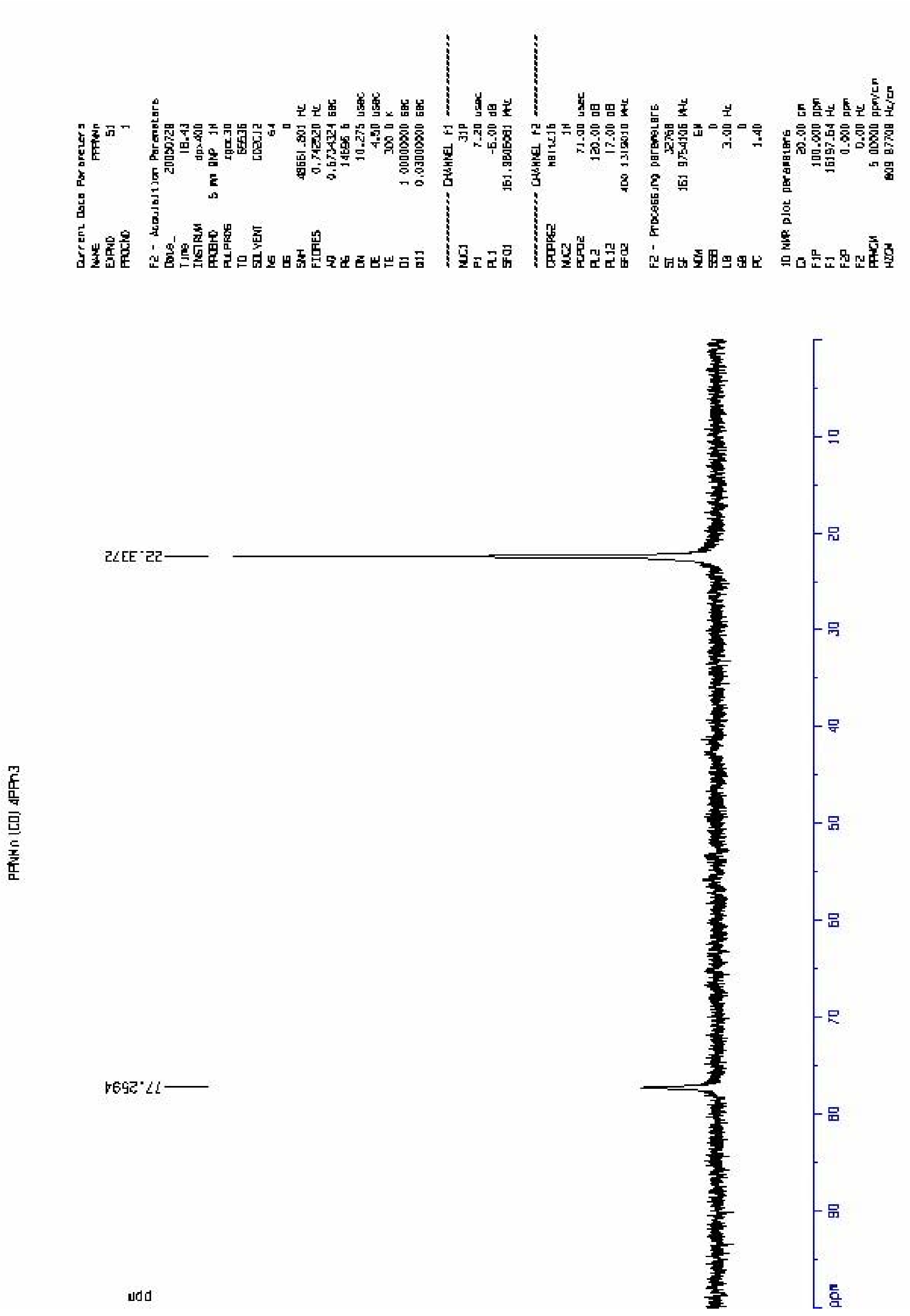

Figure 16: 161.98 MHz $^{31}P\{^{1}H\}$-NMR spectrum of [PPN][Mn(CO)$_4$PPh$_3$] (6).

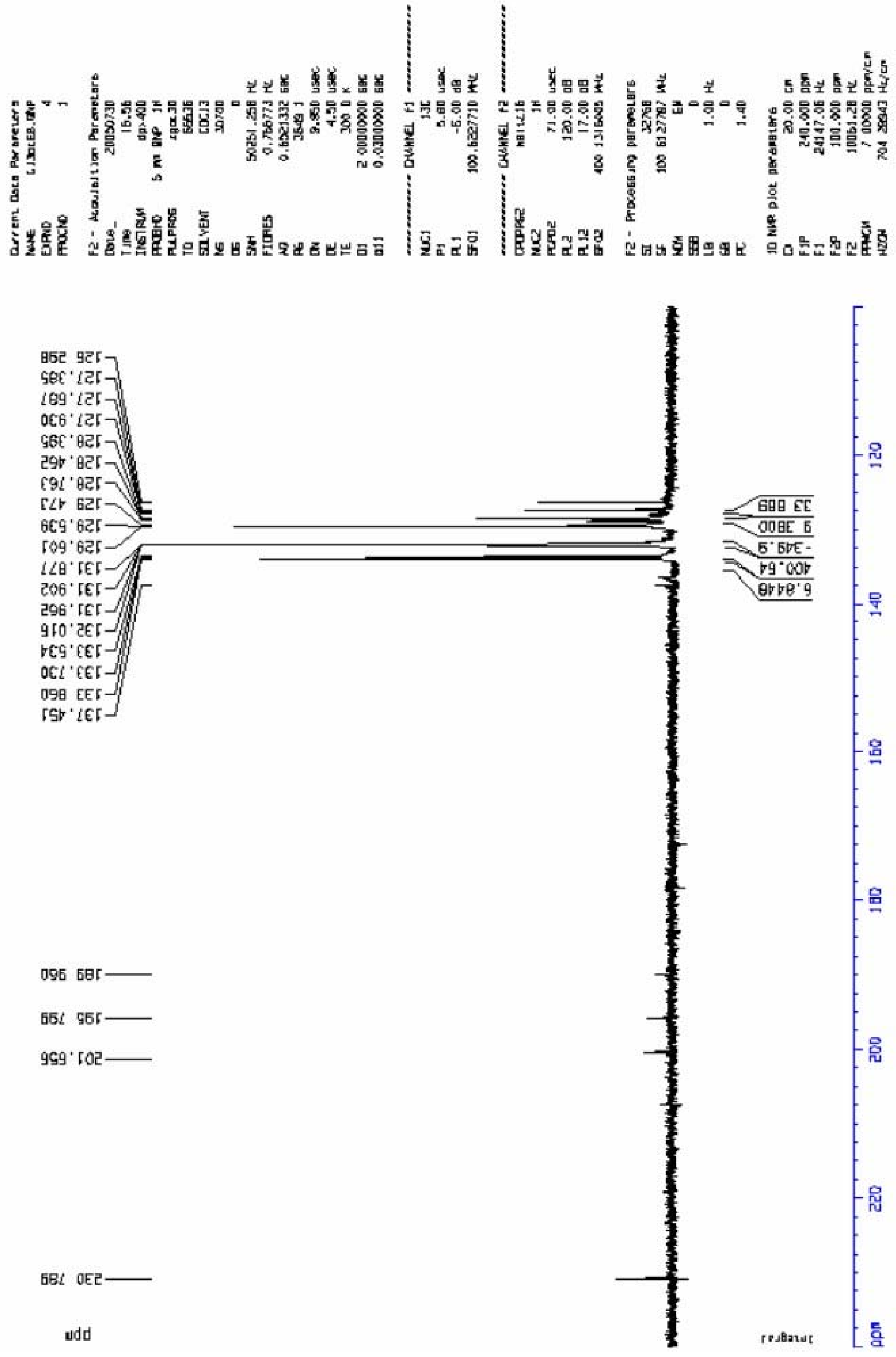

Figure 17: 100.061MHz $^{13}C\{^1H\}$-NMR spectrum of [PPN][Mn(CO)$_4$PPh$_3$] (6).

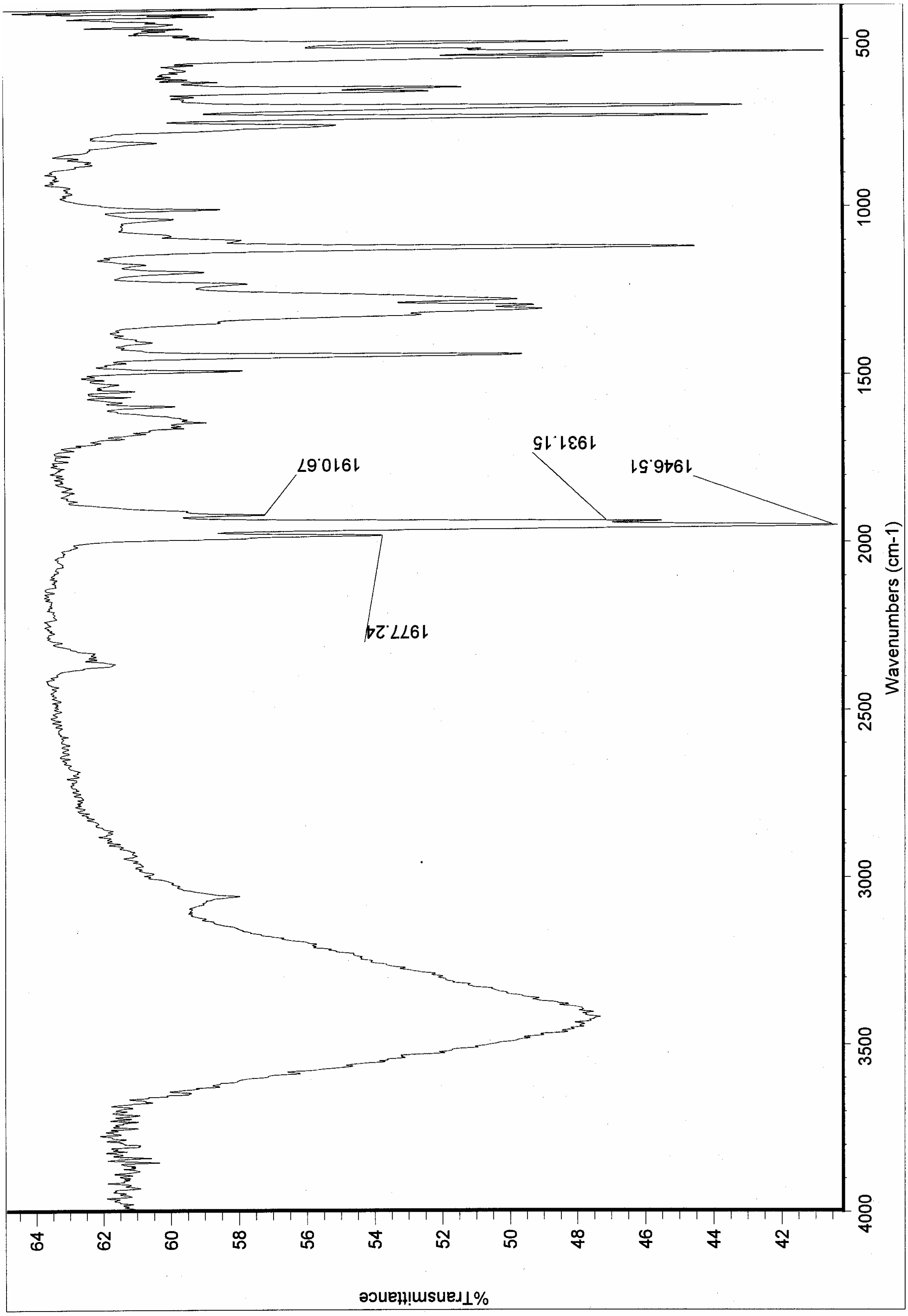

Figure 18: Infra-red spectrum of [PPN][Mn(CO)$_4$PPh$_3$] (6).

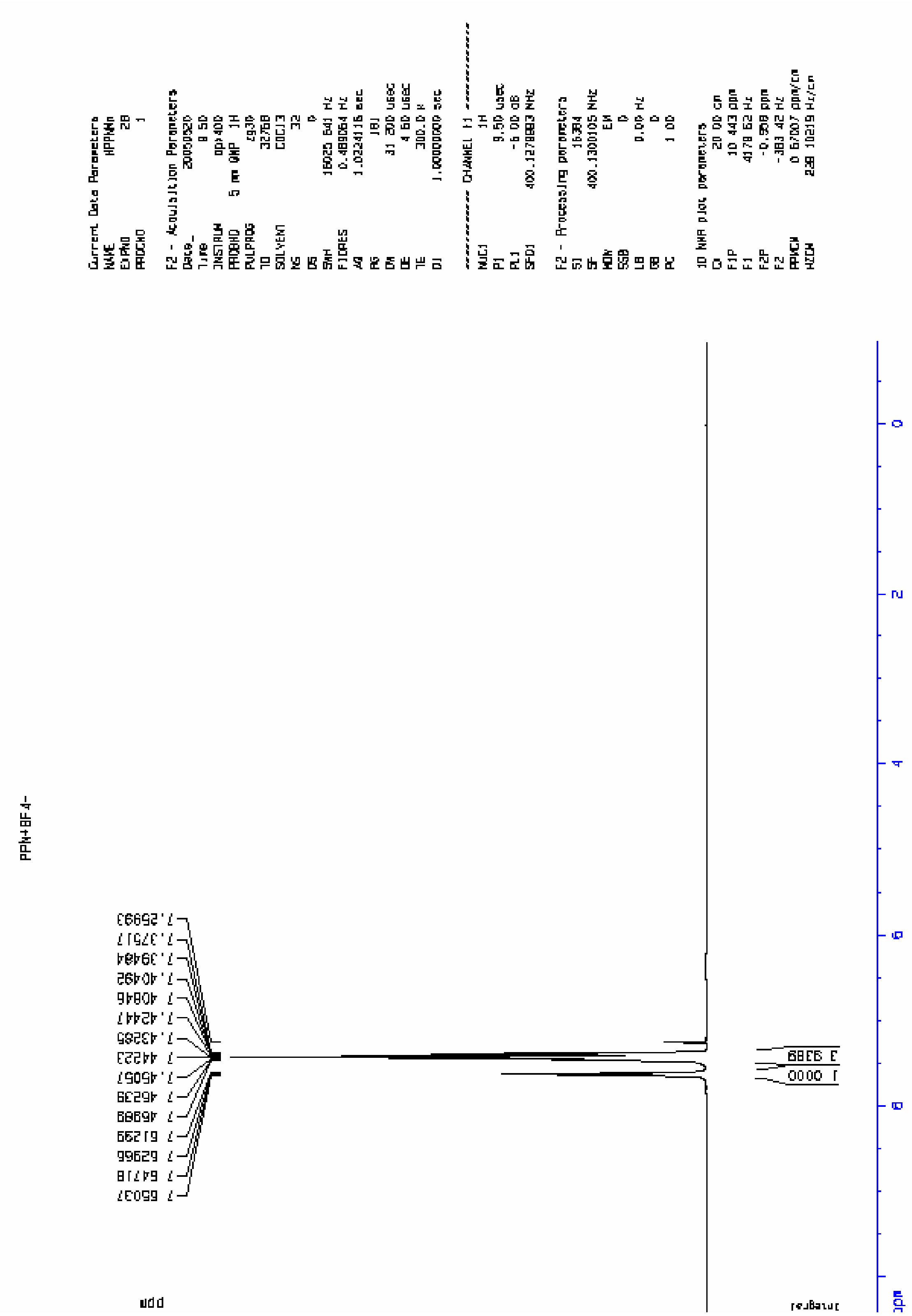

Figure 19: 400.13 MHz ^{1}H-NMR spectrum of [PPN][BF$_4$] (7).

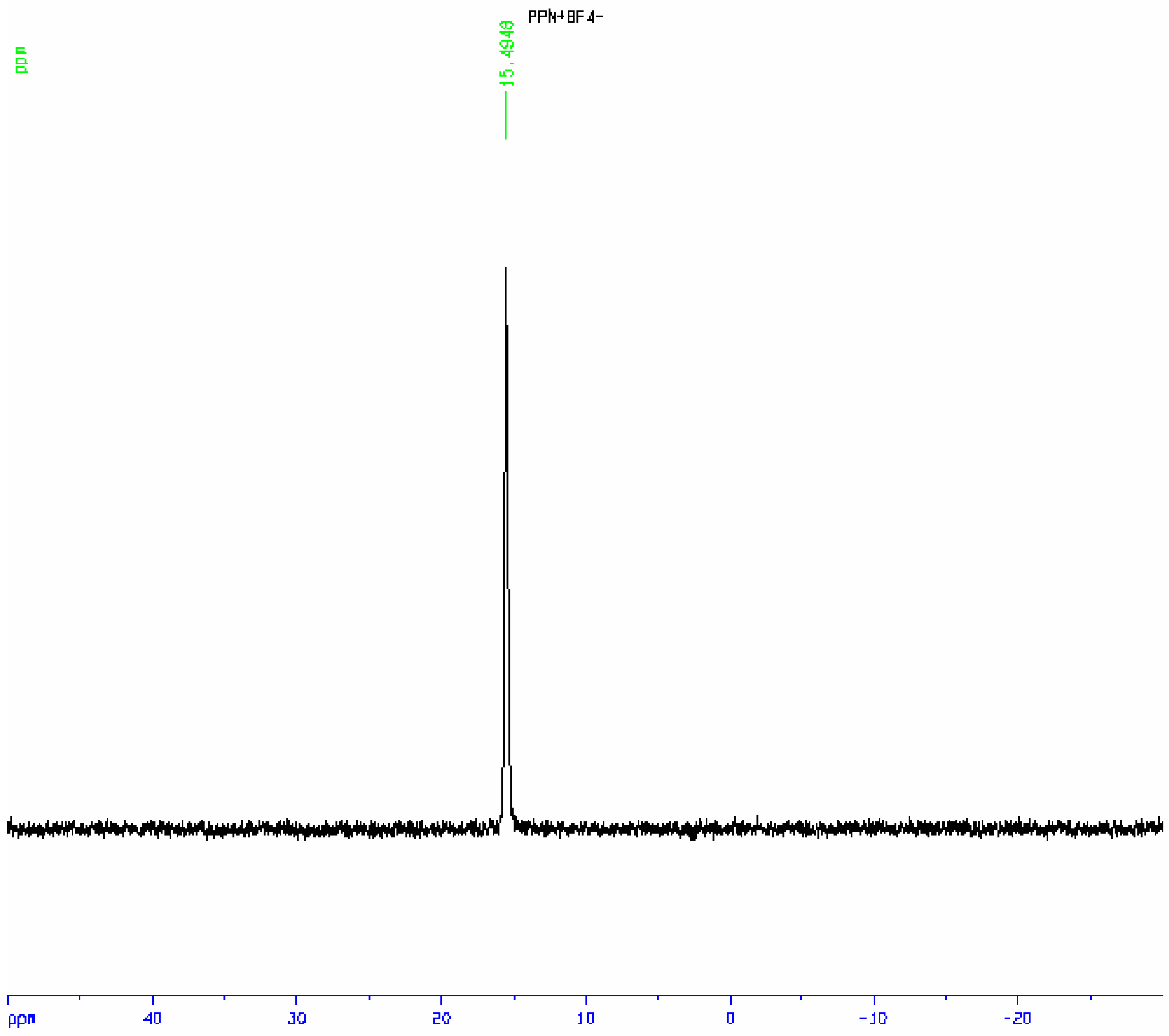

```
Current Data Parameters
NAME               PPPNM
EXPNO                 48
PROCNO                 1

F2 - Acquisition Parameters
Date_           20050520
Time                8.52
INSTRUM           dpx400
PROBHD      5 mm QNP 1H
PULPROG             zg30
TD                 65536
SOLVENT            CDCl3
NS                   103
DS                     0
SWH            32467.533 Hz
FIDRES          0.495415 Hz
AQ             1.0093044 sec
RG               11585.2
DW                15.400 usec
DE                  4.50 usec
TE                 300.0 K
D1            1.00000000 sec

============ CHANNEL f1 ============
NUC1                 31P
P1                  7.20 usec
PL1                -6.00 dB
SFO1         161.9906081 MHz

F2 - Processing parameters
SI                 32768
SF           161.9764933 MHz
WDW                   EM
SSB                    0
LB                  3.00 Hz
GB                     0
PC                  1.40

1D NMR plot parameters
CX                 20.69 cm
F1P               50.000 ppm
F1               8098.82 Hz
F2P              -30.000 ppm
F2              -4859.29 Hz
PPMCM            3.86664 ppm/cm
HZCM           626.30475 Hz/cm
```

Figure 20: 161.98 MHz $^{31}P\{^{1}H\}$-NMR spectrum of [PPN] [BF_4] (7).

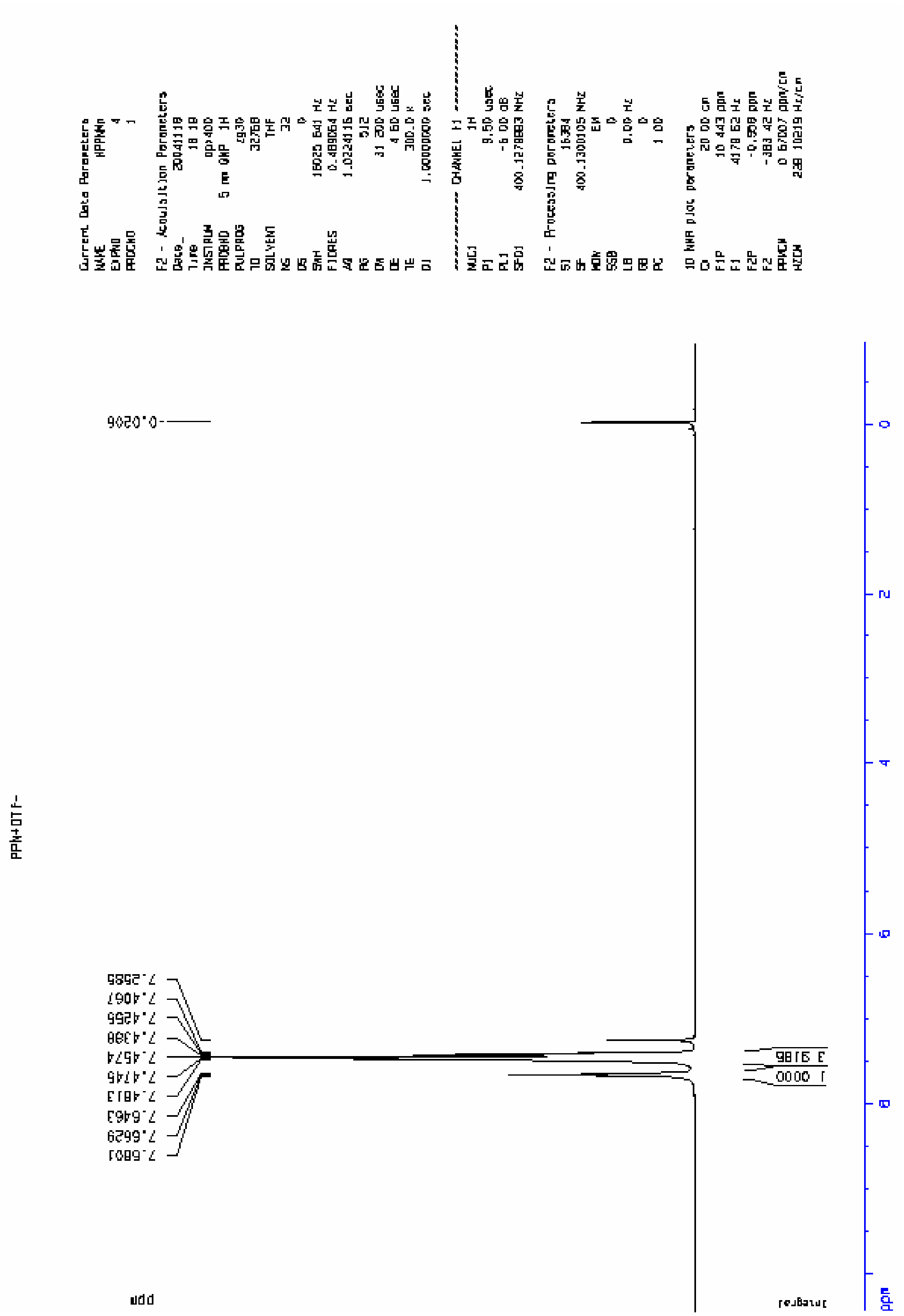

Figure 21: 400.13 MHz ^{1}H-NMR spectrum of [PPN][OTf] (8).

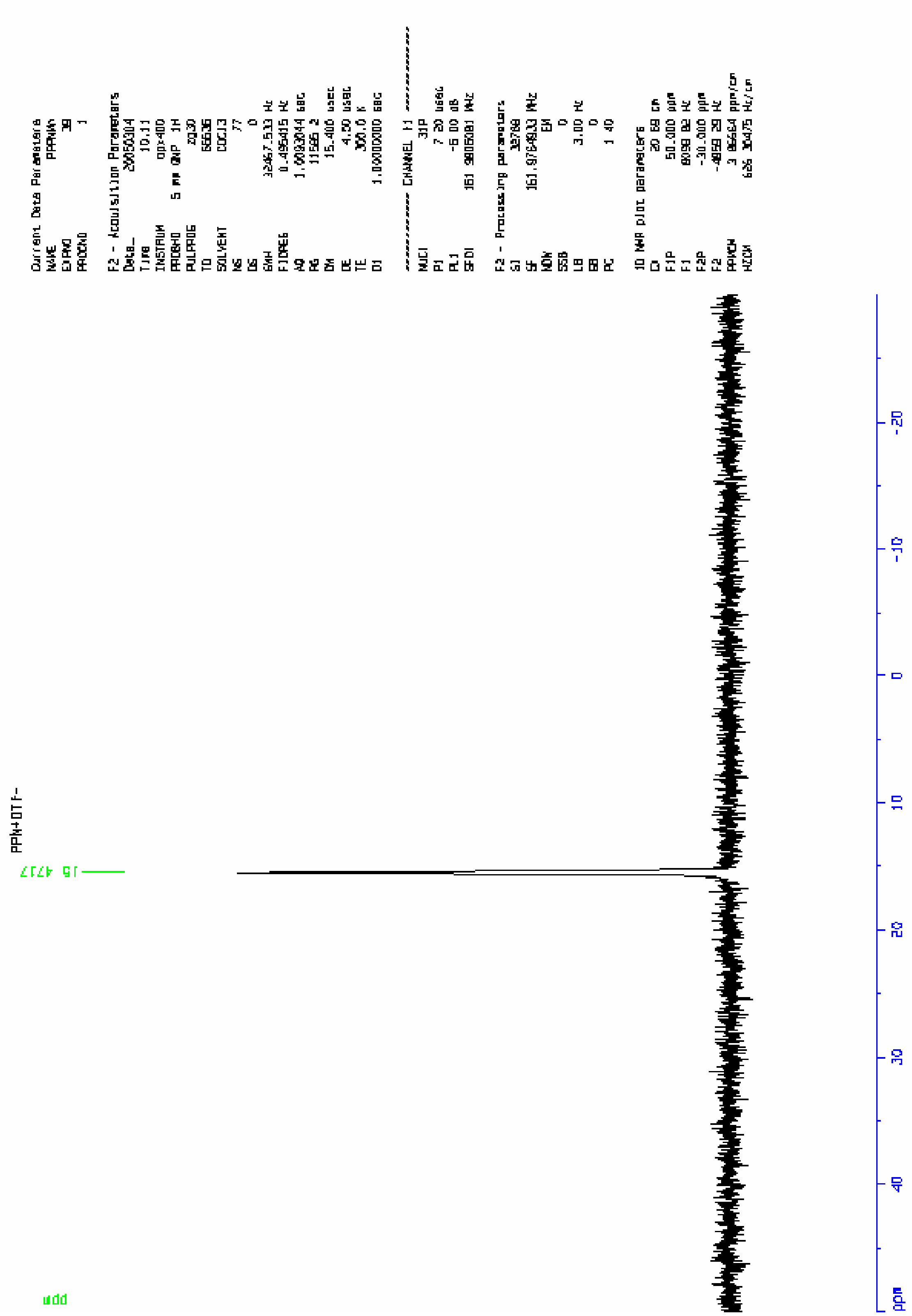

Figure 22: 161.98 MHz $^{31}P\{^{1}H\}$-NMR spectrum of [PPN][OTf] (8).

Publication

1. Wing Nga Sit, Siu Man Ng, Kar Yan Kwong, and Chak Po Lau**.,** *Coupling Reactions of CO_2 with Neat Epoxides Catalyzed by PPN Salts To Yield Cyclic Carbonates*., Journal of the Organic Chemistry., **2005**, 70**,** p 8583 – 8586.
2. Man Lok Man, King Chung Lam, Wing Nga Sit, Siu Man Ng, Zhongyuan Zhou, Zhenyang Lin, and Chak Po Lau., *Synthesis of heterobimetallic Ru-Mn complexes and coupling reactions of epoxides with carbon dioxide catalyzed by these complexes*., Chemistry - A European Journal., **2006**, *12*, 1004-1015.
3. Wing Nga Sit, Man Lok Man, Siu Man Ng and Chak Po Lau., *Desulfurization of thiiranes catalysed by the bimetallic complex [η^5-$C_5H_5Ru(CO)(\mu\text{-dppm})Mn(CO)_4$], and the monometallic complexes reaction.*, 13th IUPAC International Symposium on Organometallic Chemistry Directed Towards Organic Synthesis., P-82, 17-21, July, 2005.